T. Mehrian Isfahany

THERMODYNAMICS OF THE ADSORPTION OF ORGANIC CATIONS ON KAOLINITE

Temperature Dependence and Calorimetry

Promotor:	Prof. Dr. J. Lyklema hoogleraar in de fysische en kolloïdchemie, met bijzondere aandacht voor de grensvlak en kolloïdchemie
Co-promotor	Dr. A. de Keizer universitair docent bij de vakgroep Fysische en Kolloïdchemie

T. Mehrian Isfahany

THERMODYNAMICS OF THE ADSORPTION OF ORGANIC CATIONS ON KAOLINITE

Temperature Dependence and Calorimetry

Proefschift
ter verkrijging van de graad van doctor
in de landbouw- en millieuwetenschappen
op gezag van de rector magnificus
dr. H.C. van der Plas
in het openbaar te verdedigen
op dinsdag 20 october 1992
des namiddags te vier uur in de Aula
van de Landbouwuniversiteit te Waginngen, Nederland

دل هر ذره ای که بشکافی
آفتابیش در میان بینی

A sun is hidden in the heart of any small particle (atom).

Hatef Isfahany; Philosopher, scientist and poet; lived in the 10th century.

Cover design and photography : Gert Buurman
Text processing advice : José Zeevat-van Hommelen

To: *my father*

For: *Iraj & Katy*

Stellingen

I

De aanwezigheid van een gemeenschappelijk snijpunt in isothermen, gemeten bij verschillende zoutconcentraties, bewijst dat organische kationen met hun ladingscentrum in een vlak dicht bij het oppervlak adsorberen, maar buiten dat adsorptie vlak is de dubbellaag puur diffuus.
Dit proefschrift, hoofdstukken 4 en 5.

II

Het is logischer om de kritische hemimicelconcentratie te definieren via de concentratie van de zeepmoleculen aan het oppervlak dan via de concentratie in de bulk.

III

De drijvende krachten voor de fysische adsorptie van kationogene zepen aan kaoliniet zijn de directe aantrekking tussen de zeepmoleculen en het tegenovergesteld geladen oppervlak van kaoliniet, en de onderlinge wisselwerking tussen de hydrofobe staarten van de zeepmoleculen.
Dit proefschrift, hoofdstuk 5.

IV

De aanwezigheid van een maximum in de curven van de adsorptie als functie van de temperatuur bewijst dat de enthalpie van de vorming van een tweede laag van zeepmolekulen aan kaoliniet van de teken verandert. Daarom is het adsorptieproces in de tweede laag vergelijkbaar met dat van de micelvorming.
Dit proefschrift, hoofdstuk 5.

V

Kalorimetrische resultaten, gemeten of bij één temperatuur of over een beperkt temperatuursgebied, leveren nauwelijks een bijdrage tot een beter begrip van het adsorptiemechanisme.
Hoofdstuk 6, dit proefschrift.

VI

Propachlor, een pesticide, adsorbeert noch aan kaoliniet noch aan montmorilloniet.

VII

De zilver-thioureum methode is niet van toepassing voor de kationen-uitwisselingskappaciteit bepaling van deeltjes met veel variabele lading.

VIII

Plaatselijke verzuring van kalkhoudende gronden in kweepeer boomgaarden is een effectieve en goedkope manier om ijzerchlorose te verlichten.

M. Kalbasi; N. Manuchehri & F. Filsoof; *J. Plant Nutrition* vol. 9 , 1001-1007, 1986.

IX

Vaak is het frustrerend om in een engels-nederlands woordenboek een preciese vertaling voor wetenschappelijke termen te vinden. Zo kan men kiezen tussen een onpartijdig, neutraal, onverschilling, nogal slecht of onbelangrijk electrolyt voor het engelse "*indifferent electrolyte*".

X

Een goede elasticiteit is niet alleen wenselijk voor de schoonheid en gezondheid van de mens maar ook voor ruimteveren

XI

Alleen amfifiele mensen kunnen zich in een ander continent thuisvoelen.

Chapter 3: accepted by *Colloids Surfaces*
Chapter 4: partly published in *Colloids Surfaces*, **1990**, *51*, 339-357.
Chapter 5: published in *Langmuir*, **1991**, *7*, 3094-3098.
Chapter 6: submitted to *Colloids Surfaces*

CONTENTS

CHAPTER 1

Introduction

1.1 General

The interaction of small organic compounds with soil constituents has academic interest and is important for practice. As to the agricultural aspects, this relevance ranges from disciplines as different as plant nutrition, plant protection and environmental science. The solid phases of soils consist of inorganic and organic compounds. It is generally accepted that colloidal clay and humic acid constituents are the most active sorbents for organic molecules in the soil system. Other components, like oxides are also capable of adsorbing amounts of organic sorptives, but their surface areas are relatively low, so that they may be considered as indifferent particles compared with the clays and organic compounds with much larger surface areas. The clay mineral-organic complexes are of fundamental significance in the field of agriculture. For instance, transport and exchange processes that are vital for the uptake of nutrients through root fibrils of plants depend critically on the clay-water interaction and the effects of organic substances on these processes.

The main reason for the present study has been the environmental aspect which in these days obtains a great deal of attention. The exponential growth of the application of additives to natural soil systems confronts us with the ensuing problem of soil pollution which sooner or later leads to water contamination, one of the problems caused by industrialization. Concern with ground water contamination by organic chemicals added to soils or disposed in industrial wastes has prompted numerous investigations into their reactions and movements in soils, and has been recently reviewed by Sawhney and Brown[1].

The study of the interaction of organic molecules with mineral soil constituents is relatively young, starting in the early 1940's. This is mainly due to the lack of information about clay mineralogy[2]. The crystallinity of clay minerals is accepted since the mid 1930's. Because of the application of improved spectroscopic techniques, such as infrared

spectroscopy in conjunction with classical X-ray diffractometry to clay morphology, the knowledge about clay crystallography has strongly developed[2,3]. The importance of clay-organic systems for agriculture and a variety of industries has been the main reason for the growth of the published work in this field in the 1950's. During the last decades various groups of workers have become interested in the theoretical and experimental aspects of the interactions between clays and organic compounds[4]. Attention has been paid to elucidation of the complex mechanisms of interaction between these soil constituents and biocidal compounds such as herbicides and pesticides.

Notwithstanding the considerable progress made in understanding the behaviour of organic molecules at soil interfaces, still many gaps remain in our knowledge of the nature of the interactions between clays and organic adsorptives. This requires further research. Because of the complexity of soils, such studies are unlikely to provide basic information on the interactions responsible for the accumulation of soil particles, although the results are directly applicable under field conditions.

In this thesis we are interested in background problems and therefore prefer to work with model systems, i.e. systems resembling those occurring in nature but which are much better defined. In particular we have studied the adsorption of simple organic molecules, surfactants, on a clay mineral. A practically important feature of simple surfactants is that they are more soluble in aqueous media than most pesticides and herbicides. This enables us to use a wider concentration range. The objective has been to achieve a better understanding of the driving forces of the adsorption process, as to provide a first fundamental step to later investigations into more complex systems.

1.2 Structure and Properties of the Adsorbent

Much work on the fundamentals of the adsorption of both organic and inorganic cations on oxide materials has already been done, see e.g. references 5-9. Oxides are the most simple and well-defined constituents of the solid phase of soils and have been rather extensively studied in contrast to the study of the fundamentals of adsorption on clays.

Clay minerals are the major components of many soils and strongly influence their fertility. They also are basic raw materials in the production of building materials and are used in paper-making, enhanced oil recovery and many other industries. Clay minerals are known for their adsorption properties. The adsorption of foreign molecules and the retention of water at elevated temperature or at low vapour pressure reflect the presence of surface forces. Moreover, interparticle forces between clay minerals are strongly related to the rheological properties of clay-water mixtures[10].

In principle clays are layered aluminosilicates whose layers are built of either a Si-centred tetrahedron layer or an octahedron Al-centred one (Si/Al). Kaolinite is such an aluminiumsilicate whit a 1:1 layer structure, whose structural unit consists of one tetrahedral and one octahedral sheet. A 2:1 clay (e.g. montmorillonite) has a structural unit made of two tetrahedral and one octahedral sheet in the following order: Si/Al/Si. The asymmetric structure of kaolinite makes the growing of the particles possible by development of hydrogen bonds between octahedral and tetrahedral groups of two unit structures. Because of their symmetric structure this possibility is absent for the 2:1 clays. The multilayer structure of kaolinite reflects its low cation exchange capacity (CEC), and its relatively low surface area of about 10-20 m^2 per gram[11]. This surface area is about 50 times less than that of the single layer clays. It indicates that in one individual particle there are some 40 layers per platelet; the thickness is about 30 nm (compared with a thickness of 1 nm for single layer swelling clays). Kaolinite particles are hexagonal crystals. The kaolinite surface is more heterogeneous than 2:1 clays and its surface charge consists of a variable and a constant contribution. Having a rather small surface area, some apparent surface properties assigned to kaolinite are virtually dominated by trace of impurities of 2:1 clays.

We have given priority to kaolinite because its surface characteristics are in between those of oxides and 2:1 clay minerals. The negative charge on the basal planes, due to isomorphic substitution, is independent on pH. Therefore, in the region below the point of zero charge of the edges (epzc), basal faces are negatively charged but the edges positively. As a result, different degrees of "self coagulation" of kaolinites can be observed with changing pH. See Figure 1.

In studying an adsorption phenomenon, detailed information about the physico-chemical properties of the adsorbent is essential. Therefore, Chapter 2 will be devoted to determining the characteristics of our kaolinite sample. We will use various techniques to obtain physical and chemical information about the kaolinite-water interface. As our kaolinite sample is not contaminated with 2:1 clays, it is very likely that our data will apply generally to 1:1 clay minerals. One of the most important parameters in developing a quantitative picture of the surface is the surface charge. In oxides the surface charge can be absolutely defined if a point of zero charge (pzc) can be established. Such a pzc is usually obtained as the common intersection point of a series of acid–base titrations at different electrolyte levels. An isoelectric point (iep) can be detected using electrophoresis or another electrokinetic technique. From the pzc and the iep quantitative information about the surface charge under different conditions can be obtained. For a pristine oxide surface the iep and the pzc coincide. As far as the surface charge is concerned, clay minerals have heterogeneous surfaces. The edges resemble oxides, their surface charge density is pH-dependent and to them a pzc can be assigned. However, their plates carry a negative charge originating from the isomorphic substitution which is pH independent. As mentioned before, in 1:1 clays, including kaolinite, the contribution of the edges to the total surface charge is relatively large i.e. it has a low specific surface area with a substantial edge/plate ratio.

In Chapter 2 potentiometric acid-base titrations of Li-, Na- and Cs-kaolinite will be performed (at a safe pH range to avoid structural deterioration) and the results combined with electrokinetic measurements. The influence of the temperature on the adsorption of protons on our homo-ionic kaolinites will be also studied. All of this is meant to obtain insight into the surface charge of the clay. More specifically, the main purpose has been to obtain the ratio between the variable and constant charge of the kaolinite.

Figure 1. *Electron micrograph of Sigma Na-kaolinite, card-house structures are observable.*

1.3 Properties of the Adsorptive

The adsorptives emphasized in our work will be dodecylpyridinium chloride (DPC) and dodecyltrimethylammonium bromide (DTAB), two cationic surfactants. The term *cationic surfactant* refers to compounds containing at least one hydrophobic long chain group usually derived from either a fatty acid or petrochemical sources, and a positively charged hydrophilic head group. In general, surfactant molecules possess a dualistic character; they have a hydrophilic (water-loving) and a hydrophobic (water-fleeing) part. Many typical physico-chemical properties and numerous practical applications are based on the tendency of the nonpolar groups to avoid contact with water whereas the polar group tends to be strongly hydrated. In the adsorption of surfactants at a solid-liquid interface this amphiphilic nature is reflected. It is particularly interesting to try to discriminate between the contributions of the hydrophilic and hydrophobic parts to the adsorption. About 65 years ago it was observed that a number of physico-chemical properties of surfactant solutions may show a typical strong concentration dependence[12,13]. From such observations, which by now are known to apply to a large number of macroscopic and microscopic quantities, the concept of a critical micelle concentration (cmc) has evolved. At low

surfactant concentrations many physico-chemical properties indicate that there is no appreciable aggregation of the surfactant. At the cmc, these properties change suddenly which indicates that an extensive association to large aggregates is commencing. The driving force for micellization is *hydrophobic bonding.*

Association of ionic surfactant molecules, however, is accompanied by the creation of forces opposing the hydrophobic bonding. In the case of (cat)ionic surfactants, the repulsive force originates from the head group electrostatic repulsion. The balance between repulsive and attractive forces, which are coupled to specific regions in the molecule, leads to directional bonding and, therefore, to the formation of aggregates of a finite size and fixed shape. The tendency of such molecules to aggregate sometimes results in a superequivalent adsorption on oppositely charged surfaces.

There is a vast number of papers available on surfactant aggregation and the form of micelles. However, the temperature dependence of the form and size of the micelles and the possibility of their reformation are underexposed topics. The work of Ikeda[14] and Nusselder and Engberts[15-17] are the most recent ones dealing with this issue.

In Chapter 3 the thermodynamics of the micellization of DPC will be treated. This includes a discussion of the hydrophobic and hydrophilic contributions to the Gibbs energy of micellization and to the micellization enthalpy. The effect of one CH_2 group will be estimated by studying the thermodynamics of cationic surfactants with different chain lengths. Our results will be compared with those in the literature to obtain information about the contributions of the head groups and the counterions.

1.4 Adsorption of cationic surfactants on charged kaolinite surfaces

In Chapter 4 we consider the adsorption of two cationic surfactants with a dodecyl tail, one with a pyridinium and the other with a trimethylammonium head group, on Na-kaolinite. The key factors are: (a) the interaction of the cationic head group with the charged sites on the surface, (b) the interaction of the apolar chain with the surface, (c) association of adsorbed surfactant molecules. The last contribution varies

with increasing adsorption of amphiphilic molecules on a hydrophilic surface, because the adsorption enhances the hydrophobicity of the surface. It means that the adsorbed molecules act as centres for the aggregation at the interface. Phenomenologically this process is similar to micelle formation. Depending on the experimental pH and the epzc, different interactions between the kaolinite surface and the surfactant molecules are expected. At pH < epzc, where the edges are positively charged, electrostatic attraction exists between the plates carrying a negative charge. Then, adsorption on the edges is less probable due to the electrostatic repulsion. Therefore, the surfactant may adsorb on the plates by an exchange process in the diffuse layer or specifically in the Stern layer. At pH > epzc the edges become negative and it is possible that extra adsorption sites become available for the positively charged surfactant molecules. Since kaolinite is generally a hydrophilic particle, the interaction between the surfactant tails and the surface of kaolinite is not that important at low surfactant concentrations.

To discriminate between the adsorption of surfactants on the edges and plates, the influences of indifferent electrolyte, the surface potential and the variation of the relative surface charge in the presence of the surfactant will be studied. These results, in combination with the information to be obtained in Chapter 2, help to disentangle the contributions of basal planes and edges of kaolinite to the adsorption.

An additional issue is whether the adsorption of surfactant on kaolinite particles gives rise to a charge reversal of the adsorbent. To study this phenomenon in our system electrokinetic techniques will be used. In this way, some useful information is expected especially about the possibilities of the formation of surfactant aggregates at the interface.

A useful method to study the thermodynamics of adsorption is by investigation of the temperature dependence of the adsorption isotherms, from which the isosteric adsorption enthalpy can be calculated. Chapter 5 deals with such measurements for positive surfactant ions onto oppositely charged hydrophobic and hydrophilic surfaces. Since the kaolinite surface has a relatively hydrophilic nature, we shall compare the results of our systems (Na-kaolinite/DPC and Na-kaolinite/DTAB) with those of trimethylammonium nitrate on AgI, which is a hydrophobic substance, to

see how the hydrophobicity of an interface influences the driving forces for adsorption. At this stage we shall also try to distinguish between the electrostatic and non-electrostatic forces involved in the adsorption process.

We extend our study of the thermodynamic parameters of adsorption by doing direct isothermal microcalorimetric measurements. Microcalorimetry enables the determination of the enthalpy of interaction between the clay mineral and organic compounds. The measured enthalpy is made up from the following contributions: (i) electrostatic attraction between the negatively charged surface and the oppositely charged surfactant head group. If the adsorption takes place through exchange with the kaolinite counterions in the diffuse double layer, the adsorption enthalpy is expected to be small or zero. However, specific adsorption (in the Stern layer) has an exothermic enthalpic contribution. (ii) When the adsorption has locally developed to attain charge reversal, the repulsion between the charged head groups gives rise to an endothermic contribution to the adsorption enthalpy. (iii) If association between hydrophobic tails is important in the adsorption process, then a temperature dependent contribution typical for hydrophobic bonding must be present in the total adsorption enthalpy.

When a clay suspension is titrated by a concentrated surfactant solution in which c>cmc (post-micellar concentration), the total measured heat is the sum of the enthalpies of the dilution and the adsorption. It will be shown that these contributions can be separated.

The measured integral enthalpy can indicate the main driving force(s) for the adsorption process, especially when the measurements are carried out at different temperatures and electrolyte concentrations.

Information that we obtain from such a combination of different techniques will generally provide important insights into the nature of the interactions responsible for the adsorption of surfactants on oppositely charged heterogeneous surfaces.

1.7 References

(1) Sawhney B. L., Brown K. In "*Reactions and Movements of Organic Chemicals in Soils*", Ed. Sawhney B. L. and Brown K.; Soil Sci. Soc. Amer. Special Publ.: **1989**, pp 474.

(2) Grim R. E. In " *Clay Mineralogy*"; McGraw-Hill: New York, Toronto, London, **1953**, pp 557

(3) Brown G. In "*X-ray Identification and Crystal Structure of Clay Minerals*"; *Ed.* Brown G.,; Mineral Society: London, **1961**; pp 544.

(4) Theng B. K .G. In " *The Chemistry of Clay Organic Reactions*"; John Wiley & Sons: New York Toronto, **1974**, pp 343

(5) Harrop R. *Surface Technology*, **1987**, *7*, 81-90.

(6) Bijsterbosch B. H. *J. Colloid Interface Sci*, **1974**, *47*, 186-198.

(7) Ter-Minassian-Saraga L. *Advan. Chem. Ser.*, **1964**, *43*, 232-240.

(8) Tadros Th. F. *Colloid Interface Sci.*, **1974**, *46*,, 528-540.

(9) Rupprecht H. *J. Pharm. Sci.*, **1972**, *61*, 700-706.

(10) Weyl W. A., Ormsby W. C. In "*Rheology-Theory and Applications*", Ed. Eirich F. R., Academic Press: New York, London, **1969**, Vol. 3, pp 249-297.

(11) Sposito G. In " *The Surface Chemistry of Soils*"; Oxford University Press and Clarendon Press: New York Oxford, **1984**, pp 234

(12) Ekwall P. *Acta. Acad. Abo.*, **1927**, *4*, 1-6.

(13) Jones E. C., Bury C. R. *Phil. Mag.*, **1927**, *4*, 841-845.

(14) Ikeda S. *Colloid Polymer Sci.*, **1991**, *269*, 49-53.

(15) Nusselder J. J., Engberts J. B. F. N. *J. Phys. Chem.*, **1989**, *93*, 6142-6145.

(16) Nusselder J. J., "*Surfactant Structure and Aggregation behaviour*", PhD Thesis, State Univ. Groningen, **1990.**

(17) Engberts J. B. F. N., Nusselder J. J. *Pure & Appl. Chem.*, **1990**, *62*, 47-55.

CHAPTER 2

Surface Charge of Homo-ionic Kaolinites

Abstract

The charge on the surface of homo-ionic kaolinites is studied as a function of pH and indifferent electrolyte concentration using potentiometric titration and electrophoretic techniques. From acid–base titrations it is concluded that exchange of bound protons does not only take place at the edges, but also at the plates. The effect of the nature of counterions (Li^+, Na^+, and Cs^+) is examined. No zero point for the total charge could be detected. The point of zero charge of the edges is around pH 6.7 for Li and Na-kaolinite and 6.0 for Cs-kaolinite showing that the Cs^+ ions are specifically adsorbed. From the temperature dependence of the ad(de)sorption of protons or hydroxyl groups on Na-kaolinite it is inferred that the process is enthalpically driven.

2.1 Introduction

2.1.1 Properties of the clay mineral kaolinite

2.1.1.1 Crystal structure

Kaolinite is an aluminium silicate with a 1:1 layer of which the repeating unit structure consists of one tetrahedral and one octahedral sheet as is shown in Figure 1. In the tetrahedral sheet the silicon atoms are coordinated with four oxygen atoms. The oxygen atoms are located on the corners of a regular tetrahedron with a silicon atom in the centre. Each (individual) tetrahedron is linked with neighbouring tetrahedra by sharing three corners each. The fourth corners all point in a direction perpendicular to the sheet. In these sheets a hexagonal hole is present in the centre of each six oxygen atoms. In the octahedral sheet aluminium atoms are coordinated with six oxygen atoms or OH groups which are

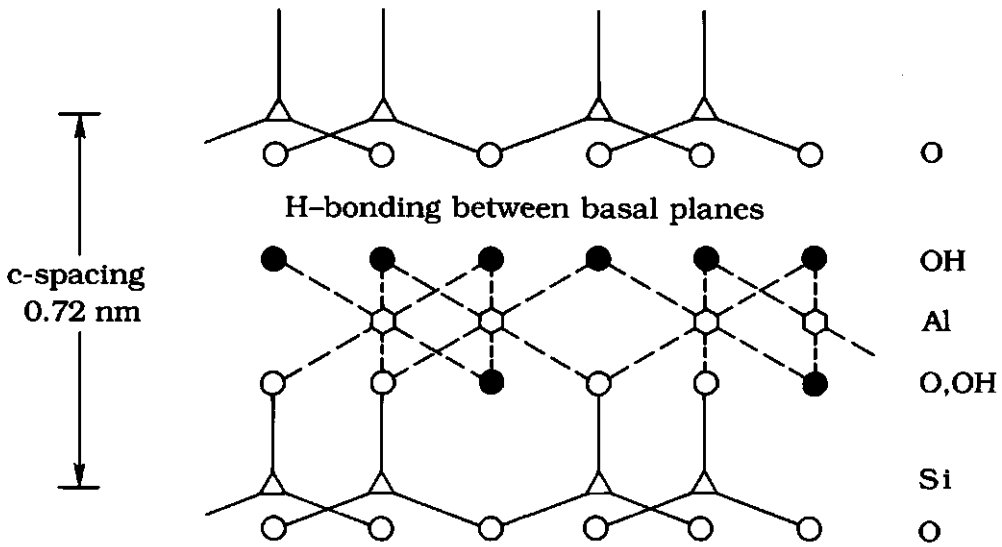

Figure 1. *Schematic structure of the repeating unit of kaolinite clay.*

located around the Al atom with their centres on the corners of a regular octahedron. The matching symmetry of the alumina and the silica sheet allows the sharing of oxygen atoms between the two. The combination of these two sheets is called a unit layer. Each unit layer repeats itself in a lateral direction. The c-spacing in kaolinite is about 0.72 nm.

Kaolinite is known as a non–swelling clay. Microscopically, kaolinite differs from swelling clays in that the platelets are multilayered and the exchangeable compensating cations are confined to the external surfaces. The multilayer structure of kaolinite is due to the asymmetry of the unit structure, such that the silicon and aluminium containing sheets are strongly bounded together through hydrogen bonding. Consequently, there is only a limited capacity for moisture absorption and swelling[1]. This also reflects its low cation exchange capacity (CEC) of some tens of μmoles g^{-1}, (in this text we refer to the "CEC" as amount of exchanged-monovalent-ions) and the low surface area of about 10-20 m^2 per gram, which is about 50 times less than that of single layer clays[2]. It indicates that some 40 layers per platelet of a total thickness of 30 nm exist in one individual particle (compare with a thickness of 1 nm for single layer swelling clays). Having a rather small specific surface area, the observed

surface properties of kaolinite are very sensitive to trace of impurities of 2:1 clays.

2.1.1.2 Isomorphic Substitution

As follows from Figure 1 an ideal kaolinite layer is electrically neutral but in reality it carries a small negative charge due to a small amount of isomorphic substitution[1,3-7]. This isomorphic substitution has taken place during the formation of the clay because the Si/Al ratio was not exactly stoichiometric. Replacement was crystallographically accepted because of the similar size of the replacing ions. Si atoms in the tetrahedral sheets have been exchanged with Al and Fe, and/or Al in the octahedral sheets with Fe, Ti, Mg or Mn. The isomorphic substitution in kaolinite is small compared to that in 2:1 clays. Hofmann et al.[8] proposed that the exchange sites are located only on the tetrahedral surface of the kaolinite crystal. This concept with its implication for the surface and colloid chemistry of kaolinite has subsequently been supported by results of electro-optical studies[9,10].

Elemental analysis is not sufficiently sensitive to prove or disprove the isomorphic substitution in kaolinite clays. If only one Si^{4+} out of every 400 in the silica sheets were substituted by Al^{3+}, the net negative charge would be as high as 30 μmole g^{-1}. Such limited substitution does not measurably alter the overall chemical composition of kaolinite.

The deficit of positive charge is mostly compensated by so-called counterions adsorbed on the surface of the particles mostly Na^+, K^+, Ca^{2+} and Mg^{2+}. If Al^{3+} is the major counterion, the negative permanent surface charge on the kaolinite can be mistakenly attributed to a pH-dependent, oxide-like charge[11]. This problem can be minimized by special treatments to remove Al^{3+} ions from the surface[6]. To detect the presence of 2:1 clay impurities the results of BET (N_2) gas adsorption is more sensitive than the X-ray patterns, since in the latter, amounts of <5% of 2:1 clays may escape detection[5]. According to Lim and co-workers[5] a BET surface area of 10-15 m^2 g^{-1} is an indication of a *2:1-clay-free* kaolinite.

2.1.1.3 Surface Charge of Kaolinite

From the structural point of view, kaolinite particles expose different crystal faces on which, in a polar (aqueous) media, electrical double layers are developed, which differ both in sign and magnitude of the (local) surface potential. It is well known that the edge surfaces of kaolinite particles differ in their structural and electrochemical properties from the platelet surfaces. In other words the overall surface charge of kaolinite is always made up of two contributions. The charge of the platelets, originating from isomorphic substitution, is always negative in sign and is responsible for the small but measurable CEC of kaolinite persisting under acidic condition. The charge on the edges, is caused by the dissociation of H^+/OH^- from the Si–O(H) or Al–OH groups. Historically, the experiment of Thiessen[12] to establish the charge of the kaolinite edges is worth mentioning here. He mixed a kaolinite suspension and a negatively charged gold sol and made an electron micrograph from the mixture. It appeared that the gold particles were adsorbed on the positively charged edges. The sign and the magnitude of the charge on the edges is pH dependent and is often referred to as the variable charge. Consequently, different modes of particle–particle interaction can occur at different pH or electrolyte environments. The electrostatic interactions between edges and faces are important in the rheology of kaolinite suspensions. With respect to the structure of kaolinite, Van Olphen[1] reported that the rheological properties agree with face-to-face aggregation dominating as soon as edge-to-face links are weakened by small concentrations of salt. However, Rand and Malton[13-15] stated that face-to-face aggregation only exists at high salt concentrations, otherwise the structure is edge-to-face and edge-to-edge. Lockhart[16] suggested that an edge-to-edge and edge-to-face association structure results from face-to-face aggregation of multilayer clay platelets with microscopic dimensions similar to the individual particle sizes, though much smaller than is suggested by the macroscopic sedimentation rates. The macroscopic structure is probably closer to a microporous "honey-comb" than a macroscopic "capillary" system.

The total (surface) charge of kaolinite (Q_{total}), (in Coulombs), consists of a variable contribution of edges (Q_{var}) and a permanent contribution of the plates (Q_{perm}).

$$Q_{total} = Q_{var} + Q_{perm} \quad (1)$$

The surface charge density of the edges (in Coulombs/m^2) is:

$$\sigma^0_{var} = Q_{var} / A_{edge} \quad (2)$$

and the surface charge density of the plates is:

$$\sigma^0_{perm} = Q_{perm} / A_{plate} \quad (3)$$

The symbol A refers to the surface area.

The averaged surface charge density (σ^0) in Coulombs/m^2 is then:

$$\sigma^0_{total} \equiv Q_{total} / A_{total} \quad (4)$$

or:

$$\sigma^0_{total} = \frac{\sigma^0_{perm} A_{plate} + \sigma^0_{var} A_{edge}}{A_{plate} + A_{edge}} \quad (5)$$

The (conventional) surface charge density is related to a measured quantity called *cation* or *anion exchange capacity* (CEC and AEC). The CEC or AEC can be obtained according to the Schofield method[3] or a similar procedure. In these methods the cations and anions which originally exist at the adsorbed phase are exchanged with a probe electrolyte. The measured amount depends on the type and concentration of electrolyte and on the pH of the solution, due to the exchange at the platelets and at the edges. Therefore, the sum of CEC and AEC can have different values at different conditions. In this chapter we use Γ_i^+ and Γ_i^- for CEC and AEC respectively, expressed in μmole g^{-1}. (Often the CEC and the AEC are expressed in centimoles per kilogram clay.) The CEC of kaolinite is rather low, in the order of 80 μmole g^{-1} of which 95% is variable according to Brady[17], 50 μmole g^{-1} according to Thomas and Hargrove[18] and 100 μmole g^{-1} according to Schofield[3]. Gonzalez et al.[19] determined the acidic centres of the kaolinite surface by n-butylamine neutralization. They found 54 μmole acidic centres per g of clay. Given the low surface

area for kaolinite even a small amount of isomorphic substitution results in a high total surface charge density. In this respect the kaolinite surface is considered as a highly-charged hydrophilic surface[20], since the (averaged) $\sigma^0_{total} \geq 10\text{-}12\ \mu C\ cm^{-2}$. The fact that different kaolinite particles show different CEC values is attributed to differences in the degree of crystallinity and the presence of impurities, particularly montmorillonite.

2.1.1.4 Changes in the Surface Properties of Kaolinite

Different pretreatments and preparation procedures can have significant effects on the surface properties of kaolinite.

(a) Dehydroxylation occurs at high temperature (T~400°C)[21,22].

(b) Ageing of the particles in acidic media or any other long time treatments of clay at extremely low pH values results within a few hours in a dissolution of clay particles, release of aluminium from the clay lattice, and eventually conversion of the H-clay to Al-M-clay[23]. Siracusa and Somasundaran[24] measured the Al content of a (Georgia) kaolinite supernatant after the particles had been treated with HCl. After 72 h, at pH 4.0, the dissolved aluminium was in the order of 10^{-4} mol/l, but it was only 10^{-6} mol/l at pH 5.0. Other investigators[7] found on US kaolinite, a dissolution of 0.7 and 0.3 mmole g^{-1} extracted at pH 3 or 5.3 respectively.

(c) Coating the surface with sesquioxides increases the buffer capacity of the particles but decreases the CEC. Further sesquioxide coatings add to the pH-dependent charge of kaolinite, resulting in a shift of the pzc towards the pzc of the coating material[25]. The iron and aluminium (hydrous) oxide coated kaolinite showed a pzc of 6.8 and <3 respectively.

(d) The minerals of the kaolin group have been traditionally classified as non-expandable clays. However, potassium ions and certain organic molecules, which have a certain size to fit into the hexagonal holes between the oxygen atoms in the tetrahedral sheets, can expand the kaolinite crystals[26]. Experimental reports are available on the penetration of certain molecules into the interlayer of kaolinite[27], like:

(i) Salts of organic acids of low molecular weight e. g. acetates.

(ii) Compounds with a strong tendency of hydrogen bond formation such as urea.
(iii) Molecules having a high dipole moment such as pyridine-oxide.
(iv) Molecules combining two or more above mentioned characteristics such as ammonium acetate.
The intercalation can increase the basal space from 0.72 to more than 1.0 nm[28].

2.1.1.5 Point of Zero Charge (pzc) of Kaolinite

According to the International Union of Pure and Applied Chemistry, (IUPAC)[29], the pzc of an oxide is the value of the negative logarithm of the activity in bulk of the charge determining ions when the surface charge is zero. For a pure oxide therefore:

$$\sigma^0_{total} = \sigma^0_{var} \equiv F(\Gamma_{H^+} - \Gamma_{OH^-})/a_{total} \qquad (6)$$

which at the pzc becomes:

$$\sigma^0_{total} = 0 \qquad (7)$$

The surface charge of clays is a determining factor for their colloidal properties. The sign and the magnitude of the surface charge of kaolinite depends on the pH. Due to the differences in the charging mechanism of the faces and the edges different points of zero charge are defined. The equilibrium potentiometric titration method has been employed to determine the pzc of kaolinite.

Even for a system containing a pure oxide there are some problems involved in the determination of the pzc from acid–base titrations. The common intersection point of charge–pH curves at different electrolyte concentrations was shown to depend on the concentration of specifically adsorbing ions in the system[30]. In other words the titrations must be performed in the presence of a real *indifferent* electrolyte. As we will show later there are even more problems involved when the above mentioned method is used to estimate a pzc for kaolinite.

Due to the operational problems in measuring the pzc of heterogeneous charged surfaces, an absolute definition does not exist. Probably this is the reason that in the literature different authors define pzc's slightly differently. According to Sposito[31], the pzc is the pH at which the total charge of the particles σ^0_{total} vanishes, the point of zero net proton charge (pznpc) is the pH value where σ^0_{var} is zero, the point of zero salt effect (pzse) is the common intersection point of σ_{H^+/OH^-}(/pH) curves at different electrolyte concentrations and finally the point of zero net charge (pznc) is the pH at which CEC = AEC[11].

The isoelectric point (iep) is defined by the IUPAC[29] as follows. A surface is at its iep if its electrokinetic charge (σ^{ek}) is zero. In the case of oxides therefore it is the pH at which the electrophoretic mobility is zero. In the heterogeneous kaolinite surface, even in the absence of specific adsorption, the iep may be (slightly) different from the pzc due to the different electrokinetic effect of the edges and the faces if oppositely charged.

In the literature there are acid-base titrations as early as in 1920's of which many are done either on H-clay or carried out at very low pH values. Different (controversial) pzc's are reported[32]. In fact the controversy is not surprising because of the significant effects of impurities (mainly 2:1 clays and oxides) and different pretreatments as mentioned earlier. Generally speaking the point of zero charge of the edges is found between 5 and 8[4].

The different behaviour of Cs^+ ions from that of NH_4^+, K^+ or Ca^{2+} with the kaolinite interface is noted. Lim et al.[5] reported that Cs^+ can even penetrate between the interlayer of kaolinite. They studied the exchange of Cs^+ by crude kaolins, and they found that Cs^+ adsorbed in greater amounts than K^+ or Ca^{2+}. The Cs^+ retention vs. replacement by NH_4^+ as compared with that by Ca^{2+} indicates that Cs^+ can penetrate further into the XY plane wedges of the mica/vermiculite than can NH_4^+ or K^+ or Ca^{2+}. Kaolins with a low intercalation index (high intercalation disorder, e.g., fireclay) fix much Cs^+ against replacement by NH_4^+ or K^+.

An oversimplified picture of kaolinite as a mixture of two oxides SiO_2 with a low pzc ($2 < pzc < 3$) and Al_2O_3 with a rather high pzc ($7.8 < pzc < 9$) fails to be perfect, since the pzc's of the two above mentioned oxides are not additive in their mixture[33].

2.1.1.6 Estimation of the Potential at the Kaolinite Surface

In general, on a homogeneous surface we can distinguish a surface potential ψ^0, a Stern layer potential ψ^d and a potential at the plane of shear ζ. Actually the first two potentials can only be derived from a theoretical model after estimation of the adsorbed charges at the surface. For kaolinite the potentials are in principle different at the edges and the faces. The ζ-potential is obtained from electrokinetic experiments e.g. electrophoresis.

The estimation of ζ-potential at a kaolinite surface is not an easy task. The calculation of the ζ-potential from electrophoretic mobilities requires a model of the electrical behaviour of the particles under shear. The heterogeneity of the surface with respect to the sign and amount of charge makes the use of simple models questionable. The Smoluchowski's equation applies to uniformly charged particles. Estimation of the ζ-potential requires a model for the electrical double layer. Each of Gouy or Gouy-Stern-Grahame model requires an estimation of charge density. The theory of O'Brien and White[34] considers in principle spherical particles. Recently Fair and Anderson[35] developed a model for ellipsoidal particles with unevenly distributed surface charges.

Ferris and Jepson[11] reviewed theories regarding face and edge properties of kaolinite. Since they find no evidence of constant cation adsorption at low pH they question the presence of isomorphic substitution. Weiss and Russow[10] recognised the fact that the two basal planes may be electrically different, the tetrahedral face being charged and the octahedral face uncharged. However, if their hypothesis is true it is probable that coagulation into doublets will occur in aqueous suspensions with the two uncharged planes in contact. Schofield and Samson[36] suggested that isomorphic substitution only occurred in the external layer of the crystals, so that a permanent charge resulted on the basal surfaces. Williams and Williams[4] have proposed an approximate method for the independent estimation of the ζ- potential of edge type surfaces. They assumed that the ζ-potential is some linear combination of the ζ-potentials of the edges of quartz and alumina. From $\zeta_{edges} = 0.5\ \zeta_{quarts} + 0.5\ \zeta_{alumina}$, they estimated the edge charge to be zero at pH ~ 6-7. Somasundaran and coworkers[37,38] studied the temperature dependence of the ζ-potentials of quartz at 20 and 40°C.

2.1.1.7 The Hydrophilic Character of a Kaolinite Surface

The hydrophilicity of a particle is defined as the affinity of water for the particle surface. One of the experimental ways to determine this affinity is by measuring the enthalpy of water adsorption. The interaction depends strongly on the type and structure of the particle and in the case of oxides and clays may range from a rather weak physical adsorption (0 - 40 kJ $mole^{-1}$) through hydrogen bonding on surface hydroxyls (50 - 70 kJ $mole^{-1}$) and ligand adsorption on Lewis acid centres (70 - 120 kJ $mole^{-1}$) to very strong chemisorption, dissociation of water molecules and hydroxyl formation (>120 kJ $mole^{-1}$). Since the heat of condensation of water is 44 kJ $mole^{-1}$, surfaces which exhibit lower heat of adsorption of water are called hydrophobic, the others hydrophilic[39,40].

Different clay types have different wetting characteristics. Talc has a completely hydrophobic surface whereas montmorillonite has a hydrophilic surface. Kaolinite is intermediate and is known as a *weakly hydrophilic clay*. The structure of kaolinite gives rise to both hydrophobic and hydrophilic surface patches. The weakly hydrophilic, almost hydrophobic character is caused by the cis-coordination of the silica tetrahedral sheet of which the external surface oxygens carry exchangeable cations. The hydrophilic nature is caused by surface OH groups of the octahedral layer [41]. The negative charge due to isomorphic substitution improves the hydrophilic nature.

Measuring the hydrophilicity of individual oxides is less complicated than that of mixed oxides and clays. The presence of two or more types of metal ions in a crystal may lead to the surface properties which are not simply an intermediate between those of pure oxides. Moreover, different crystal plates may have different hydrophobicities.

Water adsorption on oxides and clays has also been studied by measuring contact angles[42], adsorption isotherms of water vapour and by combination of the isotherm data with simultaneous microcalorimetric results[39,43]. In addition, infrared spectroscopy, dielectric measurements and NMR may serve to characterize water at the interface. Reviews have been published by Fobini and Texter[39,40]. Some investigators studied the adsorption of neutral nonpolar compounds in the vapour phase to assess the hydrophobicity of clays[44].

With respect to the hydrophilic character of a kaolinite clay, we can summarize the above mentioned investigations as follows.

The wetting contact angle for water drops on the dried surface of a pressed disk of kaolinite powder immersed in hydrocarbon liquids were measured. The smallest angle of 17.4 degrees belonged to the air/water interface. For kaolinite in hexane, octane, dodecane and cis-decaline the contact angles were 53.3, 56.9, 61.4 and 68.3 degrees respectively[42].

Conley and Althhoff[45] studied the various modes of H_2O evolution by thermogravimetric analysis. They used IR and NMR data to obtain information about the proton mobility at the crystal surfaces. Equilibrium moisture consisted of multilayer adsorption. Upon heating of aqueous kaolinite suspensions water is liberated. The liberated water consists of the following contributions: During the first stage, the outgassing temperature was above the boiling temperature and desorption became complete at about 125°C. Of the total adsorbed water 0.5% was mobile and loosely associated. However, the forces between these water molecules and the rest of the interface were stronger than van der Waals forces. At the second stage, a monolayer of water evolved which was highly ordered and far more energetically held than in the first stage. This kind of water was about 1% of the total amount of adsorbed water and was removed by outgassing only above 250°C. N_2, Ar etc. adsorption energetics differed markedly for the naked kaolinite surface than for the ordered H_2O layer. Another mode of water loss occurred between 275 and 300°C. The amount of water loss was very small (<0.05%) but it was held the most energetically, and therefore interpreted as being chemically bonded. At the fourth stage dehydroxylation occurred. The process began at about 325°C and was completed at about 700°C. The dehydroxylation process was the only process in the group which did not dominantly depend on the surface area (bulk process). The IR spectroscopy and NMR studies showed that during dehydroxylation, protons become mobile between silanol and aluminium octahedra producing exchangeable aluminium ions.

Because the adsorption of water on the kaolinite surface is an exothermic process[46] and a great amount of water adsorbs very tightly (almost irreversibly), we conclude that the kaolinite surface has a stronger hydrophilic nature.

2.1.2 Outline of this work

In this chapter we determined the characteristics of the kaolinite surface, mainly by microelectrophoresis measurements and potentiometric titrations.

As mentioned before, since the kaolinite surface is sensitive to some pretreatments and experimental conditions we avoided acid-washing and working at high temperatures. Thus extreme pH ranges are avoided as well.

The electrophoretic mobility data as a function of pH and salt concentration were measured. The reversibility of this against temperature was studied. Since the ζ-potential calculations require a proper model we avoid reporting our data in terms of ζ-potential, unless necessary.

A series of titration experiments were performed and the hysteresis between back and forward titration was studied, the electrolyte effects on the titrations measured. The effects of the nature of the different (monovalent) counterions on the H^+/OH^- ad(de)sorption were also studied.

The enthalpy of the H^+/OH^- ad(de)sorption ($\Delta_{ads(H^+/OH^-)}H_m$(isost)) was estimated from the temperature dependence of the charge/potential curves.

2.2 Experimental

2.2.1 Materials

A well crystallized sample of kaolinite (Sigma, St. Louis, USA, No.15-7375) has been used. The kaolinite particle diameter ranged between 0.1-4 μm, its CEC amounted to 57 μmole g^{-1} as measured by the silver-thiourea method[47] and 30 μmole g^{-1} according to the Schofield[3] (ammonium acetate) method. The contribution of Na^+ into the CEC was 98% and the remainder stemmed from Ca^{2+} and H^+. The BET (N_2) surface area of the kaolinite powder did not differ significantly from that of freeze-dried suspensions and amounted to 13 m^2 g^{-1}(equilibrium static method). The BET flow (dynamic) surface area was about 17 m^2 g^{-1}. The

particle density was 2488 kg m^{-3}. Hysteresis in the BET adsorption/desorption curves was negligible, indicating that the particles are not porous with respect to nitrogen gas (Figure 2). The argon adsorption experiments at 77 K (Figure 3) showed that 19.7% of the surface consisted of high energy sites assigned to the edges and the rest (80.3%) belonged to the lower energy sites attributed to be the basal surface area[48]. This results in an edge/basal surface ratio of 0.25. From the argon adsorption experiments (sensitive to the surface texture and rugosity) it was concluded that the lateral faces are heterogeneous whereas from nitrogen adsorption (more sensitive to the polar sites and chemical nature) the surface looked particularly homogeneous.

Elemental analysis was performed by Röntgen Fluorescence, melting the Na-kaolinite in $Li_2B_4O_7$, maximum temperature 1100°C. The structural formula calculated from elemental analysis was as follows: $Si_4Al_{3.9}Ti_{0.07}Fe_{0.03}Na_{0.02}(OH)_{8.5}O_{10.45}$. The loss of ignition at 900°C was 14.38%. Since as a result of the ignition process, the white colour of the

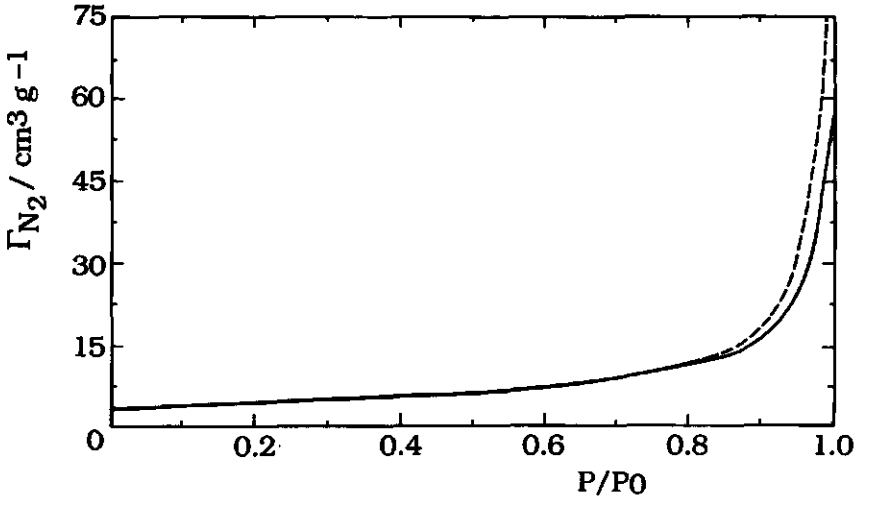

Figure 2. *Hysteresis of the BET-N_2 experiment. Solid curve is for adsorption and dashed curve for desorption.*

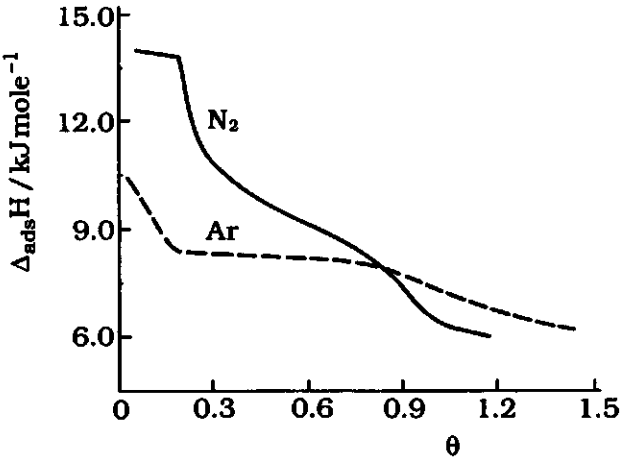

Figure 3. *Ar and N_2 adsorption measurements on kaolinite surface combined with the calorimetry of adsorption at 77 K.*

clay powder did not change there was no evidence for organic contaminations. Thus the loss of ignition was attributed to the water content, mainly present inside the interlayers. In the literature the structural formula of an *ideal* kaolinite is given as: $Si_4Al_4(OH)_8O_{10}$[21]. In our kaolinite sample, the elemental analysis gives 59 µmol total cations (mainly sodium) per gram which is close to the CEC measured by silver thiourea method.

The X-ray diffraction measurements showed a sharp peak at 0.72 nm attributed to the kaolinite crystals. Other peaks were almost not detectable, implying that no significant amounts of impurities exist. The diffraction peak was narrow and sharp, indicating that the particles are well-crystallized. The electron micrographs as presented in Figure 4 show hexagonal flat particles with well defined edges.

Freshly distilled water (using a Wagner & Münz instrument) has been boiled before use for 30 minutes to remove dissolved gases, especially CO_2. All other chemicals were of pro analyse quality and used without further purification.

2.2.2 Methods

2.2.2.1 Estimation of the kaolinite specific basal (a_{plate}) and specific lateral surface areas (a_{edges})

Using the electron micrographs (see Figure 4) the total surface area and that of the plates and the edges can be estimated[48]. Assuming that the kaolinite crystallites have a hexagonal shape, those two parameters can be related to the average diameter $\overline{D}$, the average height $\overline{h}$ and the density of the particles d, respectively. It is therefore possible to calculate a_{edge} and a_{plate} as follows:

$$a_{edge} = \frac{8}{\sqrt{3}.d.\overline{D}} \qquad (8)$$

$$a_{plate} = \frac{2}{d.\overline{h}} \qquad (9)$$

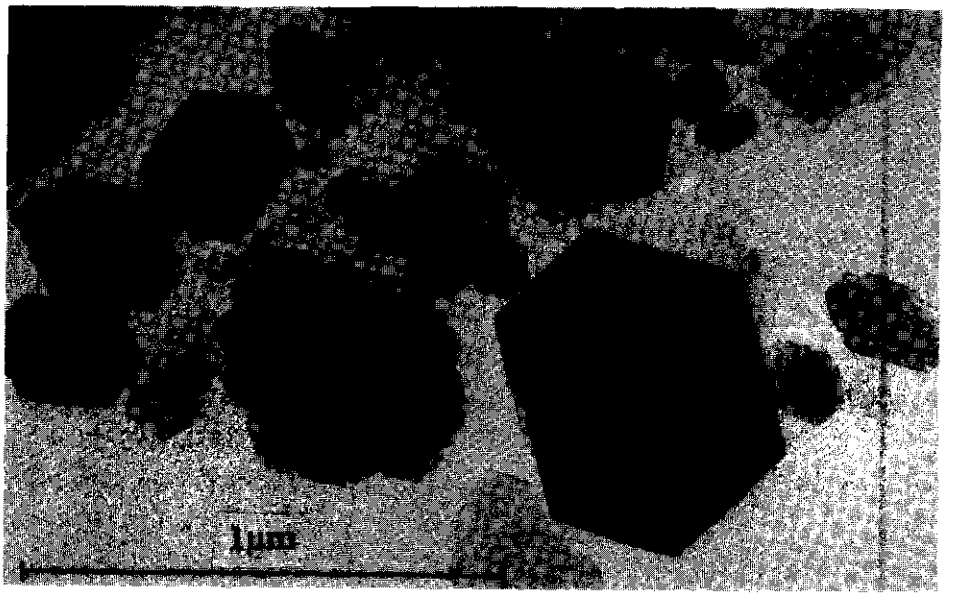

Figure 4. *Electron micrograph of Na-kaolinite.*

2.2.2.2 Preparation of a homo-ionic clay suspension

Homo-ionic clays are prepared according to the following procedure. A sample of 50 gram kaolinite was suspended in 2 dm^3 water, then the sample was shaken with a 1 M MCl (M = Li, Na or Cs) solution for 3 hours. After centrifuging, the supernatant was removed and the treatment repeated until the concentration of ions other than M^+ could not been detected by flame photometry. Always after the second treatment the supernatant was found to be free of unwanted cations, nevertheless we repeated the procedure three times. Then the clay was washed till the conductivity of the suspension was below that of $<10^{-4}$ M MCl. The M-clay fraction of <1μm was separated by settling during 31h. The suspension did not settle markedly during 3-4 days. After longer periods, 10 min. of shaking was enough time to redisperse the suspension. The pH of the suspension was 6.8±0.3 in all M-kaolinites and its final concentration was 11-13 g dm^{-3}. The BET surface area of the suspensions did not show a significant difference with that of the original powder. The suspensions were kept in the dark at a constant temperature of 20°C.

2.2.2.3 Electrophoresis

Electrophoretic mobilities were measured at different temperatures by a microelectrophoresis Zetasizer-II (Malvern, Instruments Ltd.) apparatus, unless stated otherwise.

The kaolinite suspension was diluted 25 times (volume ratio) in an MCl solution. The pH was adjusted using 0.05 M HCl or NaOH standard solutions. The suspension was then dispersed during 10 min. in an ultrasonic bath. Afterwards the electrophoretic mobility was measured.

2.2.2.4. Acid-base titrations

In order to use thermodynamic interpretations, we made an effort not only to perform the acid-base titrations under equilibrium conditions but also to choose experimental conditions such that structural deterioration was not significant during the experiment.

The automatic titration experiments were carried out using the procedure described by Fokkink et al.[49]. The titration cell was a thermostatted 500 ml double-walled pyrex glass vessel. To remove any trace of CO_2 a constant flow of pure N_2 was passed through the titration vessel from 15 hours before each titration up to the very end of the experiment. After about 12 hours of N_2 passage a constant cell potential was obtained. The Nernstian behaviour of the pH electrodes was examined by measuring standard buffers of pH 4, 7, 8 and 10.

A volume of a concentrated suspension of M-kaolinite, containing about 2.7 g of kaolinite was added to an MCl solution in the titration cell. The pH of the suspension was around 6.8±0.3 in all cases. The potential was sampled every minute under a non-stirring condition. Each single titration curve was made up of 25–30 experimental points. For each point the maximum equilibration time being between 4 and 70 minutes has been checked. After the first acid titration the hysteresis between two acid or two base titration curves was negligibly small, independent on the titration speed. However, a pronounced hysteresis effect was found (again independent on the titration speed) between the acid and the base titration curves. The maximum equilibrium time was set to 15 minutes. The maximum standard deviation amounted to 0.6 mV and the maximum drift was 0.02 mV/min. Equilibrium was controlled by a microcomputer. Since the clay surface properties are rather sensitive to extreme pH values our pH limits were 4.5 - 10.0. After completion of a given titration, the electrolyte level was raised by addition of dry MCl and the titration was carried out at the new electrolyte level. A blank titration was performed before and after each experiment under similar conditions as the clay titration.

A scanned titration curve was measured as follows. We started from the alkaline region. The starting pH value was ~10 and the final pH ~ 9.2. A series of acid/base/acid titration was carried out in this region. The same procedure was repeated within the pH ranges as is given in Table 1.

Dissolution of Na-kaolinite in acid media is examined by the following experiment. Different amounts of 0.05 M HCl were added to a clay suspension of the same concentration as used for the potentiometric

Table 1. *Starting and end points of the scanned potentiometric titration curves of Na-kaolinite, see Figure 11.*

Region	Begin pH	End pH
A-B	10.00	9.25
B-C	9.25	8.00
C-D-E	8.00	6.95
E-F-G-H	6.95	5.92
G-H-I-J-K	5.92	4.75

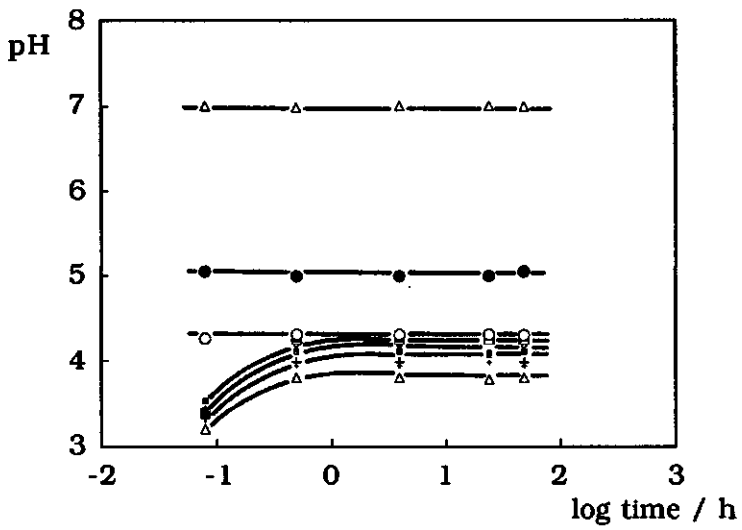

Figure 5. *pH change of Na-kaolinite as a function of time.*

titrations. The pH is measured as a function of time, as is shown in Figure 5.

In all cases of pH values less than 4.2 extra adsorption sites were formed. These extra sites came probably from the structural deterioration of the crystals[23]. More protons then adsorbed on the clay particles such that the pH increased to about 4 after a few hours. After that no significant pH change with time was observed. At pH values higher than

4.2 the change in the pH with time was of the order of experimental error (±0.1 unit).

In the acid-base titrations we obtained the depletion of protons by measuring the proton activity in the bulk and comparing that with the proton activity of a blank. The amount depleted per unit mass of M-kaolinite is therefore $(\Gamma_{H^+} - \Gamma_{OH^-})$. The relative (titration) specific surface charge of the particles due to the ad-(de)sorption of protons and/or hydroxyls is defined according to :

$$\Delta\sigma^0_{total} = \frac{F(\Gamma_{H^+} - \Gamma_{OH^-})}{a_{total}} \qquad (10)$$

The relative specific charge density is calculated from the potentiometric titrations data as follows:

$$\Delta\sigma^0_{total} = \frac{F\left((V.c)_{susp} - (V.c)_{bl}\right)}{ma_{total}} \qquad (11)$$

where V is the volume of referred titrant added, c is its concentration, subscripts (susp) and (bl) are referred to the suspension and the blank respectively, m is the weight of dry M-kaolinite and a_{total} is the (total) specific surface area. When we were interested in the charge density per unit of mass, we omitted a_{total} in (11).

The relative positions of the titration curves of each M-clay was determined in a similar batch experiment by increasing the indifferent electrolyte concentration at some initial pH value without addition of acid or base. Changes of pH due to the electrolyte addition were corrected by using the data obtained for a blank.

2.3 Results

2.3.1 Kaolinite Specific Surface Area, Edge/Plate Ratio

Different methods give different results for the total as well as the edge/plate ratio of kaolinite surface. From BET measurements the total surface area measured by N_2 was 13, whereas from the electron microscopy an a_{total} of 19.6 m^2/g was obtained. The a_{edge} was 20 and 41% from Ar adsorption calorimetry and electron microscopy, respectively.

2.3.2 Electrophoresis

A plot of the electrophoretic mobility U/X of Na-kaolinite as a function of pH is shown in Figure 6. The mobility decreases with pH especially at lower pH values. As we explained elsewhere[50], electrophoresis shows no isoelectric point (iep) in the pH range of 3–10. However, extrapolation to U/X = 0 indicates that the iep is near pH = 2. These results agree with earlier measurements on the same kaolinite[51].

The salt effect at two pH values is given in Figure 7. The value of U/X decreases with increasing electrolyte concentration. At electrolyte concentrations higher than a few hundredths of a molar, coagulation of the particles starts, making the results less reliable than those at lower concentrations, although this is not readily apparent from the experimental results.

The effect of temperature on U/X is shown in Figure 8. A measurement at 20°C was performed first, then at 40°C, finally the sample was kept at 60°C during a few hours and after cooling down to 20°C, the measurement was repeated. The value of U/X became significantly more negative upon increasing temperature. It appeared that heating the sample to 60°C has no influence on the results of the electrophoretic mobilities at 20°C. This indicates that the electrical properties are not irreversibly effected by a variation of the temperature, within our experimental temperature range. The effect of the temperature on the mobilities of quartz and Na-kaolinite is studied by Ramachandran and Somasundaran[38]. The mobilities are translated to ζ-potentials using the

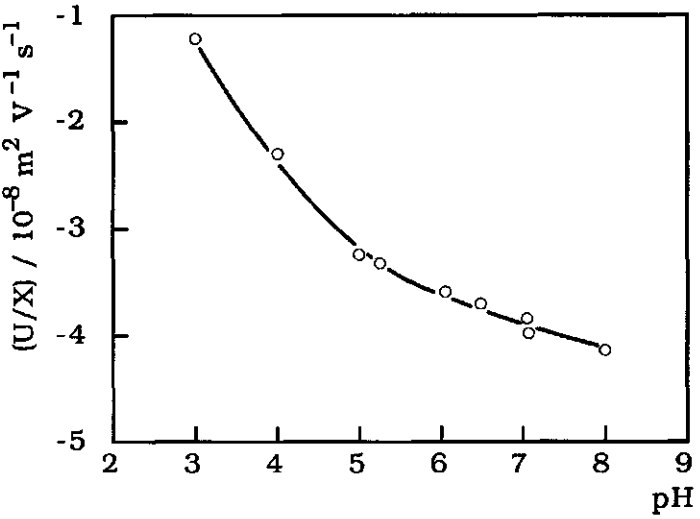

Figure 6. *Electrophoretic mobility of a Na-kaolinite suspension as a function of pH; T = 25°C, c_{NaCl} = 5 mM.*

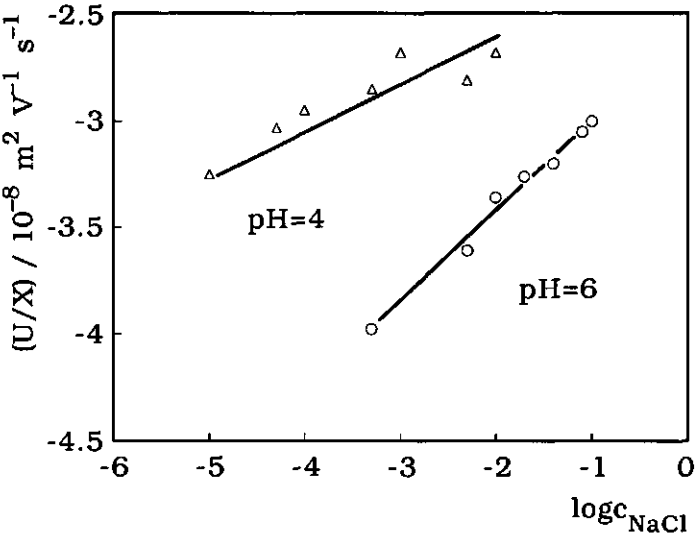

Figure 7. *Electrophoretic mobility of Na-kaolinite suspension as a function of NaCl concentration; T = 25°C, pH values are indicated.*

Helmoltz-Smoluchowski equation. The trend is similar to what we found, more negative mobility at a higher temperature. However the hysteresis that were present in their systems is absent in ours.

At a certain pH and electrolyte concentration the electrophoretic mobility of Cs-kaolinite is about17% less (negative) than that of Na-kaolinite as it is given in the Table 2.

Table 2. *Electrophoretic mobilities of M-kaolinite in ($10^{-8}V^{-1}m^2s^{-1}$), measured by Malvern Zetasizer III. T = 25°C, pH = 6.1.*

c_{salt} / mM	Na-kaolinite	Cs-kaolinite
0.5	–2.35	–2.00
5.0	–2.87	–2.39

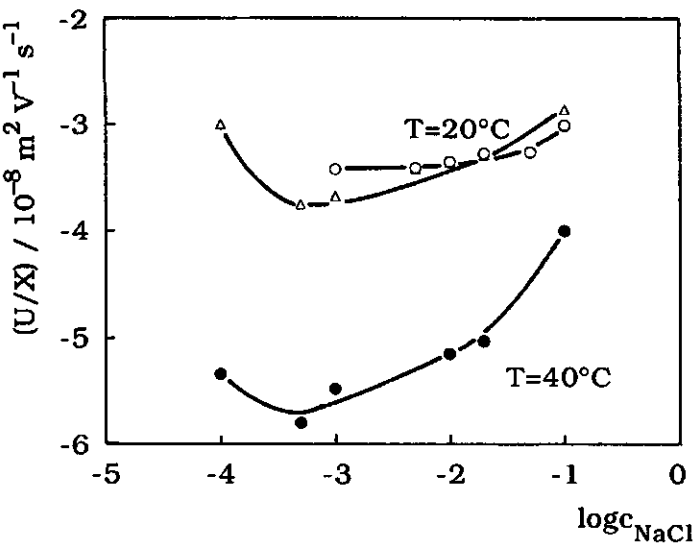

Figure 8. *Reversibility of electrophoretic mobilities of Na-kaolinite against temperature change. pH =5, Δ and O are the pre-warmed (60°C) and not pre-warmed samples respectively.*

2.3.3 Acid-base titrations of kaolinite

A typical example of a set of base titration curves for the blank and in the presence of kaolinite is given in Figure 9. The curves are well reproducible and hysteresis is absent within experimental error. For the acid titration curves we arrived at the same conclusion. However, there is always a constant hysteresis between back and forward titrations as is shown in Figure 10. This hysteresis appears to be hardly dependent on the indifferent electrolyte concentration.

To obtain more information on this phenomenon, a scanning titration has been performed (Figure 11). Obviously above pH=8 both back and forward titrations are hysteresis free. The hysteresis begins to appear at pH values below 8 and increases in the acid range. The maximum

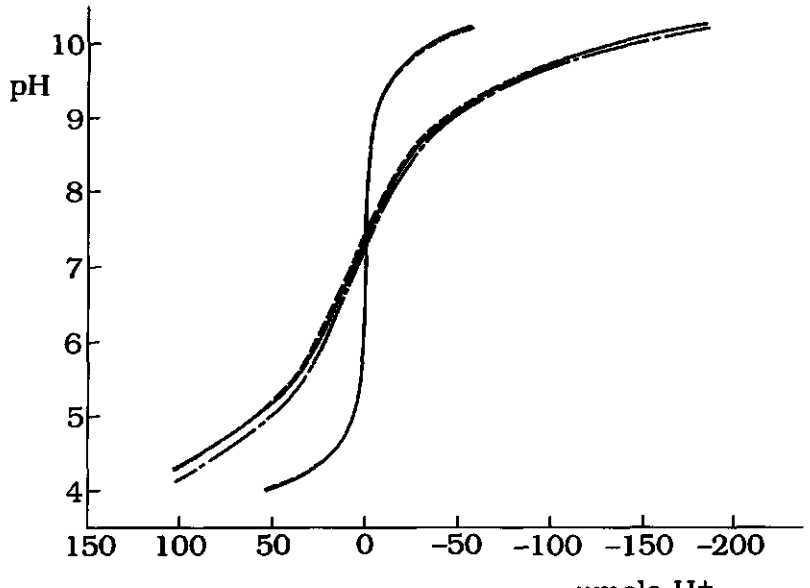

Figure 9. *Hysteresis of acid - base titration curves of the same nature, the equilibration time per each titration point in solid, dashed and stippled curves is 4, 15 and 70 minutes, respectively;* $m_{kaolinite}$ *= 2.7 g,* c_{NaCl} *= 20 mM and T = 20°C.*

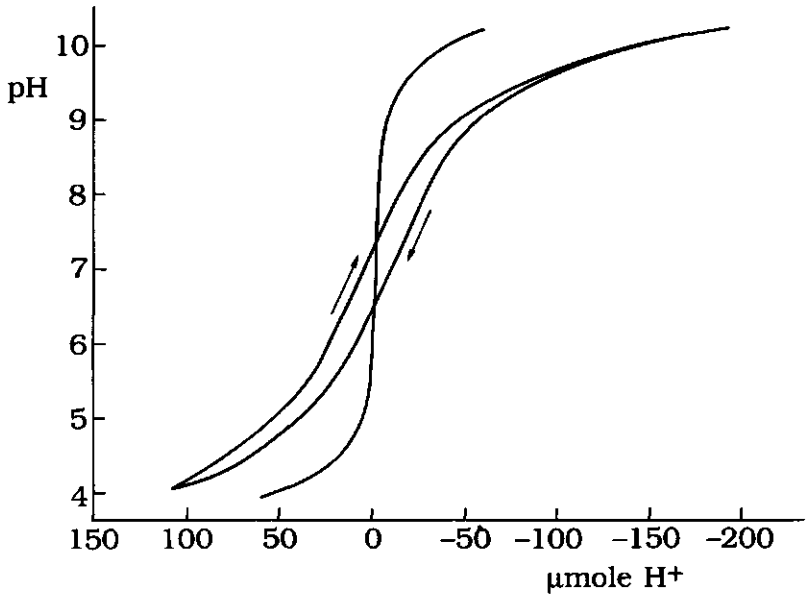

Figure 10. *Hysteresis of back-forward potentiometric titration curves.* c_{NaCl} *= 20 mM, T = 20°C,* $m_{kaolinite}$ *= 2.7 g. Arrows show the titration directions.*

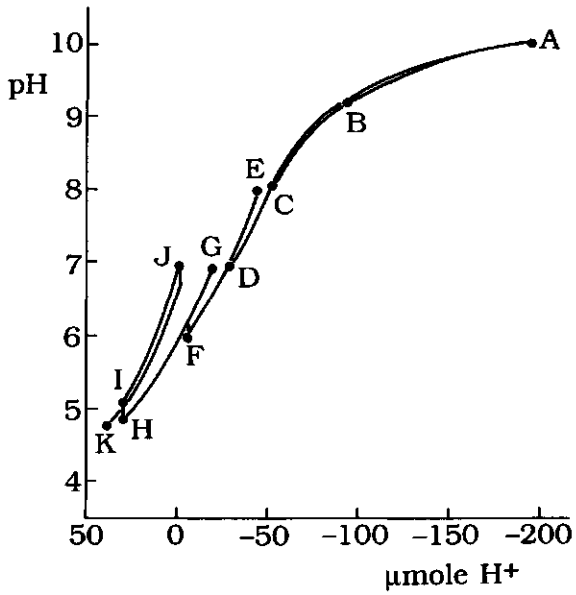

Figure 11. *Scanning curve, acid-base titration of Na-kaolinite at 20 mM NaCl;* $T = 20°C$ $m_{kaolinite}$ *= 2.7 g. See Table 1.*

hysteresis amounted to 6.3 μmole g^{-1} and is independent on the salt concentration.

The (relative) surface charge/pH curves at 20°C and three electrolyte concentrations are shown for Li- Na- and Cs-kaolinite in Figures 12a, 12b and 12c respectively. The relative surface charge ($\Delta_{H^+/OH^-}\sigma$) becomes more negative (depletion of protons or adsorption of hydroxyl groups) upon increasing electrolyte concentration. The curves do not show a common intersection point, but close to pH = 7 their is a minimum of the electrolyte effect. A similar result has been found for Birch Pit kaolinite[52] and for Ward's Scientific (uncovered) kaolinite clay API no.5[25].

In Figure 13a, 13b and 13c the effect of temperature on the $\Delta_{H^+/OH^-}\sigma$ of Na–kaolinite at 5, 20 and 100 mM NaCl, respectively, is presented. The adsorption of protons on Na-kaolinite decreases at all electrolyte concentrations showing that the adsorption process is exothermic.

2.4 Discussion

All evidence such as elemental analysis, BET experiments, X-ray patterns, electron micrographs and the shapes of the titration curves show that our kaolinite is not contaminated with impurities and is a good representative of a *kaolinite clay*.

The discrepancy of the surface areas measured by different methods is due to the different affinities of the adsorbates for the different adsorption sites of the clay surface. From our adsorption measurements of dodecylpyridinium chloride (DPC) and dodecyltrimethyl ammonium bromide (DTAB) as we will discuss in Chapters 4 and 5, we estimated a contribution of the edges to the total surface area of 35%. However, the proton adsorption measurements for M-kaolinite showed an average of about 55%. See Table 4.

The electrokinetic charge of the clay particles is negative over the whole pH range examined (See Figure 6). The same has been found for other kaolinites such as English China Clay[4] and Macon Georgia[53]. The majority of evidence[1,3,4] suggests that isomorphic substitution contributes significantly to the surface charge.

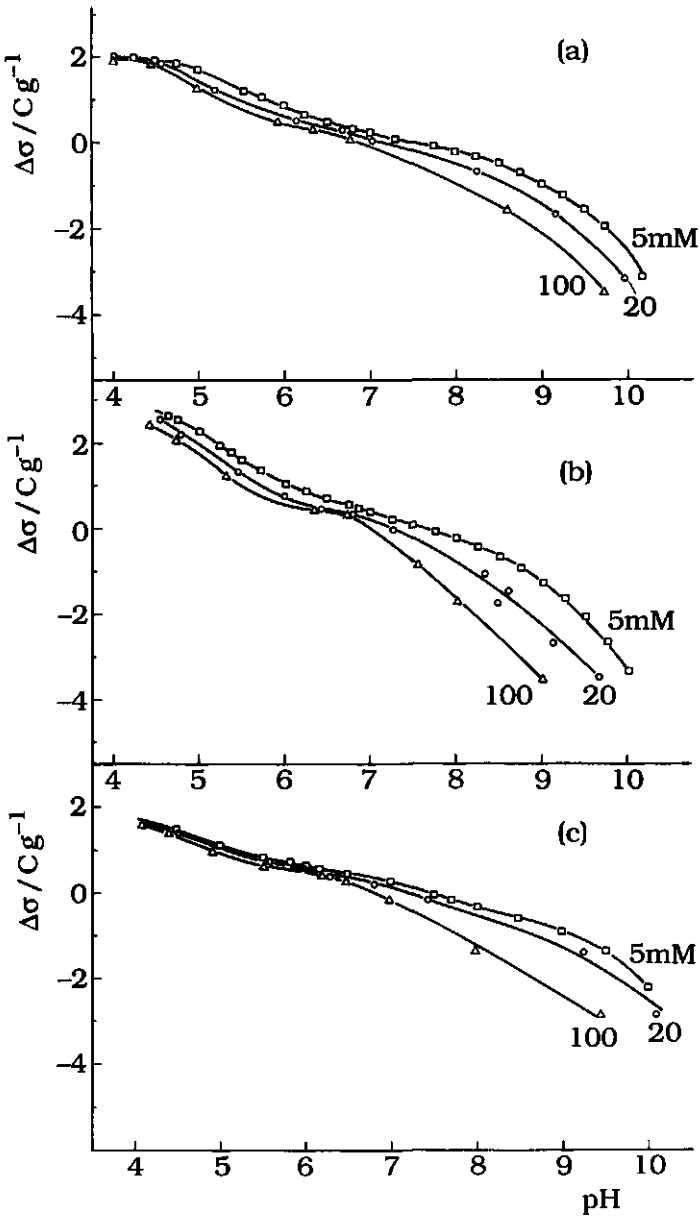

Figure 12. *Effect of the (indifferent) electrolyte concentration on the relative surface charge density of (a) Li-kaolinite, (b) Na-kaolinite and (c) Cs-kaolinite. T = 20°C.*

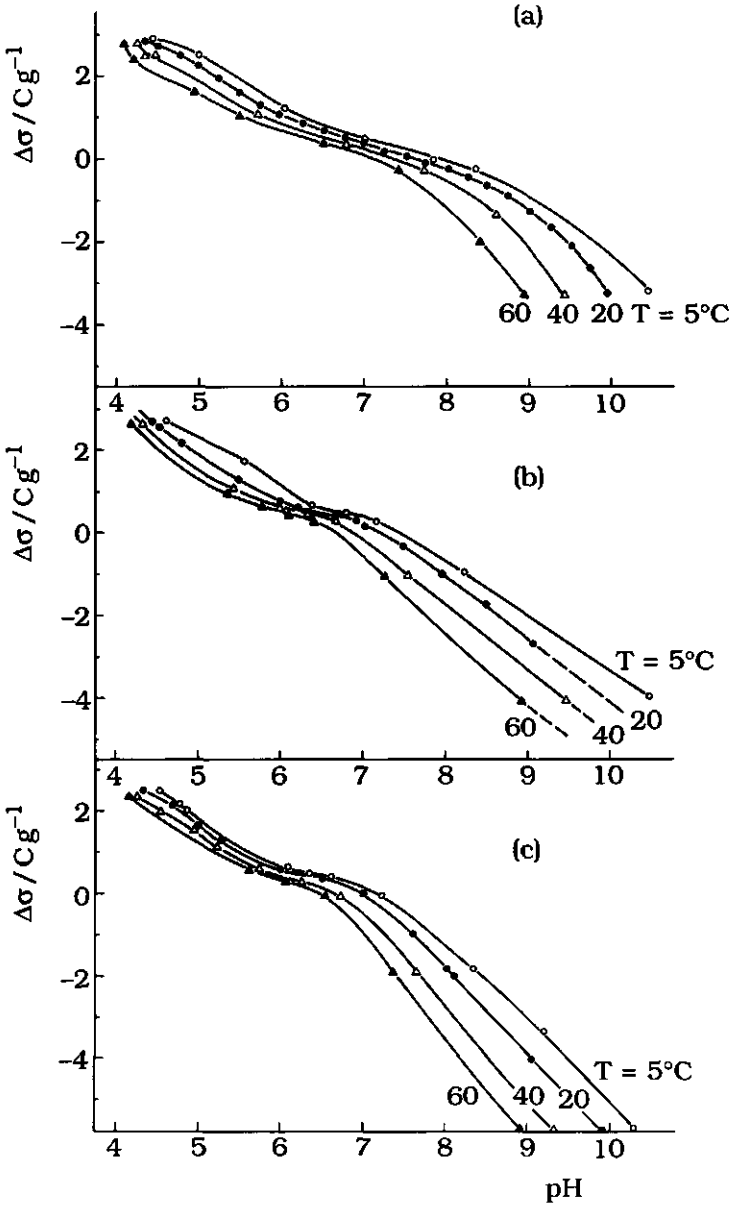

Figure 13. *Temperature dependence of the the relative charge-potential curves of Na-kaolinite (a) at 5, (b) 20 and (c) 100 mM NaCl.*

Since the mobility of Cs-kaolinite is less (negative) than that of Na-kaolinite, the Cs^+ is specifically adsorbed at the surface, resulting in a decrease in the negative surface charge (potential).

The use of potentiometric titrations to determine absolute charge-pH curves is subject to a number of problems. First of all, there is the hysteresis between acid and base titration curves mainly occurring in the acidic range (the maximum being 0.6 C/g). Neither the existence nor the extent of the hysteresis depends on the equilibrium time chosen (in the range of practical feasibility) for each titration point. Apparently this is not an "artifact" either, because there is no hysteresis between two curves of the same nature. The origin of this hysteresis effect is not completely clear. Since below pH 8 the edges of the particles become positively charged an electrostatic attraction between the edges and the negatively charged plates could lead to a "card-house" type of structure, see Figure 1 of Chapter 1. Due to the fact that the BET (N_2) surface area of the kaolinite powder did not differ significantly from that of the ultrasonically treated freeze-dried suspensions, the attraction is electrostatic and relatively strong. From the fact that hysteresis starts below pH 8, it can be speculated that in this region the attraction between the particles decreases the number of the proton adsorption sites. The formation and destruction of the card-house structure does not take place at the same pH value but both processes are somewhat "retarded". The fact that the hysteresis is hardly dependent on the salt concentration implies that the surface potential is probably only slightly affected by the electrolyte, whereas changing the pH has a much larger effect on the surface potential ψ^0.

The second problem is the determination of the absolute value of the surface charge, i.e. the estimation of the point of zero charge. The most striking feature of the charge–potential curves of kaolinite is the absence of a (common) intersection point for curves at different electrolyte concentrations. Above pH 7 the trend is similar to that for a negative oxide surface, i.e. the surface charge increases with increasing electrolyte concentration and the capacity (i.e. the derivative of the charge–pH curve) increases with increasing pH as in the Gouy–Chapman theory. Extrapolating this trend would lead to a common intersection point around pH 7. The explanation is that the oxide-like behaviour is due to the edges of the kaolinite clay. Above pH 7, the contribution of the faces

is negligible because protons do not contribute to the surface charge on the faces due to the fact that the proton concentration is negligible compared to other cations. Below pH 7 other processes than exchange at the edge sites take place. It is likely that specific adsorption of protons at the faces is not negligible any more at higher proton concentrations. However, if we increase the electrolyte concentration two processes take place simultaneously: an increase of proton adsorption at the edges due to the increased screening by the (indifferent) electrolyte and a decrease of proton adsorption at the faces due to exchange for the electrolyte cations. The latter effect is dominating so that at low pH values the surface charge becomes more negative with increasing electrolyte concentration.

It may be concluded that the point of zero charge of the edges (epzc) is around 7 in agreement with other evidence from literature. A more quantitative measure of the epzc is probably the inflection point of the charge–pH curves, which is the point where the second derivative is zero. This is in fact the pH at which the first derivative of the charge potential curves changes sign as is the case of the pure oxides. These values are given in Table 3. The epzc's are independent on the salt level but only in one case on the nature of the cation. The averaged epzc in the presence of CsCl is about 0.7 lower than for LiCl and NaCl indicating the stronger specific adsorption of Cs[54].

To obtain some semiquantitative information about the ad-(de-)sorption of protons/hydroxyl groups on the variable and specifically exchange sites, we chose arbitrarily two pH values symmetrical with respect to the epzc's and considered the change in proton adsorption for an increase of the electrolyte concentration from 5 to 100 mM. When pH >> epzc:

$$\Delta\Gamma^{\text{total}}_{(H^+-OH^-)} = \left|\Delta\Gamma^{\text{exch.}}_{(H^+-OH^-)}\right| \qquad (12)$$

and at pH < epzc:

$$\Delta\Gamma^{\text{total}}_{(H^+-OH^-)} = \left|\Delta\Gamma^{\text{exch.}}_{(H^+-OH^-)}\right| + \Delta\Gamma^{\text{edge}}_{(H^+-OH^-)} \qquad (13)$$

Table 3. *The pzc of the edges of kaolinite particles (defined as the inflection point in charge potential curves) for LiCl, NaCl and CsCl at three concentrations. T = 20 °C.*

salt	c_{salt} /mM	pzc	Av. pzc
LiCl	5	7.00	
	20	6.55	6.70
	100	6.65	
NaCl	5	6.87	
	20	6.61	6.68
	100	6.55	
CsCl	5	6.00	
	20	6.00	5.99
	100	5.98	

Table 4. *Column 2 and 3: Charge difference in C/g between 5 mM and 100 mM salt, column 4 and 5: individual contribution of the plates and of the edges, column 6: percentage of exchange contribution. Data calculated from Figures 12a - 12c.*

counterion	$\Delta\sigma^0_{total}$ (epzc+1.5)	$\Delta\sigma^0_{total}$ (epzc−1.5)	$\Delta\sigma^0_{var}$	$\Delta\sigma^0_{perm}$	% plate
Li^+	0.45	0.95	0.95	1.40	59.6
Na^+	0.60	1.80	1.80	2.40	57.1
Cs^+	0.15	1.20	1.20	1.35	52.9

The results are presented in Table 4. From these results we infer that specific adsorption of protons on the faces contributes significantly to the total adsorption at low pH values.

The total change in the relative surface charge with pH in the presence of different ions of the lyotropic series follows from Figures 12a, 12b and 12c. The results are presented in Table 5.

Table 5. *Difference in the* $\Delta\sigma^0_{total}$ *of M-kaolinite;* c_S *= 5 mM, pH = 4.5-10.0.*

Clay-counterion	$\Delta\sigma^0_{total}$ /C g^{-1}
Li^+	4.4
Na^+	6.1
Cs^+	3.8

The behaviour of Na^+ and Li^+ are due to the effect of the size of their hydrated ions. Na^+ being smaller is able to approach the closer vicinity of the surface and results in an increase of $\Delta\sigma$ (negative charge). The behaviour of Cs^+ in this respect is not fully understood. The fact that $\Delta\sigma^0_{total}$ is less sensitive to the pH may be correlated with the specific adsorption of the Cs^+ ions on the plates which results in a decrease of the contribution of the edges in the $\Delta\sigma^0_{total}$. This conclusion is confirmed at least qualitatively by the comparison of the mobility of Cs-kaolinite with that of Na-kaolinite, see Table 2.

From the titration curves, a rough estimation of the total proton adsorption at pH = 4 gives an average value of 2 C/g. An extrapolation to pH = 2, which is probably the pzc of kaolinite, shows a value of around 5 C/g, total charge. Realizing that from the CEC (silver thiourea) a value of 5.5 C/g is obtained it follows that at pH 4 about half the surface charge is compensated by the adsorption of protons. The total charge estimated from the potentiometric titrations is not far from an estimation of the pzc around pH = 2.

We have estimated the isosteric molar enthalpy of the adsorption of protons on kaolinite at different temperatures and electrolyte concentrations using the van 't Hoff equation:

$$\left[\frac{\partial pH}{\partial(1/T)}\right]_{\sigma^0_{total},c_{NaCl}} = \frac{\Delta_{ads(total)}H_m(isost)}{2.303R} \qquad (14)$$

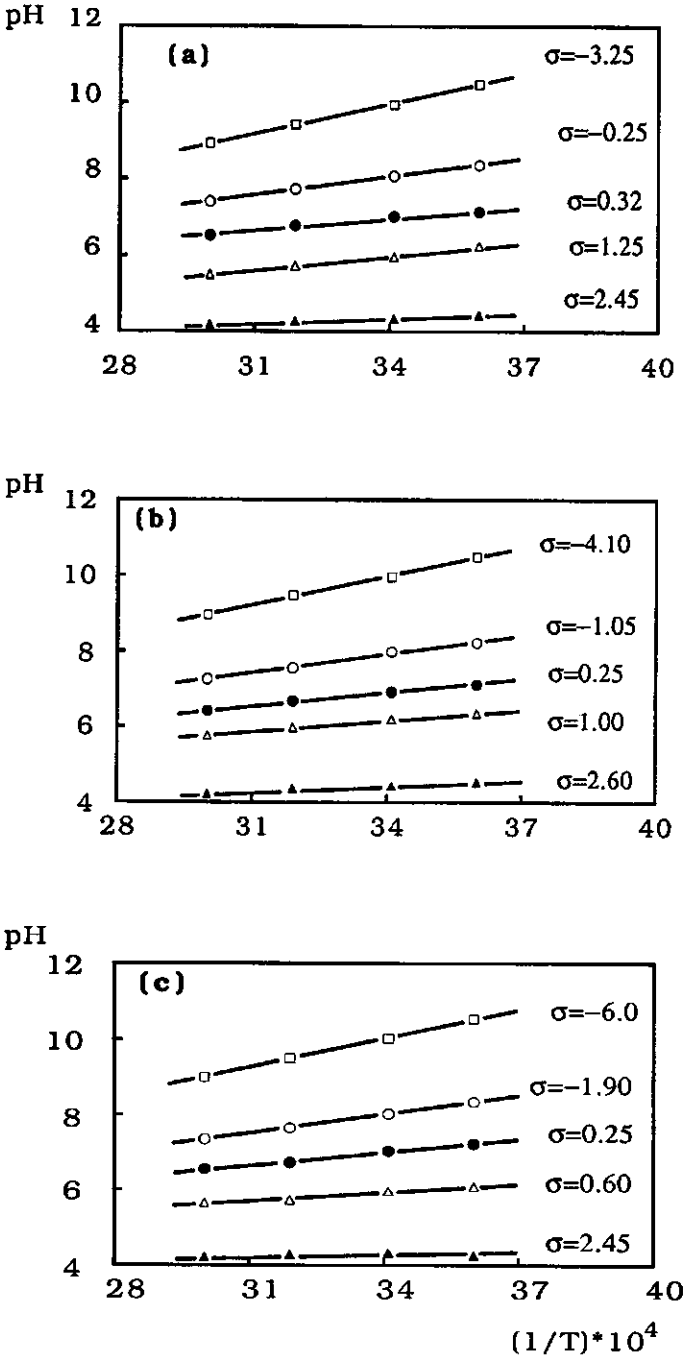

Figure 14. *pH/(1/T), at different relative* σ^0_{total}*, used for the estimation of proton adsorption enthalpy on Na-kaolinite. (a) at 5, (b) 20 and (c) 100 mM NaCl.*

Curves of pH against 1/T obtained from Figures 13a, 13b and 13c are presented in Figures 14a, 14b and 14c for 5, 20 and 100 mM NaCl, respectively. The pH is a linear function of 1/T, hence $\Delta_{ads(total)}H_m(isost)$ is not a function of T at a given σ^0_{total}. The enthalpies at 20°C calculated according to (14) are presented in Figure 15.

The enthalpies of proton adsorption in 20 mM NaCl, as a function of pH at different temperatures are shown in Figure 16. Similar results are obtained for 5 and 100 mM salt concentration. The enthalpies range from -10 kJ mole^{-1} at pH = 4 to -50 kJ mole^{-1} at pH = 10.

Three important conclusions are drawn. (a) Adsorption of protons onto the kaolinite surface is always an exothermic process. In other words the enthalpy contributes positively to the driving force. (b) The adsorption enthalpy increases progressively with increasing pH, i.e. as the surface becomes more negative. (c) The adsorption enthalpy does not depend on the electrolyte concentration. The latter two conclusions may seem contradictory with respect to the importance of contributions of electrostatic interactions on the adsorption enthalpy of protons. Probably, the surface potential is only slightly affected by the electrolyte, whereas changing the pH has a much larger effect on the surface potential ψ^0. This is in accordance with the electrokinetic results at different pH and electrolyte concentrations.

Fokkink et al.[49] have investigated the enthalpy of proton adsorption on rutile and hematite. They found an adsorption enthalpy of -17.6 kJ mole^{-1} and -36.3 kJ mole^{-1} for rutile and hematite, respectively. These values are also exothermic and in the same range as our values for kaolinite. Contrary to our results their enthalpies for proton adsorption on these well-defined Nernstian oxide surfaces are independent on both electrolyte concentration as well as the pH. Apparently the anomalous behaviour of the charge-pH curves of kaolinite is reflected in the non-ideal (oxide) behaviour of the enthalpies.

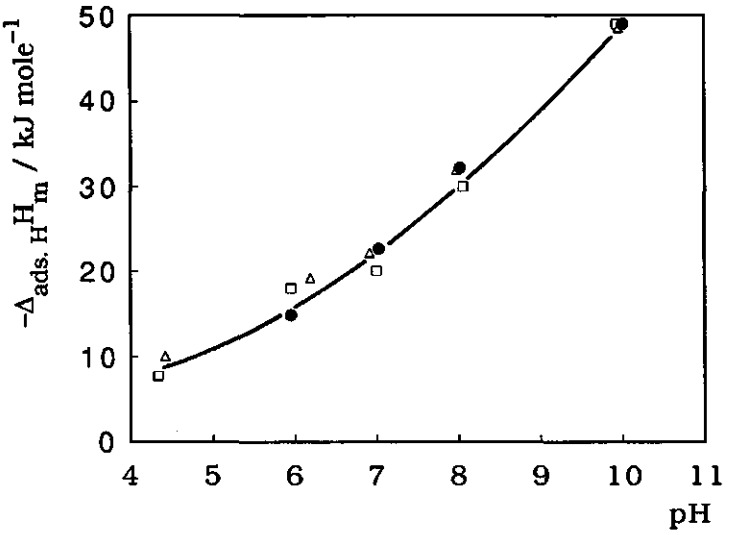

Figure 15. *Enthalpy of proton adsorption on Na-kaolinite as a function of pH; at □ 5, △ 20 and ● 100mM NaCl, T = 20°C.*

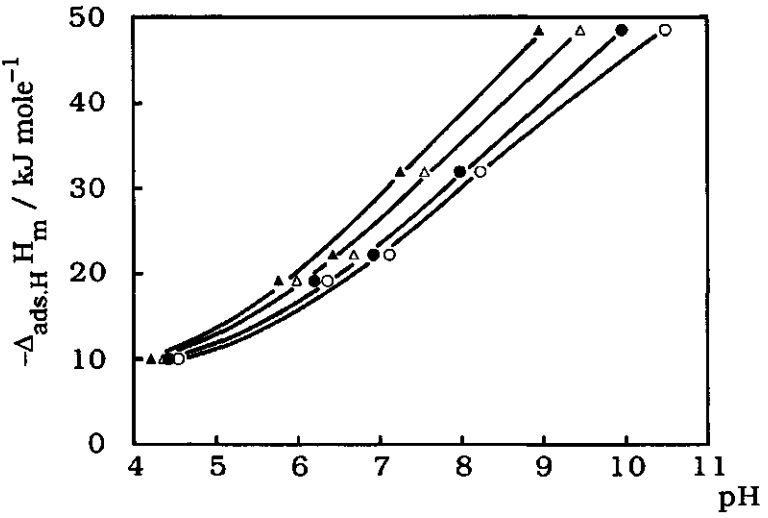

Figure 16. *Enthalpy of proton adsorption on Na-kaolinite as a function of pH; c_{NaCl} = 20 mM, at o 5, ● 20, △ 40 and ▲ 60°C.*

Comparison of our results with that of Fokkink et al.[49] leads to some interesting conclusions. The total enthalpy of the adsorption of protons on kaolinite can be separated into the contributions of Al- and Si-containing groups on the plates as well as on the edges. To get some semiquantitative information about the different contribution to the enthalpies at different pH values we averaged the enthalpies presented in the Figure 15 within four pH ranges. The results are presented in Table 6, together with $\Delta_{ads(total)}H_m(isost)$ of some oxides with the pzc's which are in these pH ranges. The similarity between the enthalpies of the proton adsorption on our kaolinite clay and on these oxides suggests that at different pH values one of the existing groups has a more important contribution to the total enthalpy. At pH > 8 the $\Delta_{ads(total)}H_m(isost)$ is similar to that of alumina, therefore the role of the Al-containing groups is more dominant. In the pH range of 5-7 the averaged enthalpy suggests that the groups on the edges are more important. At pH < 4 therefore the Si groups must have the dominant effect. It can be seen from the extrapolation of the curve presented in Figure 15 towards low pH values that the enthalpy of the adsorption of protons on silica surface would be roughly about 10 kJ $mole^{-1}$. Provided that one is aware of the approximations which are involved in the estimation of the $\Delta_{ads(total)}H_m(isost)$, a reasonably well qualitative information is obtained.

2.5 Conclusions

Various physico-chemical techniques such as X-ray diffractometry, electron microscopy, Ar/N_2 adsorption calorimetry and BET are used to characterize the surface. All evidence proves that our sample is very pure and especially 2:1 clay-free. Potentiometric titrations show that the clay surface in uncovered with any other oxide coatings[25].

Constant hysteresis observed between back- and forward potentiometric titrations approves the hetereogeneity of the surface charge and the possibility of edge-plate interactions resulting in a so called card-house packing. Combined electrophoresis measurements and

Table 6. *Comparison of the averaged enthalpies of the proton adsorption on Na-kaolinite with the enthalpies of the proton adsorption on some oxides. Column 3 is the enthalpy of proton adsorption on oxides from the reference mentioned in column 4, The values corresponding to alumina are calculated from the temperature dependence results of ref. 55, column 6 is the averaged enthalpies calculated using data presented in Figure 15. Enthalpies are in kJ mole^{-1}.*

Oxide	pzc	$\Delta_{ads(total)}H_m$(isost) oxide	ref.	pH (Fig. 15)	$\Delta_{ads(total)}H_m$(isost) (Fig. 15)
alumina	9.1	-24.9*	55	9-10	-42
hematite	8.7	-36.3	49	8-10	-37
rutile	5.7	-17.6	49	5-7	-15
silica	2-3	?		<4	(~ -10)

potentiometric titration data reveal information about the specification of a representative of 1:1 clay groups.

The ratio of the edge/plate surface area depends on the method used, being 0.35 from the DPC adsorption, 0.55 from potentiometric titration, 0.20 from Ar adsorption calorimetry and 0.41 from electron microscopy. The majority of evidence[1,3,4] suggests that isomorphic substitution contributes significantly to the surface charge. This is indeed the case for our kaolinite from which about 50% of the surface charge is caused by the isomorphic substitution (CEC measured by silver thiourea method[47] amounts to 57 μmole/g whereas CEC determined by ammonium acetate[3] is 30 μmole/g). The plates carrying the permanent charge are homogeneous but the edges, with the variable charge produced from the proton-selective functional groups, are more heterogeneous in nature.

In our experimental pH range, no point of zero charge for the entire particles has been detected either by electrophoresis measurements or by acid-base titrations. Extrapolation of the electrophoretic data gives an estimated pzc of 2. In the charge-potential curves, at different electrolyte concentrations, an inflection point is detected which is located in a region where the curves approach each other. This inflection point is attributed to the zero point of charge of the edges, being 6.7 for Li- and Na-kaolinite and 6.0 for Cs-kaolinite, implying more specific adsorption

of Cs^+. The relative change of the surface charge density of M-kaolinites corresponds well with the relative size of hydrated ions of Li and Na. Cs^+ deviates from this trend in a way that the relative surface charge of Cs-kaolinite is less sensitive to a pH change. We infer that this behaviour is due to the specific adsorption of Cs^+ at the plates. This conclusion is reinforced by the fact that the electrophoretic mobilities of Cs-kaolinite is less than that of Na-kaolinite.

Temperature dependence of the specific adsorption of protons on homo-ionic kaolinite shows that the process is enthalpically driven. The adsorption enthalpy increases drastically with increasing pH but it is hardly dependent on the electrolyte concentration. This suggests that the pH change has a more pronounced effect on the surface potential than that of the indifferent electrolyte. From the fact that electrophoretic mobilities change stronger with pH than with electrolyte concentration we come to the same conclusion. The proton adsorption enthalpies at each pH range show a qualitative similarity to that of oxides with similar pzc's.

2.6 Acknowledgments

The performance of X-ray measurements and elemental analysis by the Soil Science and Geology Department of Wageningen Agricultural University, and the nitrogen-argon-calorimetric adsorption measurements by Mr. Grillet (Centre de Microcalorimétrie Marseille) are highly appreciated.

2.7 References

(1) Van Olphen H. In " *An Introduction to Clay Colloid Chemistry*"; Wiley (Interscience): New York, **1977**.

(2) Sposito G. In " *The Surface Chemistry of Soils*"; Oxford University Press and Clarendon Press: New York Oxford, **1984**.

(3) Schofield R. K. *J. Soil*, **1949**, *1*, 1-8.

(4) Williams D. J. A., Williams K. P. *J. Colloid Interface Sci.*, **1978**, *65*, 79-87.

(5) Lim C. H., Jackson M. L., Koons R. D., Hemke P.A. *Clays and Clay Minerals*, **1980**, *28*, 223-229.

(6) Bolland M. D. A., Posner A. M., Quirk J. P. *Clays and Clay Minerals*, **1980**, *28*, 412-418.

(7) Bolland M. D. A., Posner A. M., Quirk J. P. *Aust. J. Soil Res.*, **1976**, *14*, 197-216.

(8) Hofmann U., Boehm H. P., Gromes W. *Z. Anorg. Allgem. Chem.*, **1961**, *308*, 143-154.

(9) Cashen G. H. *Trans. Faraday Soc.*, **1959**, *55*, 477-486.

(10) Weiss A., Russow J., Proceedings: *"Proc. Int. Clay Conf."*, Ed. Stockholm, **1963.**

(11) Ferris A. P., Jepson W. B. *J. Colloid Interface Sci.*, **1975**, *51*, 245-259.

(12) Thiessen P. A. *Z. Electrochem.*, **1942**, *48*, 675-681.

(13) Malton I. E., Rand B. *J. Colloid Interface Sci.*, **1977**, *60*, 331-339.

(14) Rand B., Malton I. E. *J. Colloid Interface Sci.*, **1977**, *60*, 308-320.

(15) Malton I. E., Rand B. *J. Colloid Interface Sci.*, **1977**, *60*, 320-330.

(16) Lockhart N. C. *J. Colloid Interface Sci.*, **1980**, *74*, 520-528.

(17) Brady N. C. In " *The Nature and Properties of Soils*"; Macmillan Publishing Company: New York, **1990**.

(18) Thomas G. W., Hagrove W. L. In " *Soil Acidity and Liming*"; Ed. Adams F.; American Society of Agronomy, Inc. Crop Science Society of America, Inc. Soil Science Society of America, Inc.: Madison Wisconsin, **1984**; Vol. 12, p 380.

(19) Gonzalez L., Marti P., Ibarra L. *British Polymer J.*, **1989**, *21*, 327-332.

(20) Ingram B.T., Ottewill R. H. In " *Adsorption of Cationic Surfactants at Interfaces*"; Ed. Rubingh B. N. and Holland P. M.; Marcel Dekker Inc.: New York and Basel, **1991**; p 87-140.

(21) Newman A. C. In " *Chemistry of Clays and Clay Minerals*"; **1989**.

(22) Torres Sanchez R. M., Aglietti E. F., Poto Lopez J. M. *Materials Chemistry and Physics*, **1988**, *20*, 27-38.

(23) Bolt G. H., Bruggenwert M. G. M., Kamphorst A. In "*Soil Chemistry. A Basic Element*", Ed. Bolt G. H. and Bruggenwert M. G. M.; Elsevier Scientific Publishing Company: Amsterdam - Oxford - New York, **1978**, Vol. A, pp 281.

(24) Siracusa P. A., Somasundaran P. *Colloids and Surfaces*, **1987**, *26*, 55-77.
(25) Hendershot W. H., Lavkulich L. M. *Soil Sci. Soc. Am. J.*, **1983**, *47*, 1252-60.
(26) Wada K. *Am. Mineralogist*, **1961**, *46*, 78-91.
(27) Weiss A., Thielepape W., Goring G., Proceedings: *"Int. Clay Conf."*, Jerusalem, **1966.**
(28) Theng B. K .G. In " *The Chemistry of Clay Organic Reactions"*; John Wiley & Sons: New York Toronto, **1974**.
(29) Lyklema J. *Pure & Appl. Chem.*, **1991**, *63*, 895-906.
(30) Lyklema J. *Chemistry and Industry*, **1987**, *2*, 741-47.
(31) Sposito G. *Soil Sci. Soc. Am. J*, **1981**, *45*, 292-297.
(32) Marshall C. E. In " *Soil Materials."*; Wiley: New York, **1964**.
(33) Tschapek M. T., Tscheichvili L., Wasowski C. *Clay Minerals*, **1974**, *10*, 219-229.
(34) O'Brien R. W., White L. R. *Farad. Trans. II*, **1987**, *74*, 1607-1626.
(35) Fair M. C., Anderson J. L. *J. Colloid Interface Sci.*, **1988**, *127*, 388-400.
(36) Schofield R. K., Samson H R. *Discuss. Faraday Soc.*, **1954**, *18*, 135-145.
(37) Somasundaran P., Kulkarni R. D. *J. Colloid Interface Sci.*, **1973**, *45*, 591-607.
(38) Ramachandran R., Somasundaran P. *Colloids and Surfaces*, **1986**, *21*, 355-369.
(39) Fobini B., Bolis V., Stone F. S. *Solid State Ionics*, **1989**, *32/33*, 258-269.
(40) Texter J., Klier K., Zettlemoyer A. C. *Prog. Surf. Membrane Sci.*, **1976**, *12*, 327-350.
(41) Forslind E., Jakobsson A. In " *Water: A Comprehensive Treatise"*; Ed. F. Franks; Plenum Press: New York, London, **1975**; Vol. 5, p 366.
(42) Janczuk B., Bialopiotrowicz T. *Clays Clay Minerals*, **1988**, *3*, 243-248.
(43) Partyka S., Rouquérol F., Rouquérol J. *J. Colloid Interface Sci.*, **1979**, *68*, 21-30.
(44) Sawhney B. L., Gent M. P. N. *Clays Clay Minerals*, **1990**, *38*, 14-20.

(45) Conley R. F., Althoff A. C. *J. Colloid Interface Sci.*, **1971**, *37*, 186-194.

(46) Fripiat J., Cases J., Francois M., Letellier M. *J. Colloid Interface Sci.*, **1982**, *89*, 378-400.

(47) Chabra R., Pleysier J., Cremers A. *Proc. Intern. Clay Conf*, **1975**, 439.

(48) Cases J. M., Cunin P.; Poinsignon C. ; Yvon J. *Clay Minerals*, **1986**, *21*, 55-68.

(49) Fokkink L. G. J.; de Keizer A., Lyklema J. *J. Colloid Interface Sci.*, **1989**, *127*., 116-131.

(50) Mehrian T., de Keizer A., Lyklema J. *Langmuir*, **1991**, *7*, 3094-3098.

(51) de Keizer A. *Progr. Colloid Polym Sci.*, **1990**, *83*, 118-126.

(52) Verburg K., *personal communication*, **1989.**

(53) Cases J. M., Touret-Poinsignon Ch., Vestier D. *C. R. Acad., Ser. C.*, **1971**, *272*, 728-731.

(54) Lyklema, J. *J. Colloid Interface Sci.*, **1984**, *99*, 109-117.

(55) Tewari P. H., McLean A. W. *J. Colloid Interface Sci.*, **1972**, 40, 267-272.

CHAPTER 3

Thermodynamics of Micellization of n-Alkylpyridinium Chlorides.

Abstract

The effect of temperature on the thermodynamic parameters of micellization of a homologous series of n-alkylpyridinium chlorides has been studied by isothermal microcalorimetry. The decyl-, dodecyl- and tetradecyl-compounds were studied both in water and in 0.1 M NaCl in the temperature range of 6 - 60°C.

Enthalpies and entropies of micellization are strongly temperature dependent whereas there exists only a weak temperature dependence for the standard Gibbs energies. With increasing temperature the micellization process changes from endothermic to exothermic, indicating the importance of hydrophobic bonding. The transition temperature decreases with increasing chain length which is interpreted in terms of a relation between the temperature and the enthalpy per CH_2. It is concluded by extrapolation that this enthalpy was zero at a temperature of about −12°C.

Enthalpies of micelle formation calculated from the temperature dependence of the critical micelle concentrations compare satisfactorily with those obtained microcalorimetrically.

3.1 Introduction

During the last two decades the study of the thermodynamics of micellization of ionic and non-ionic surfactants has obtained much attention[1-20]. Studies involving calorimetry and the temperature dependence have proven powerful to elucidate the mechanism of the micellization process. A better insight into this process also contributes to a better understanding of many other physical and biological processes such as adsorption of surfactants, solubilization and membrane formation.

Probably the most characteristic aspect of the temperature dependence of the thermodynamic parameters of micellization is that, as a rule, the enthalpy decreases strongly with temperature (i.e. becomes more exothermic), whereas the standard Gibbs energy, obtained from the position of the critical micelle concentration (cmc), is hardly or only moderately temperature dependent. Apparently, there exists an enthalpy-entropy compensation[10,21,22]. Mechanistically the micellization process can be separated into a contribution of the tails, a non-electric contribution of the head groups and, in the case of ionic surfactants, a contribution of the formation of an electrical double layer due to the charged head groups. It is generally assumed that the temperature effect is mainly due to the tails, reflecting hydrophobic bonding.

For non-ionic surfactants with linear alkyl chains the molar enthalpy of micellization decreases linearly with its length (the number of alkyl groups in the tail) whereas the corresponding molar entropy increases linearly. This implies that the contributions per segment are constant. For these systems the micellization standard molar Gibbs energy decreases with approximately –3 kJ per mole CH_2.

For ionic surfactants the micellization process is much more complicated than for non-ionics due to the effect of repulsion between the head groups, formation of an electrical double layer and possible specific adsorption of counterions. Both the entropy and the enthalpy can be influenced by the concentration and the nature of the background electrolyte.

In this work, the partial molar enthalpies of micellization of n-decyl, n-dodecyl, and n-tetradecyl pyridinium chlorides in aqueous solutions are obtained by isothermal calorimetric titration experiments in the temperature range of 6-60°C. Other properties of micellization are also evaluated and compared with data for other surfactants. In this way, important information about the driving forces for the aggregation of cationic surfactants is obtained.

3.2 Experimental

3.2.1 Materials

The n-alkylpyridinium chlorides have been synthesized from 1-chloro-alkane and pyridine, both of PA grade, and purified according to the method of Colichman[23]. The curves of surface tension against the logarithm of the concentration show no dip, indicating that the surfactants are surface-chemically pure. From NMR measurements no chemical impurities could be detected. For our calorimetric experiments we used concentrated stock solutions of 0.4 M decylpyridinium chloride (DePC), 0.25 M dodecylpyridinium chloride (DPC) and 0.04 M tetradecyl-pyridinium chloride (TPC). For our experiments at 0.1 M NaCl the last solution contained additionally 0.06 M NaCl.

All solutions are prepared by weight. Double distilled water has been boiled for 30 minutes before use to remove dissolved gases. All other chemicals were of pro analyse quality and used without further purification.

3.2.2 Methods

Our experiments were performed with a Thermal Activity Monitor (TAM) isothermal microcalorimeter (Thermometric LKB 2277, Sweden), including a large volume (25 ml) stainless steel stirred titration cell fitted into a single detector measuring cylinder. The titration cell was especially designed for the study of mixing liquids and adsorption from solution. A second cylinder, containing a 25 ml ampoule is used as a reference. The use of a reference cell reduces the noise of the baseline by a factor of 2-3. Both cylinders are positioned in a 25–litre thermostatted water bath functioning as a heat sink. The bath is connected to a pre-thermostat resulting in a temperature control down to $\pm 2 * 10^{-4}$ °C within the working range of 5 - 80°C.

The procedure is controlled by a personal computer with the program "DigiTAM v.1.05" (ThermoMetric AB, Sweden), which integrates the output signal and performs an analysis of the output data. Calibration of

the calorimeter was performed prior to and after each experiment by passing a known current through a 50 Ω built-in resistance. Probably due to a heat leakage from the measuring cell, the constant baseline level was slightly exothermic below room temperature, and increasingly endothermic above. However, there are no indications that this has affected our experimental results. For more details about the instrument see the Appendix A1.

The enthalpy of demicellization is obtained by titrating a concentrated surfactant solution into water or 0.1 M NaCl. During a stepwise titration experiment the surfactant concentration in the cell increases up to the critical micelle concentration ("pre-cmc region"). If the titration is continued no further demicellization takes place, but only dilution of micelles, at a practically constant monomer concentration ("post-cmc region"). In the region of c<<cmc, the total measured heat q_{dil} is the sum of the heat of demicellization q_{dem} and the heat of dilution of the concentrated micellar solution $q_{dil'}$.

$$q_{dil} = q_{dem} + q_{dil'} = -q_{mic} + q_{dil'} \tag{1}$$

The partial molar enthalpies $\Delta_{dil}H_m$, $\Delta_{mic}H_m$ and $\Delta_{dil'}H_m$ expressed per mole of monomers are calculated from the corresponding integral enthalpies according to Equations 2-4.

$$\Delta_{dil}H_m = \frac{q_{dil} / V_{titrant}}{(c_{titrant} - cmc)} \tag{2}$$

$$\Delta_{dil'}H_m = \frac{q_{dil'} / V_{titrant}}{(c_{titrant} - cmc)} \tag{3}$$

$$\Delta_{mic}H_m = -\Delta_{demic}H_m = \Delta_{dil'}H_m - \Delta_{dil}H_m \tag{4}$$

In (2) and (3) $c_{titrant}$ and $V_{titrant}$ are the concentration and the volume of the added surfactant stock solution, respectively.

Duplicates were usually reproducible within 2 mJ (i.e.1%). Comparison with independent measurements by a different laboratory with the same equipment showed a difference of about 7%. Due to the lower critical

micelle concentrations the experimental error increases with increasing alkyl chain length. The resulting average overall error for DePC, DPC and TPC amounts to 0.03, 0.1 and 1 kJ per mole of monomers, respectively. (See Appendix A1.)

3.3 Results and Discussion

3.3.1 Calorimetric enthalpies of micellization

Enthalpies of dilution of concentrated solutions of DePC, DPC and TPC in water and 0.1 M NaCl as a function of the surfactant concentration in the calorimetric cell, at different temperatures, are presented in Figures 1-6.

The general trend in the enthalpy curves at a given temperature and electrolyte concentration is that a more or less constant $\Delta_{dil}H_m$ is obtained before the cmc, whereas $\Delta_{dil}H_m$ is relatively small or even zero after passing the cmc. In between, a break corresponding to the cmc occurs. In order to determine these "calorimetric" cmc's more accurately, cumulative enthalpies were plotted against the concentration of the surfactant. (An example is given in Appendix A2.) The calorimetric determination of the cmc is a sensitive method as long as $\Delta_{dil}H_m$ differs substantially from zero, i.e. if a break is clearly detectable. In that case it has the advantage above some surface tension methods to be independent on the contact angle. The numerical values of the cmc's for our alkylpyridinium chlorides correspond well with the results from other methods. Therefore we used our calorimetric cmc values in order to calculate the $\Delta_{dil}H_m$ curves by iteration according to Equations 1-4.

The numerical values of the cmc's at different temperatures and ionic strengths are collected in Tables 1-3. As expected, the cmc decreases with increasing electrolyte concentration. This is due to screening of the repulsion of the head groups facilitating the formation of micelles. However, the salt effect strongly increases with increasing chain length. Whereas for DPC the cmc decreases by a factor of 3 independent on

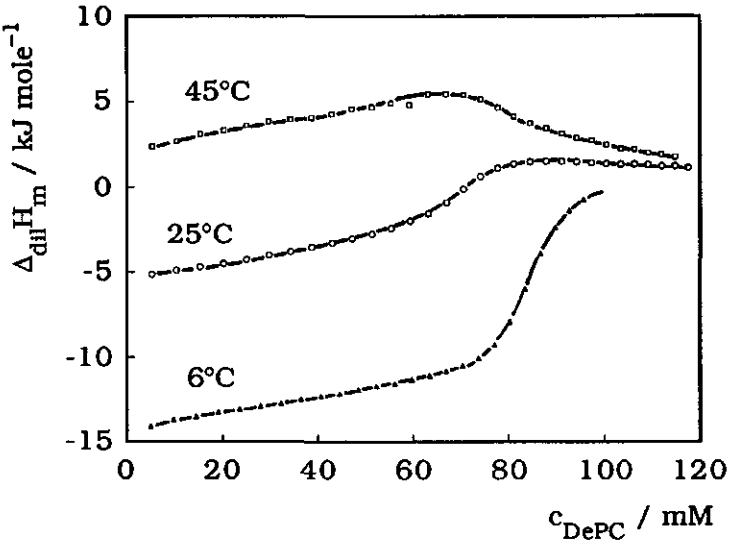

Figure 1. *Enthalpy of dilution of 0.4 M DePC in water.*

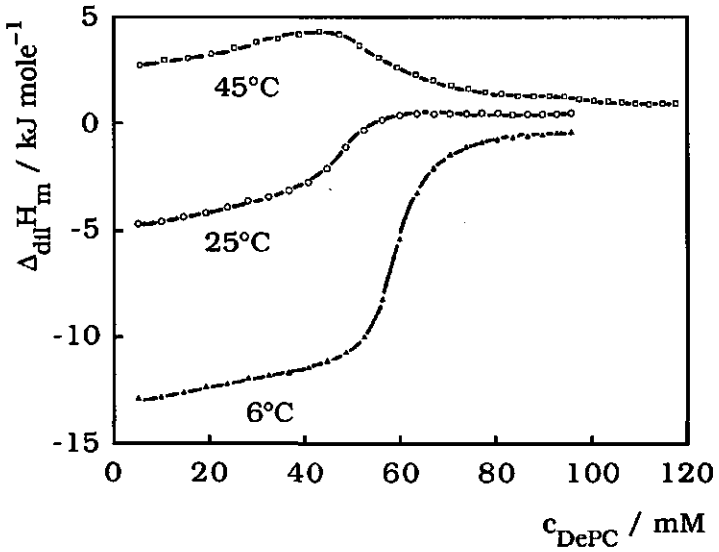

Figure 2. *Enthalpy of dilution of 0.4 M DePC in 0.1 M NaCl.*

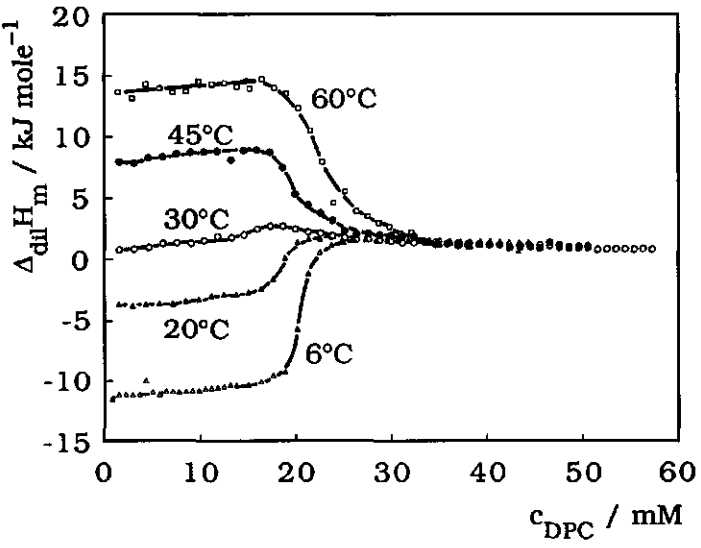

Figure 3. *Enthalpy of dilution of 0.25 M DPC in water.*

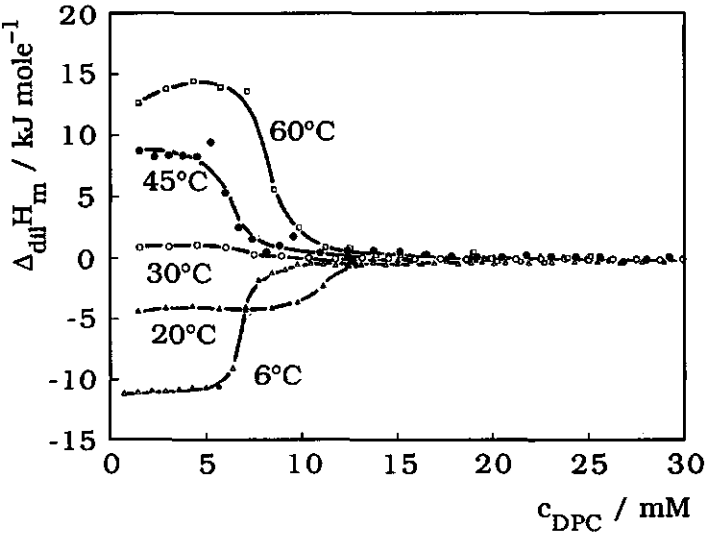

Figure 4. *Enthalpy of dilution of 0.25 M DPC in 0.1 M NaCl.*

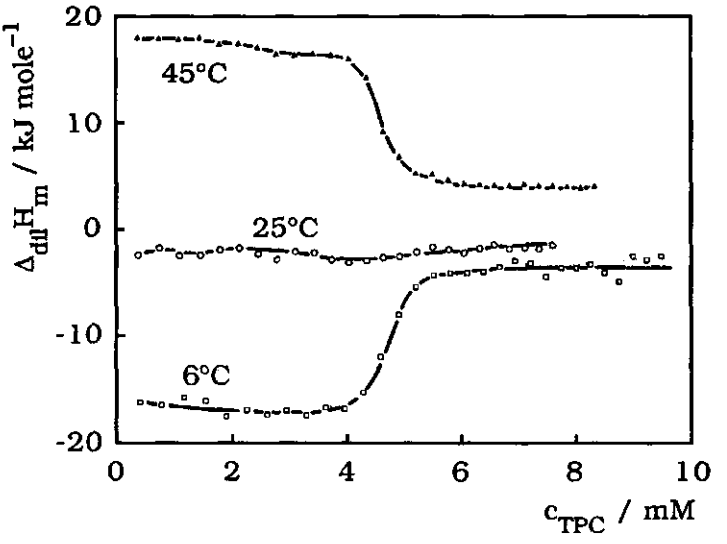

***Figure 5**. Enthalpy of dilution of 0.04 M TPC in water.*

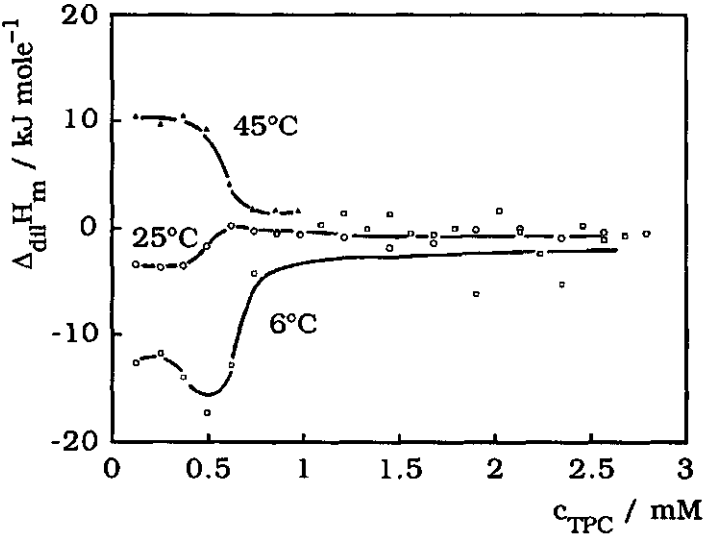

***Figure 6**. Enthalpy of dilution of 0.04 M TPC (and 0.06 M NaCl) in 0.1 M NaCl.*

temperature when changing from water to 0.1 M NaCl, we find a factor of 1.3 and 9 for DePC and TPC, respectively. This can be, at least partly, attributed to the fact that upon micelle formation in water the charges of the head groups are significantly screened when the equilibrium concentration of the monomers is high as in the case of DePC (around 80 mM). However for TPC the equilibrium concentration is only abount 4 mM. As a consequence the difference between the ionic strength of 0.1 M NaCl and the cmc is much larger. A second feature is that the cmc shows a minimum as a function of temperature both in water and in 0.1 M NaCl. Below we will discuss the implications of this minimum.

The curves of the heat of dilution for DPC, DePC and TPC give more or less well-defined limiting values below and above the cmc. These values, called $\Delta_{dil}H_m$ and $\Delta_{dil'}H_m$, respectively, are also included in Tables 1-3. The value of the molar enthalpy of micellization follows from Equation 4 assuming $\Delta_{dil}H_m$ to be constant over the entire concentration range.

The heats of dilution in the post-cmc region $\Delta_{dil'}H_m$, are relatively small compared to the enthalpy of micellization. For more details see Appendix A4. One would expect the heat of dilution of a concentrated micellar solution into a solution just above the cmc to be equal to zero as no demicellization takes place. However, the process is more

Table 1. *Thermodynamic data and cmc-values for DPC.*

c_{NaCl} mM	T °C	cmc mM	$\Delta_{dil}H_m$ kJ/mole	$\Delta_{dil'}H_m$ kJ/mole	$\Delta_{mic}H_m$ kJ/mole	$\Delta_{mic}G_m^0$ kJ/mole	$T\Delta_{mic}S_m^0$ kJ/mole
0	6	19.3	-10.8	1.4	12.2	-18.5	30.7
	20	17.50	-3.7	1.4	5.1	-19.6	24.7
	30	12.4	1.1	0.9	-0.2	-21.2	21.0
	45	20.0	8.5	1.1	-7.4	-20.9	13.5
	60	24.1	14.0	1.6	-12.4	-21.4	9.0
100	6	6.0	-11.1	-0.4	10.7	-21.2	31.9
	20	5.8	-4.1	0.0	4.1	-22.3	26.4
	30	6.5	0.9	-0.2	-1.1	-22.8	21.7
	45	7.0	8.6	0.0	-8.6	-23.7	15.1
	60	8.4	13.9	-0.2	-14.1	-24.3	10.2

Table 2. *Thermodynamic data and cmc-values for DePC.*

c_{NaCl} mM	T °C	cmc mM	$\Delta_{dil}H_m$ kJ/mole	$\Delta_{dil'}H_m$ kJ/mole	$\Delta_{mic}H_m$ kJ/mole	$\Delta_{mic}G_m^0$ kJ/mole	$T\Delta_{mic}S_m^0$ kJ/mole
0	6	83.2	-13.7	-0.7	13.0	-15.1	28.1
	25	63.3	-5.0	1.4	6.4	-16.8	23.2
	45	80.0	3.8	1.8	-2.0	-17.3	15.3
100	6	58.7	-12.6	-0.6	12.0	-15.9	27.9
	25	48.7	-4.3	0.5	4.8	-17.4	22.2
	45	62.5	3.8	0.9	-2.9	-17.9	15.0

Table 3. *Thermodynamic data and cmc values for TPC.*

c_{NaCl} mM	T °C	cmc mM	$\Delta_{dil}H_m$ kJ/mole	$\Delta_{dil'}H$ kJ/mole	$\Delta_{mic}H_m$ kJ/mole	$\Delta_{mic}G_m^0$ kJ/mole	$T\Delta_{mic}S_m^0$ kJ/mole
0	6	4.5	-17.9	-4.0	13.9	-21.8	35.7
	25	3.5	2.4	1.7	-0.7	-24.0	23.3
	45	4.5	16.8	3.6	-13.2	-24.9	11.7
100	6	0.5	-10.3	-1.7	8.6	-26.9	35.5
	25	0.4	3.5	0.7	-2.8	-29.3	26.5
	45	0.7	13.7	0.8	-12.9	-29.8	16.9

complicated, because it is possible that the shape and the aggregation number are concentration-dependent. It seems, however, that among the dodecylpyridinium surfactants only the iodide compound is able to form rod-shape micelles at room temperature[24]. The effect of temperature and chain length on the shape of these micelles is unfortunately unknown. However, it is likely that a change in the shape with surfactant concentration will be temperature dependent, see Appendix A4. Secondly, dilution of a concentrated micellar solution into water changes the repulsion between the head groups and the binding of the counterions. The screening of the charge of the head groups will give rise to an exothermic effect while the change in the binding of the counterions will be endothermic. Both effects are probably independent

of temperature and will be much smaller for dilutions in 0.1 M NaCl. Pilcher et al.[8] calculated the enthalpy of dilution of sodium n-dodecylsulphate micelles (considered as rigid spherical particles) and concluded that the endothermic nature of the dilution was due to the ionization of the micelles and removal of the counterions from the micelles. An endothermic effect has also been reported by Kresheck et al.[10] for other ionic surfactants but they did not find the effect for non-ionics. For n-alkylpyridinium surfactants we found a pronounced effect of the presence of 0.1 M NaCl. Moreover, for dilution of a concentrated micellar solution of DPC in water we found an endothermic effect, indicating that counterion binding is also in this case the origin of the finite positive value of $\Delta_{dil}H_m$. If we neglect the small negative value at 6°C, the same conclusion can be drawn for DePC. On the other hand, the strong temperature dependence of $\Delta_{dil}H_m$ for the longer TPC suggests a possible change with surfactant concentration in either the shape or the aggregation number.

3.3.2 Isosteric Enthalpies of Micellization

The enthalpy of micellization can also be derived from the temperature dependence of the cmc. To that end we are obliged to adopt a model for the micellization process. In addition, a model enables us to derive values of the standard molar Gibbs enthalpy and the molar entropy of micellization from the cmc's. For our purpose we used the mass action model for micelle formation. According to this model a relation exists between the concentration of surfactant monomers and the concentration of micelles. Although micelles can be polydisperse and polymorphic, in the model the micellar solution is generally assumed to be homodisperse. For non-ionic surfactants the model can be easily implemented but for ionic surfactants the binding of counterions complicates it. However, in the following we assume that the degree of counterion binding of monomers and micelles is small and identical, the aggregation number is high and the activity coefficients are equal to unity. The Gibbs energy, the enthalpy and the entropy of micellization can then be expressed by the following (general) equations. The derivation of Equations 5 and 6 is given in Appendix A3.

$$\Delta_{mic}G_m^0 = RT \ln cmc \tag{5}$$

$$\Delta_{mic}H_m = -RT^2\left(\frac{\partial \ln cmc}{\partial T}\right)_{P,c_{salt}} = R\left(\frac{\partial \ln cmc}{\partial (1/T)}\right)_{P,c_{salt}} \tag{6}$$

$$\Delta_{mic}S_m = (\Delta_{mic}H_m - \Delta_{mic}G_m^0)/T \tag{7}$$

In Tables 1-3 we calculated $\Delta_{mic}G_m^0$ according to Equation 5 with the cmc expressed as a mole fraction. The values of $\Delta_{mic}S_m$ follow from Equation 7 with $\Delta_{mic}G_m^0$ calculated according to Equation 5 and the calorimetric $\Delta_{mic}H_m$. These values will be discussed below.

The isosteric enthalpy of micellization is derived from the temperature dependence of the calorimetric cmc according to Equation 6. In Table 4 we compare the isosteric and the calorimetric enthalpies of micellization

Table 4. *Comparison of micellization enthalpies of n-alkylpyridinium chlorides from microcalorimetry and temperature dependence of the cmc.*

Surfactant	T/°C	Water		0.1 M NaCl	
		$\Delta_{mic}H_m$ calorimetric	$\Delta_{mic}H_m$ isosteric	$\Delta_{mic}H_m$ calorimetric	$\Delta_{mic}H_m$ isosteric
DePC	6	13.0	14.3	12.0	8.2
	25	6.4	5.5	4.8	1.5
	45	-2.0	-13.3	-2.9	-47.5
DPC	6	12.2	7.0	10.7	4.7
	20	5.1	4.9	4.1	3.0
	30	-0.2	0.0	-1.1	-9.8
	45	-7.4	-14.5	-8.6	-12.8
	60	-12.4	-20.8	-14.1	-15.0
TPC	6	13.9	16.6	8.6	15.1
	25	-0.7	0.0	-2.8	-12.3
	45	-13.2	-20.8	-12.9	-19.9

both in water and 0.1 M NaCl. The differences are caused by assumptions made in the isosteric enthalpies and in experimental errors involved in both techniques. For instance the isosteric enthalpies are obtained by differentiating cmc-temperature curves consisting of 3-5 experimental points. This gives inevitably rise to substantial interpolation errors which are enlarged in the derivative. Moreover, in order to derive the isosteric heats a model has to be adopted taking into account the micellar size and the binding of the counterions. This problem is particularly relevant for ionic surfactants. For non-ionics agreement between the two methods was reported by Corkill et al.[6]. For ionic surfactants good agreement was found for sodium dodecyl sulphate and dodecyltrimethylammonium bromide, but poor agreement for dodecyl pyridinium iodide[10]. Further we have to be aware that the microcalorimetrically measured demicellization enthalpy is an integral heat, i.e. micelles are broken down into monomers so that the enthalpy of breaking down an electrical double layer has to be accounted for. On the other hand, when we derive isosteric heats from the cmc, equilibrium between monomers and micelles is maintained, resulting in a differential quantity, i.e. upon the process the double layer remains intact. Although we are aware of these differences between the two enthalpies, comparison gives at least an indication of the validity of thermodynamic conditions of equilibrium and reversibility. In both techniques the isosteric enthalpies show a transition from endothermic to exothermic with increasing temperature. It may be noted that according to Equation 6 this transition corresponds with the minimum in the cmc mentioned above. As a trend, it seems that the isosteric enthalpies are somewhat more exothermic than the calorimetric values. The reason for this discrepancy is not clear; in fact from the differential character of the isosteric heat we just expect it to be more endothermic. In spite of the quantitative uncertainties we may conclude that the agreement between isosteric and calorimetric enthalpies is at least satisfactory within the context of experimental and theoretical uncertainties. As the calorimetric values are more reliable than the isosteric heats, below we use the former.

3.3.3 Temperature dependence of the thermodynamic parameters

Considering the enthalpies of micellization (Tables 1-3), a number of interesting trends emerge. It appears that $\Delta_{mic}H_m$ is clearly temperature dependent. The most striking feature is that for all surfactants $\Delta_{mic}H_m$ changes from endothermic to exothermic with increasing temperature. The estimated transition temperatures (T_{trans}) are given in Table 5. They

Table 5. *Transition temperatures of n-alkylpyridinium chloride solutions.*

surfactant	c_{NaCl} (mM)	T_{trans} (°C)
DePC	0	40.1
	100	37.5
DPC	0	29.7
	100	28.0
TPC	0	24.7
	100	21.1

depend strongly on the chain length, but to a lesser extent on the electrolyte concentration. This is an indication that the reason for the occurrence of the transition stems mainly from interactions of the tails and not from the charges of the surfactants. Below we will show that the effect of the chain length on T_{trans} is intimately related to the thermodynamic parameters of hydrophobic bonding.

The enthalpy of micellization is more positive in water than in 0.1 M NaCl due to the screening of the charge of the head groups. For DePC and DPC the difference is almost independent on temperature and chain length and amounts to about 1.2 kJ mole^{-1}. On the other hand, the salt effect for TPC is larger than for DPC and DePC and depends on temperature. The former observation is possibly a consequence of the change in ionic strength due to the monomer concentration although we took an averaged enthalpy value before the cmc and not at the cmc as discussed above. The dependence on the temperature of the salt effect of TPC may be due to possible changes in the shape and/or the aggregation

number as we suggested already in relation to the post-cmc dilution enthalpies.

Comparison of the micellization enthalpy in water for different chain lengths is not straightforward because the effect of the ionic strength differs between the different n-alkylpyridinium surfactants due to differences in the cmc values. It is therefore more straightforward to compare $\Delta_{mic}H_m$ at 0.1 M NaCl as then the electrostatic contribution is constant and relatively small. Then it is found that with increasing chain length $\Delta_{mic}H_m$ shifts to more exothermic values. The averaged

Table 6. *Heat capacities of C10 to C14 surfactants with different head groups. The unit of* ΔC_P^0 *is J mole*$^{-1}$ *K*$^{-1}$.

head group	C_{10}	C_{12}	C_{14}
PyCl in water	-382	-462	(-621)
PyCl in 0.1M salt	-374	-467	-552
TABr in water (ref. 14)	-302	-409	-499

contribution per CH_2 depends on the temperature and amounts to 0.85, 1.9 and 2.5 kJ mole^{-1} at 6, 25 and 45°C, respectively. This temperature trend is a clear indication of the importance of hydrophobic bonding to the process. Below we will compare these values with data from other hydrophobic bonding processes.

Heat capacities ΔC_P^0 are calculated from the slopes of the micellization enthalpy-temperature curves (Figs. 7 and 8). The values are independent of temperature. In Table 6 we compare our values of ΔC_P^0 for a series of alkylpyridinium chlorides with a corresponding series of alkyltrimethylammonium bromides after Bashford and Wooley[14]. Kresheck[10] found a value of -460 J mole^{-1} K^{-1} for DPC. The changes in ΔC_P^0 per CH_2 are identical within experimental error and amount to -45 J mole^{-1} K^{-1}, independent on the nature of the head group. Extrapolation of the micellization enthalpy–temperature curves at different chain length gives a common intersection point at about -12 °C. For the homologous series of n-alkyltrimethylammonium bromides in water an intersection point was found at the same temperature. At this imaginary point the

contribution of a CH_2 to the micellization enthalpy is zero which implies that at that point the net contribution of the alkyl chain to the micellization process would be purely entropical. As the temperature increases every CH_2 contributes equally to the micellization enthalpy which is due to either an increase of the bond strength between alkyl chains or to a breakdown of water bonds surrounding the chain. The latter is most likely since the bond strength between alkyl chains is determined by the Hamaker constant which is almost independent on temperature. The latter conclusion is supported by Kresheck et al[10] who also concluded that the heat capacity reflects mainly solvent effects. From this behaviour it follows that the transition temperature T_{trans} shifts towards lower temperatures with increasing chain length.

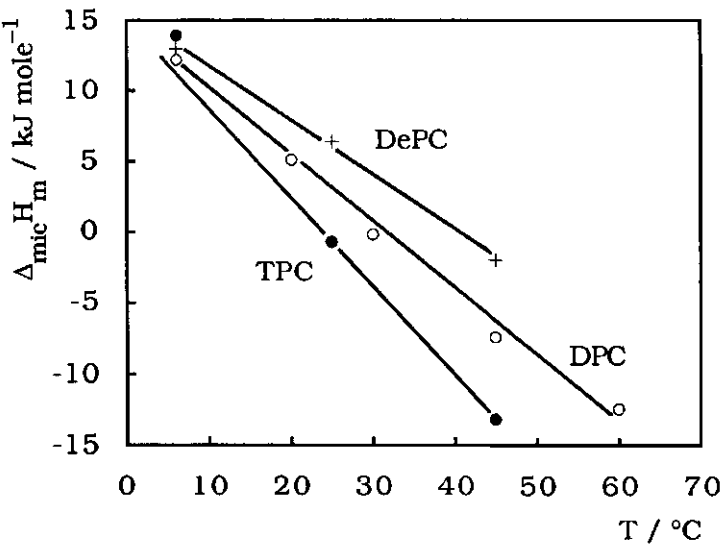

Figure 7. *Enthalpy of micellization of DePC, DPC and TPC in water as a function of temperature.*

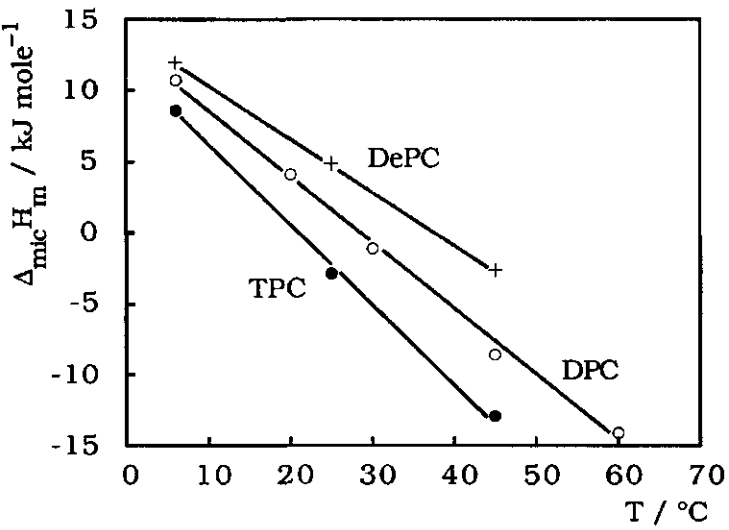

Figure 8. *Enthalpy of micellization of DePC, DPC and TPC in 0.1 M NaCl as a function of temperature.*

In Figures 9-10 the behaviour of DePC and DPC around $T=T_{trans}$ is given. Here micellization is mainly driven by entropy changes. The data points are identical with those of the corresponding curves in Figures. 1-4. The enthalpy curves deviate from the general trend discussed above showing an endothermal maximum near the cmc. We cannot exclude the possibility that at temperatures away from T_{trans} this effect also exists, but is invisible because it is hidden in the break. Taken into account the salt effect in Figure 9 and 10 it seems that near the cmc the process becomes enthalpically less favourable implying that the repulsion between the head groups is not completely compensated by attraction between the tails.

If we compare the enthalpy, entropy and Gibbs energy of micellization (Tables 1-3) the most striking feature which emerges is that the strong temperature dependence of the enthalpies is largely compensated by the temperature dependence of the $T\Delta S$-term. In the literature this effect is known as the enthalpy/entropy compensation effect[10,21,22] and it is intimately related to hydrophobic bonding. For instance, enthalpies and entropies of hydration of hydrophobic solutes of varying chain length also exhibit this compensation effect[21]. The increase in the entropy caused by

the release of water molecules from the so called "ice structure" around the hydrophobic tails of the surfactant monomers, is the main driving force for the micellization process when $T<T_{trans}$. At $T> T_{trans}$ the enthalpy also favours micellization. With a further increase in temperature the enthalpy always overcompensates the decrease in entropy gain and as a result the Gibbs energy only slightly increases with temperature.

3.3.4 Contributions to the Gibbs energies and enthalpies of micellization

For non-ionic surfactants with an n-alkyl chain and a head group the enthalpies and entropies of micellization can, to a first approximation, be rather straightforwardly decomposed into a contribution per CH_2-group of the tail and a contribution of the head group. Several examples are given in the literature, e.g. references 1-5.

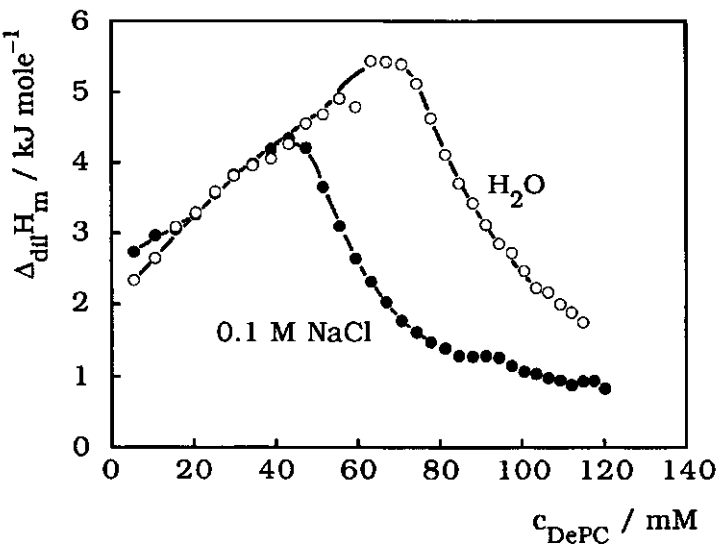

Figure 9. *Enthalpy of dilution of a concentrated solution of DePC at 45°C.*

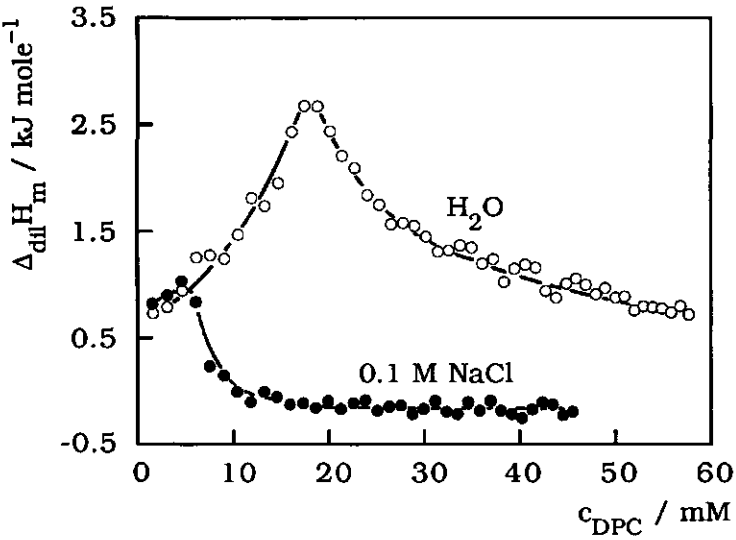

Figure 10. *Enthalpy of dilution of a concentrated solution of DPC at 30°C.*

For ionic surfactants with an n-alkyl chain and a charged head group the analysis of the thermodynamic parameters is more complicated than for non-ionic surfactants. The problems start already when considering the demicellization process. One titrates a concentrated surfactant solution into water or into an aqueous solution. Usually the ionic strengths in the stock solution and the mixing chamber are not equal. This gives rise to enthalpic and entropic changes due to alteration of the electric screening and, hence, of the activity coefficients. Moreover, association of counterions depends on electrolyte concentration. Associated with the effect of counterion binding there is the release of water molecules giving rise to both enthalpic and entropic contributions. As surfactants with different chain length have different solubilities, and critical micelle concentrations, the separation of the contributions of solvation of the head group and structuring around the hydrocarbon chain is complicated.

As a model, the following subprocesses can be distinguished when a monomer penetrates into a micelle. First, consider the hydrophobic tail which is transferred from water (or an aqueous solution) into the interior of a micelle. The interior of the micelle behaves as a liquid hydrocarbon and, hence, the release of structured water around the alkyl chain gives

rise to an increase in entropy and enthalpy characterizing hydrophobic bonding (hb). This process is strongly temperature dependent. To a first approximation the effect on enthalpy and entropy is proportional to the number of CH_2-groups. A second effect is the electrical contribution (el). The surfactant head group charges approach each other resulting in an electrostatic repulsion and formation of an electrical double layer. Finally, besides coulombic repulsion between head groups there will be a non-electrostatic contribution to the interaction which we call the chemical contribution (chem) and which may be due to e.g. association of pyridinium groups, a difference in counterion binding between micelles and monomers and (non-electrical) contributions of displaced ions or solvent molecules. Thus, the differential Gibbs energies, enthalpies and entropies can be separated into three terms according to Equations 8, 9 and 10.

$$\Delta_{mic}G_m^0 = \Delta_{mic}\,G_m^{el} + \Delta_{mic}\,G_m^{chem} + n.\Delta_{mic}\,G_m^{hb} \qquad (8)$$

$$\Delta_{mic}H_m^0 = \Delta_{mic}\,H_m^{el} + \Delta_{mic}\,H_m^{chem} + n.\Delta_{mic}\,H_m^{hb} \qquad (9)$$

$$\Delta_{mic}S_m^0 = \Delta_{mic}\,S_m^{el} + \Delta_{mic}\,S_m^{chem} + n.\Delta_{mic}\,S_m^{hb} \qquad (10)$$

In the literature several attempts have been made to estimate these individual components[1-5]. The contribution of hydrophobic bonding can be estimated by transferring a methyl group from water to the interior of the micelles or another hydrophobic medium. Alternatively, one could measure the thermodynamic parameters for a homologous series. A review is given in Table 7. Considering the values presented in this table, the general trend is that on average the Gibbs energy decreases by about –3.1 kJ per mole of CH_2 which is calculated using Traube's rule. This Gibbs energy decrease is composed of a decrease of the enthalpy of 1.8 and a $T\Delta S$ increase of 1.3 kJ $mole^{-1}$. The entropy change is always positive indicating that the release of structured water around the hydrocarbon always favours the micellization process. However, at room temperature the enthalpy of this process is also favourable. Our measurements with a homologous series of n-alkylpyridinium surfactants

Table 7. *Thermodynamic parameters for the transfer of CH_2 from water to a hydrophobic phase to at 25°C.*

ΔG^0 kJ mole^{-1}	ΔH^0 kJ mole^{-1}	$T\Delta S^0$ kJ mole^{-1}	Process	Ref.
-4.2	-3.3	0.9	water to liquid hydrocarbon	1
-3.4	-0.8	2.6	R-OH, water to pure alcohol	25
-4.0	-2.6	1.4	C_nH_{2n+2}, water to hydrocarbon	26
-3.2	-0.3	2.9	$C_6H_5C_nH_{2n+1}$, water to hydrocarbon	26
-3.0	-2.0	1.0	micellization of R-E_6	6
-2.0	-1.3	0.7	micellization of C_nE_6.	6
-3.3	-1.5	1.8	micellization of alkyl-sulphoxides	27
-2.0	-1.8	0.2	alkyl-Py, micellization in water	Our work
-3.0	-1.9	1.1	alkyl-Py, micellization in 0.1M NaCl	Our work

at high salt concentration are in perfect agreement with the averaged values cited above. As explained earlier, for the dilution of ionic surfactants in water the values are not well suited for comparison due to ionic strength effects.

Now we are able to assign numerical values to the different contributions defined in Equations 8-10 for our n-alkylpyridinium surfactants based on the micellization in 0.1 M NaCl. We set $\Delta_{mic} G_m^{hb}$, $\Delta_{mic} H_m^{hb}$ and $T\Delta_{mic} S_m^{hb}$ equal to -3.0, -1.9 and 1.1 kJ mole^{-1} CH_2, respectively. If we presume that at 0.1 M salt the electrostatic interactions are largely suppressed and realise that the screening is different for different surfactants then the parameters for the electrical part of the Gibbs energy, the enthalpy and the entropy can be estimated

Table 8. *The thermodynamic parameters of the micellization of n-alkylpyridinium chlorides in water at 25°C.*

surfactant	Parameter	total	i≡hb	i≡el	i≡chem
DePC	$\Delta_{mic} G_m^i$	-16.8	-30	0.6	13
	$\Delta_{mic} H_m^i$	6.4	-19	1.6	25
DPC	$\Delta_{mic} G_m^i$	-20.4	-36	2.2	13
	$\Delta_{mic} H_m^i$	3.1	-23	1.0	26
TPC	$\Delta_{mic} G_m^i$	-24.0	-42	5.3	13
	$\Delta_{mic} H_m^i$	-0.7	-27	2.1	22

from the difference between $\Delta_{mic}G_m^0$'s in water and in high salt concentration, as presented in Tables 1-3. In this procedure, the values of $\Delta_{mic} G_m^{chem}$ and $\Delta_{mic} H_m^{chem}$ are rest terms. The results are presented in Table 8.

Some interesting conclusions can be drawn. It is evident that the electrostatic contribution to the Gibbs energy and the enthalpy of micellization is relatively small and positive. The fact that the values increase with chain length is an artifact as discussed above. The most interesting aspect is the fact that the "chemical" contribution to the Gibbs energy and to the enthalpy is practically constant and positive. It means that a strong unfavourable enthalpic contribution exists which is partly compensated by a favourable entropic term. It is well possible that this is due to disturbance of the hydrophobic effect near the head group or to a decrease in hydration forces of solvent around the head group. The signs of the enthalpy and the entropy indicates that probably the latter contribution dominates.

3.4 Conclusions

The effect of temperature on the thermodynamic parameters of micellization obtained from calorimetry contributes to our insight into the mechanism of the micellization process.

The most striking property of the enthalpy of micellization is its strong temperature dependence. At the imaginary point at a temperature of -12°C the enthalpy contribution due to the CH_2 groups is zero and the process is determined by the $T\Delta S$ effect due to the structured solvent around the alkyl chain, counteracted by an endothermic contribution of the head groups. With increasing temperature the gain in entropy due to the liberation of the structured water decreases, but this effect is more than compensated by a decrease (more exothermic) of enthalpy. The enthalpic contribution also originates from changes in the solvent structuring. At a temperature T_{trans} the endothermic enthalpy effect of the head groups is compensated by the exothermic effect of the alkyl chain. Obviously T_{trans} decreases with increasing chain length.

For our surfactants, the directly measured heats of micellization agree at least semi-quantitatively with the ones calculated from the shift in the cmc's with increasing temperature.

From the heat of dilution of post-cmc solutions there is some circumstantial evidence that a change in the shape and/or the aggregation number occurs during demicellization of TPC.

The value of $\Delta_{mic}G_m^0$ has been split up into its hydrophobic, electric and chemical contributions. For our system, the different contributions were well additive. The contribution of $\Delta_{mic}G_m^{el}$ is small and inhibits the micellization process. The most striking feature is the presence of a constant $\Delta_{mic}G_m^{chem}$ term which was ascribed to a decrease in hydration forces of the solvent around the head group.

3.5 Acknowledgement

The contributions of Mr. A. J. Korteweg in the experimental work and Mr. M. Bakkenes for synthesizing our surfactants are gratefully acknowledged.

3.6 References

(1) Tanford C., In: *"The hydrophobic effect: Formation of micelles and biological membranes"*, Wiley, New York, **1973**.

(2) Couper A., In *"Surfactants"*, Ed. Tadros Th. F., Academic Press, London, **1983**, p.19.

(3) M.J. Rosen, In:*"Surfactants and Interfacial Phenomena"*, Second ed., Wiley, New York, **1989**, pp 431

(4) Zana R., In: *"Cationic Surfactants"*, Eds. Rubingh D. N. and Holland P. M., Marcel Dekker, New York, **1991**, Vol. 37, p 41.

(5) Clint J. H., In: *"Surfactant Aggregation"*, Blackie, London, **1992**.

(6) Corkill J. M., Goodman J. F., Tate J. R., *Trans Faraday Soc.*, 60 **(1964)** 996-1002

(7) Adderson J. E., Taylor H. *J. Colloid Sci.*, 19 **1964** 495-502.

(8) Pilcher G., In: *Proceedings of the International Symposium "Calorimetry in Chemical and Biological Sciences"*, Guildford, Surrey (UK), **1969**, p.31.

(9) Waligóra B., Góralczyk D., *Bull. Acad. Polon. Sci., Sér. Sci. Chim.*, 19 **1971** 465.

(10) Kresheck G. C., Hargraves W. A., *J. Colloid Interface Sci.*, 48 **1974** 481-486.

(11) Musbally G. M., Perron G., Desnoyers J. E., *J. Colloid Interface Sci.*, 54 **1976** 80-86.

(12) De Lisi R., Ostiguy C., Perron G., Desnoyers J. E., *J. Colloid Interface Sci.*, 71 **1979** 147-152.

(13) Woolley E. M., Burchfield T. E., *J. Phys. Chem.*, 89 **1985** 714-722.

(14) Bashford M. T., Woolley E. M., *J. Phys. Chem.*, 89 **1985** 3173-3178.

(15) Sharma V. K., Bhat R., Ahluwalia J. A., *J. Colloid Interface Sci.*, 115 **1987** 396-402.

(16) van Os N M., Daane G. J.,Bolsman T. A. B. M., *J. Colloid Interface Sci.*, 115 **1987** 402-409.

(17) van Os N M., Daane G. J.,Bolsman T. A. B. M., *J. Colloid Interface Sci.*, 123 **1988** 267-274.

(18) van Os N. M., Daane J. G., Haandrikman G., *J. Colloid. Interface Sci.*, **1991**, *141*, 199-217.

(19) Moroi Y., Matuura R., Kuwamura T., Inokuma S., *Colloid Polymer Sci.*, **1988**, *266*, 374-379.

(20) Keh E., Partyka S., Zaini S., *J. Colloid Interface Sci.*, 129 **1989** 363-369.

(21) Krishnan C. V., Friedman H. L., *J. Solution Chem.*, **1973** 37 119-125.

(22) Jolicoeur C., Philip P. R., *Can. J. Chem.*, **1974**, *52*, 1834-1839.

(23) Colichman E. L., *J. Am. Chem. Soc.*, **1950**, *81*, 1834-1840.

(24) Ikeda S., Fujijo K., 7th ICSCS, Compiègne, France, **1991** Vol.1 Part1, p.142.

(25) Arnett E.M., Kover W. B., Carter J. V., *J. Am. Chem. Soc.* **1969** 91 4028-4035.

(26) Gill S. J., Nichols N. F., Wadsö I., *J. Chem. Thermodynamics*, **1976** 8 445-452.

(27) Clint J. H., Walker T., *J. Chem. Soc. Faraday I*, **1975**, *71*, 946-952.

APPENDIXES TO CHAPTER 3

A1. Description of the microcalorimeter and the calorimetric procedure

Our experiments were performed with a Thermal Activity Monitor (TAM) isothermal microcalorimeter, (Thermometric LKB 2277, Sweden). The LKB microcalorimeter is a free-standing multi-channel microcalorimeter as it is shown schematically in figure A1. The instrument is especially designed for the study of mixing of liquids and adsorption from solution. It involves the introduction of adsorbate from outside the instrument into a solution or suspension, maintained in a homogeneous state by effective stirring. Continuous heat leakage measurements are conducted in an isothermal system. All routine operator controls are situated under a hinged protective cover on the top of the instrument. A display panel on the front of these controls continuously monitors the status of the instrument on an built-in digital voltmeter. A multi-position switch used in conjunction with the digital voltmeter allows the operator access to all necessary information, without interrupting the measurement. The bath is connected to a pre-thermostat resulting in an improved temperature control and hence in a great sensitivity and a high level of precision of the microcalorimetric system. The heat sink is a 25-litre thermostatted water bath, maintained to $\pm 2 * 10^{-4}$ °C, within the working range of 5 - 80°C. For the internal thermostat, two thermistors monitor the water temperature. One thermistor is in operation for water temperatures below 50°C and the other above 50°C.

Samples are presented to the TAM in measuring cylinders which are maintained at constant temperature in the water thermostat. Each cylinder, together with its individual signal amplifier, forms a "channel". The heat of dilution of a concentrated surfactant solution is measured in a 25-ml stainless steel titration cell (especially designed for batch measurements of the heat of adsorption with suspended materials)

1. *Temperature control unit*
2. *Water bath circulation pump*
3. *Water bath*
4. *Measuring cylinder*
5. *Heat exchanger*

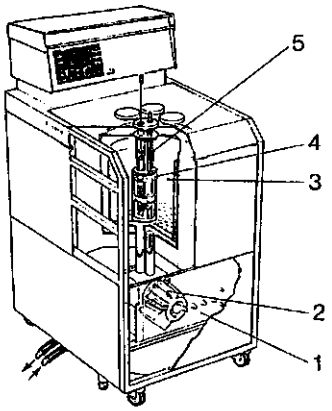

Figure A1. *Schematic presentation of the LKB" Thermal Activity Monitor".*

sandwiched between a pair of thermopile heat sensors. These sensors were in contact with a metal heat sink.

The titration cell fitted into a single detector measuring cylinder. A second cylinder containing a 25 ml ampoule is used as a reference. The procedure is controlled by a personal computer with the program "DigiTAM v. 1.05" (ThermoMetric AB, Sweden), which also integrates the output signal and performs an analysis of the output data. Calibration was performed prior to each experiment and afterwards. A known current is passed through a 50 Ω resistance, built in the calorimeter, during a certain time period. The amplifiers are adjusted to the known amount of heat, when necessary.

The use of a reference cell ameliorates the final results, because external perturbances appear in the form of noise both in the reference and the measuring channel. As an example we compared the noise measured in measuring cell, the reference cell and the difference signal, for an arbitrary experiment. The results are given in Table A1. Clearly the reference cell improved the results by reducing the noise of the signals to about 40%.

Due to a constant small heat leakage from the calorimeter cell, the base line signals deviated from zero, being slightly exothermic at $T < 20°C$ and endothermic when $T > 20°C$ as shown in figure A2, where the raw signal

Table A1. *An example of the base line noise in μW for channels 1 - 3.*

Channel	Mean value	standard deviation
1, measuring cell	-58.6	0.5
2, reference cell	-32.5	0.5
3, difference signal	-31.6	0.2

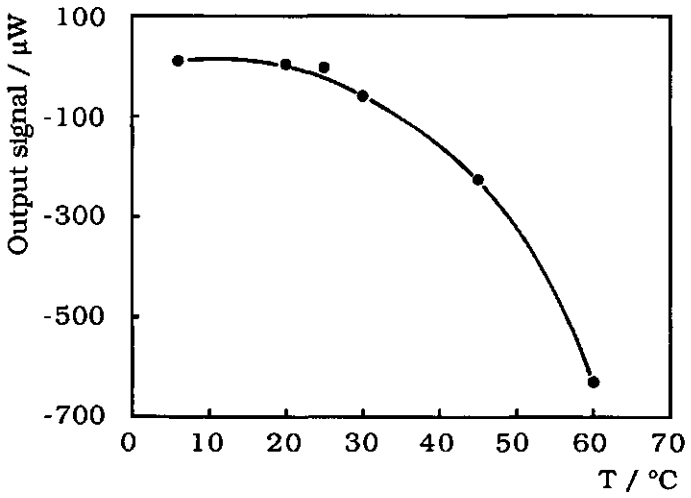

Figure A2. *Base line of the calorimetric signals at different temperatures*

is drawn as a function of the experimental temperature. The signal could not be adjusted to zero. When the temperature difference between the calorimeter and the environment was low (20-30°C) the base-line signal was very close to zero. Because the base line did not shift significantly during a titration step, the above mentioned deviation did not affect our experimental results.

A typical example of the calorimetric output signal of a dilution experiment is presented in figure A3. The experiment is performed at 20°C. The cell contained 17 g distilled water. A 0.25M DPC solution was added in steps of 100 μl into the titration cell from a "Hamilton

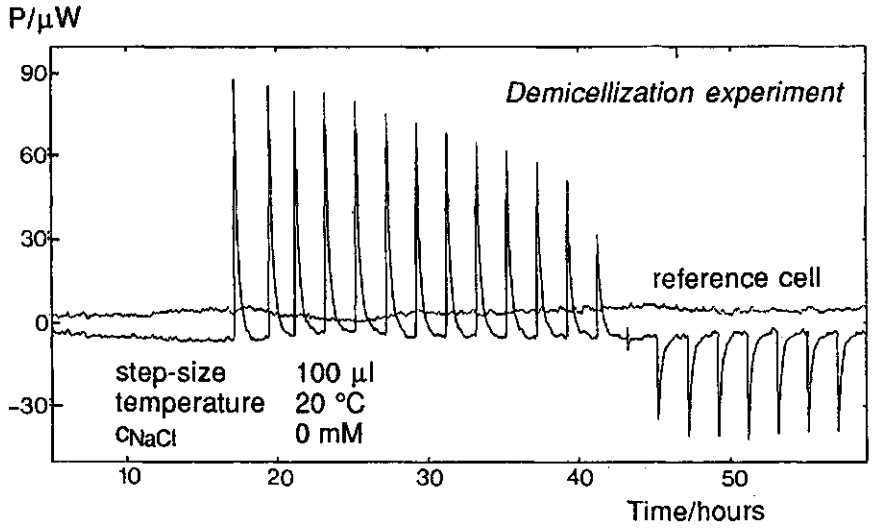

Figure A3. *A typical example of calorimetric output signal; demicellization experiment in water.*

Microlab M" burette through a capillary at a sufficiently low speed (0.5 μl s^{-1}) to allow for thermal equilibrium. Every peak, in figure A3 represents one titration step. The starting exothermic peaks refer to the sum of demicellization enthalpy and the enthalpy of the dilution of micelles. As the concentration becomes closer to the cmc the area under each peak decreases. When c>cmc the sign of the signals changes, explaining the endothermic nature of the dilution of post-micellar solutions.

The enthalpy of dilution of 7 mM DPC (monomers) into a 0.1M NaCl solution at 20°C is –0.02 kJ $mole^{-1}$, which falls within the range of experimental error.

The experiments were very well reproducible, as shown in figures A(4a) and A(4b). From the results presented in figure A(4a), it is concluded that the difference between the duplicates is on average only 1.3 mJ as compared with the total enthalpy of 250.7 mJ. This means

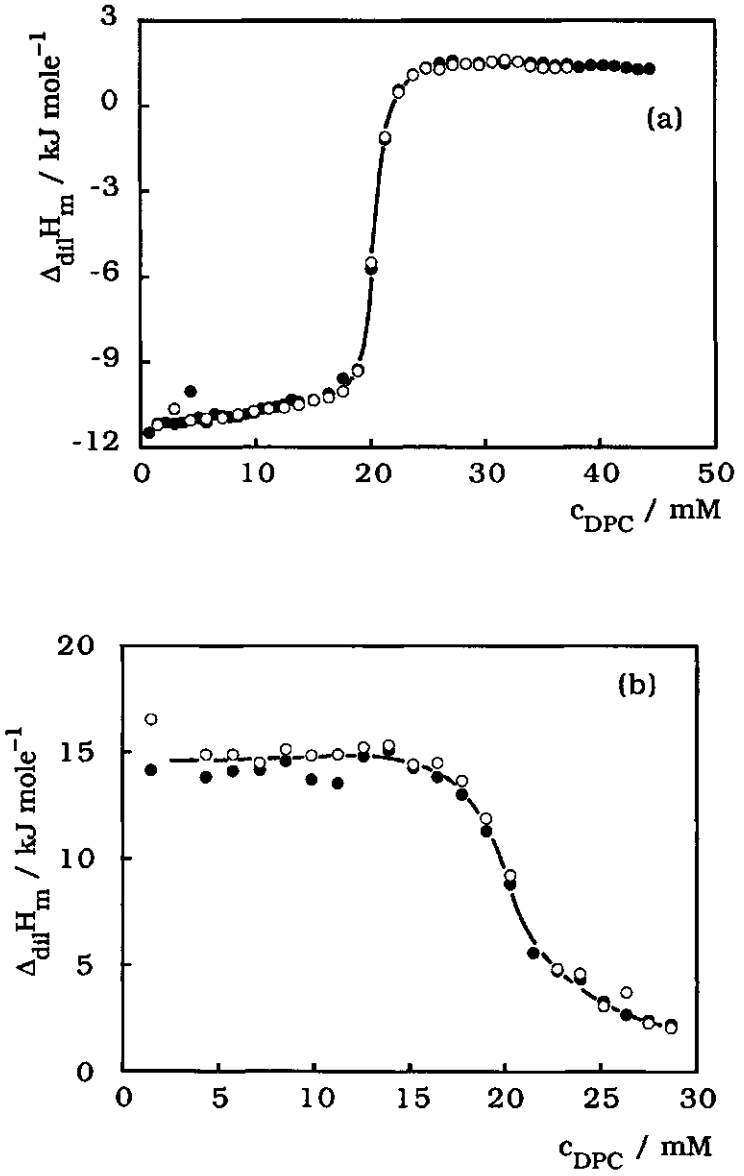

Figure A4. *Reproducibility of $\Delta_{dil}H_m$ of DPC, (a) our identical experiments except for V_{DPC} = 100 μ (●) and V_{DPC} = 50 μ l (o), T = 6°C, (b) comparison of our work (o) with that of KSLA "Shell Amsterdam" (●); T = 60°C.*

error of less than 0.5%. In figure A(4b) the difference between the duplicates is on average about 7%. These differences correspond to an uncertainty of 0.1 and 1 kJ/mole in the molar micellization enthalpy for figures A(4a) and (4b), respectively. We recall here that the experiments presented in figure A(4b) are not only performed by two completely independent laboratories and technicians, but also at two very different experimental conditions. (Note that the temperatures were 6 and 60°C for figures A(4a) and A(4b), respectively.) The errors in the measured enthalpies affect the $\Delta_{mic}H_m$ differently because, as shown in equations (1-3), the titrant volume, the titrant molarity and the total measured heat influence $\Delta_{mic}H_m$. The resulting average overall error for DePC, DPC and TPC amounts to 0.03, 0.1 and 1 kJ/ mole, respectively.

A2 Calculation of the cmc using cumulative enthalpies

In order to determine the cmc's more accurately the cumulative enthalpies were plotted against the concentration of surfactant. An example is shown in figure A5. We started with an estimation of the cmc to calculate the total molar enthalpy. After that, the cumulative curve is drawn (see figure A5) on the basis of that cmc. A slightly different break point was found. The new cmc is used for recalculation of the $\Delta_{dil}H_m$. The iteration process is continued until the cmc coincided with the break point.

A3 Evaluation of thermodynamic parameters from the mass action model

According to the mass action model a relation exists between the concentration of surfactant monomers and the concentration of micelles. Although in principle micelles can be polydisperse in size as well as in shape, in the model the micellar solution is generally assumed to be homodisperse. For non-ionic surfactants the model can be easily implemented but for ionic surfactants the binding of counterions

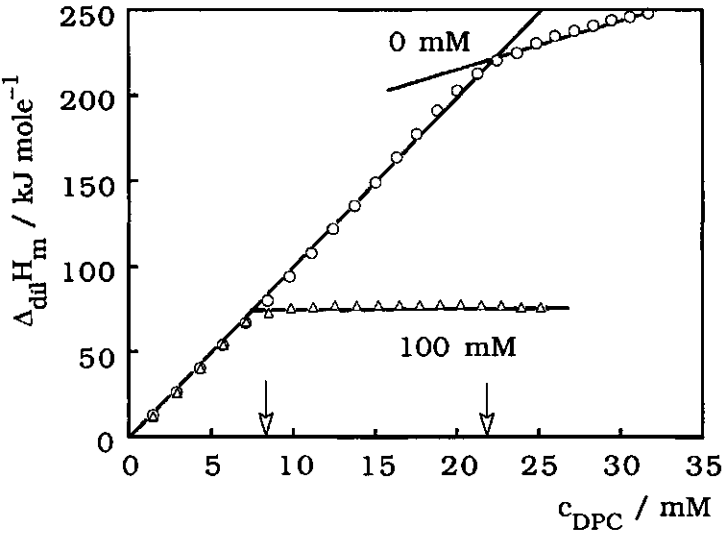

Figure A5. *Cumulative* $\Delta_{dil}H_m$ *of 0.25M DPC; T = 60°C; (added) NaCl concentration is indicated.*

complicates it severely. For simple ionics, such as our alkylpyridinium surfactants, the dissociation of monomers is complete, but the charge of micelles is usually partly compensated by specifically adsorbed counterions.

Let us consider an ionic surfactant molecule LA where L is the surfactant ion with valency z_L and A the counterion with valency z_A. The following equilibrium equation can then be formulated for the formation of homodisperse micelles from n surfactant ions and m counterions

$$nL + mA \rightleftarrows M \qquad (A1)$$

Thermodynamic equilibrium implies

$$n\mu_L + m\mu_A = \mu_M \qquad (A2)$$

The chemical potential follows from

$$\mu_i = \mu_i^o + RT\ln a_i \qquad (A3)$$

and the standard Gibbs energy of micelle formation expressed per mole of surfactant monomers is given by (A4).

$$\Delta_{mic}G_m^0 \equiv \left(\mu_M^0 - n\mu_L^0 - m\mu_A^0\right)/n = -RT\left(\frac{1}{n}\ln a_M - \ln a_L - \frac{m}{n}\ln a_A\right) \qquad (A4)$$

The partial molar enthalpy of micelle formation follows from the temperature dependence of the μ's. However, we have to realize that the aggregation number n and the extent of the counter ion binding may also depend on temperature. In the following we assumed the pressure to be constant. From (A2) it follows:

$$\frac{\partial(n\mu_L/T)}{\partial T} + \frac{\partial(m\mu_A/T)}{\partial T} = \frac{\partial(\mu_M/T)}{\partial T} \qquad (A5)$$

Since:

$$\frac{\partial(\mu_i^0/T)}{\partial T} = -\frac{h_i^0}{T^2} \qquad (A6)$$

where h_i^0 is the standard enthalpy of species a. Therefore

$$\frac{\partial(\mu_i/T)}{\partial T} = -\frac{h_i^0}{T^2} + R\frac{\partial \ln a_i}{\partial T} \qquad (A7)$$

From (A5) and (A7) it follows:

$$n\left(-\frac{h_L^0}{T^2} + R\frac{\partial \ln a_L}{\partial T}\right) + \frac{\mu_L}{T}\frac{\partial n}{\partial T} + m\left(-\frac{h_A^0}{T^2} + R\frac{\partial \ln a_A}{\partial T}\right) + \frac{\mu_A}{T}\frac{\partial m}{\partial T} = \left(-\frac{h_M^0}{T^2} + R\frac{\partial \ln a_M}{\partial T}\right) \qquad (A8)$$

or:

$$Rn\frac{\partial \ln a_L}{\partial T} + Rm\frac{\partial \ln a_A}{\partial T} - R\frac{\partial \ln a_M}{\partial T} = m\frac{h_L^0}{T^2} + m\frac{h_A^0}{T^2} - \frac{h_M^0}{T^2} - \frac{\mu_L}{T}\frac{\partial n}{\partial T} - \frac{\mu_A}{T}\frac{\partial m}{\partial T} \qquad (A9)$$

$$RT^2\left(n\frac{\partial \ln a_L}{\partial T} + m\frac{\partial \ln a_A}{\partial T} - \frac{\partial \ln a_M}{\partial T}\right) = -\Delta h^0 - \left(\frac{\partial n}{\partial T}\right)T\mu_L - \left(\frac{\partial m}{\partial T}\right)T\mu_A \qquad (A10)$$

Where

$$\Delta h^0 = h_M^0 - nh_L^0 - mh_A^0 \qquad \text{(A11)}$$

$$\Delta_{mic}H_m \equiv \left(h_M^0 - nh_L^0 - mh_A^0\right)/n =$$

$$= RT^2\left\{\left(\frac{1}{n}\frac{\partial \ln a_M}{\partial T} - \frac{\partial \ln a_L}{\partial T} - \frac{m}{n}\frac{\partial \ln a_A}{\partial T}\right) - \left(\frac{\partial n}{\partial T}\right)\left(\frac{T\mu_L}{n}\right) - \left(\frac{\partial m}{\partial T}\right)\left(\frac{T\mu_A}{n}\right)\right\} \qquad \text{(A12)}$$

It is reasonable to neglect the temperature dependence of the aggregation number n and the counterion binding m. Thus (A12) becomes:

$$\Delta_{mic}H_m = RT^2\left\{\left(\frac{1}{n}\frac{\partial \ln a_M}{\partial T} - \frac{\partial \ln a_L}{\partial T} - \frac{m}{n}\frac{\partial \ln a_A}{\partial T}\right)\right\} \qquad \text{(A13)}$$

Generally, the values for the enthalpy and the Gibbs energy are obtained from the cmc or the temperature dependence of the cmc. We assume the activity coefficients unity and (1/n) being small for large n in (A4) and (A13). Now we have to distinguish between the situation with and without electrolyte. In the absence of indifferent electrolyte, $c_L = c_A$ and it follows from (A4) that

$$\Delta_{mic}G_m^0 = RT\left(1 + \frac{m}{n}\right)\ln cmc \qquad \text{(A14)}$$

and from (A13) that

$$\Delta_{mic}H_m = -RT^2\left(1 + \frac{m}{n}\right)\frac{\partial \ln cmc}{\partial T} \qquad \text{(A15)}$$

If no counterion binding occurs m/n=0, with 100% counterion binding m/n=1. If the electrolyte concentration is much higher than that of the surfactant then $\ln a_A \sim \ln c_{salt}$ and $\ln a_L \sim \ln cmc$. (A4) and (A13) can be written as (A16) and (A17).

$$\Delta_{mic}G_m^0 = RT\left(\ln cmc + \frac{m}{n}\ln c_{salt}\right) \qquad (A16)$$

$$\Delta_{mic}H_m = -RT^2\frac{\partial \ln cmc}{\partial T} = R\frac{\partial \ln cmc}{\partial(1/T)} \qquad (A17)$$

$\Delta_{mic}G_m$ and $\Delta_{mic}H_m$ are dependent on the choice of the value of m/n.

A4 Enthalpy of Dilution of Post-Micellar Solutions

In the post-cmc region the enthalpies of dilution of micelles, $\Delta_{dil}H_m$ (when c>cmc), presented in figures A6 and A7, are to a large extent dependent on the electrolyte concentration. The observed $\Delta_{dil}H_m$ is the sum of the next different contributions:

(i): Geometrical change in the shape of the micelles (e.g. rod-like to spherical)

(ii): Change in the aggregation number and porosity (packing) of the micelles.

(iii): Interaction between micelles.

(iv): Interaction between the charged head groups.

(v): Interaction between head groups and oppositely charged counter ions.

(i) and (ii) are supposedly temperature dependent, because the hydrophobic effects are sensitive to the temperature change. The rest are electrostatically determined and rather insensitive to the temperature.

The dilution enthalpy of monomers and dilution of the indifferent electrolyte are negligible, and we do not take those into account. What are the contributions of (iii)-(v) to $\Delta_{dil}H_m$? When charged micelles are in close vicinity they repel each other. There are enthalpy and entropy changes involved in this electrostatic repulsion. If we consider the enthalpy change in this process, dilution of micelles leads to a decrease in repulsion and must be exothermic. On the other hand, in diluted micelles, especially at low electrolyte concentration, the counterions partly dissociate which is an endothermic process. The endothermic contribution is thus due to:

- dissociation of a neutral compound into charged species.

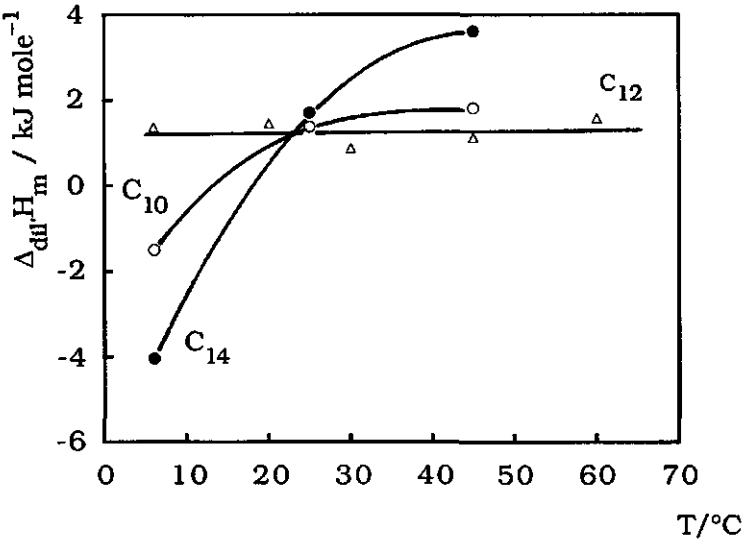

Figure A6. *$\Delta_{dil}H_m$ (c>cmc), for DePC, DPC and TPC in water as a function of temperature.*

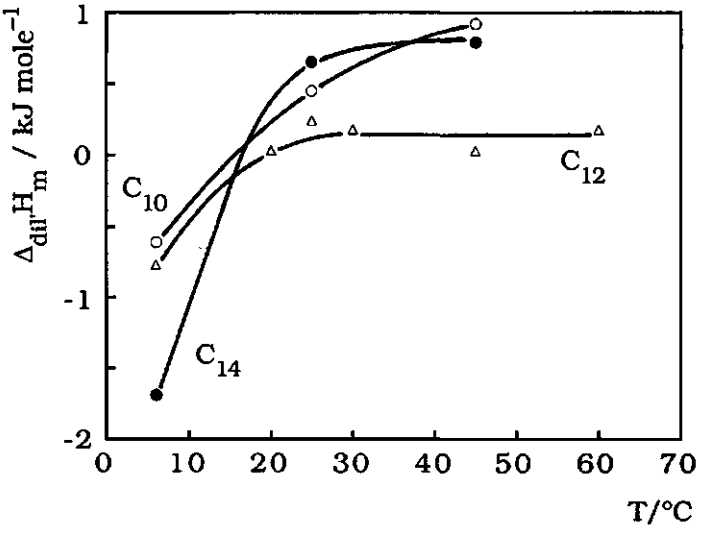

Figure A7. *$\Delta_{dil}H_m$ (c>cmc), for DePC, DPC and TPC in 0.1 M NaCl as a function of temperature.*

- increasing repulsion between the charged head groups being a part of micelles.

In our experiments $\Delta_{dil}H_m$ for DePC and TPC in water is temperature dependent. It seems that in the case of DPC the hydrophobic effect and the electrostatic contribution compensate each other. TPC has the highest values of $\Delta_{dil}H_m$ suggesting that some change in the aggregation number and/or in the micellar shape occurs. The stepwise form of the microcalorimetric titration curves of TPC as it is shown in figures 5 and 6, confirms this conclusion. The fact that a sharp change in the slope of $T/\Delta H_{dil}$ curves occurs around $T = T_{trans}$ is another evidence for the presence of a change in the shape and aggregation number of micelles. This trend can be related to the aggregation number change or to the micellar form change as well. In the case of DePC it is much less pronounced.

Table A2. *Shift in $\Delta_{dil}H_m$ of differential enthalpy curves of DePc, DPC and TPC at different electrolyte concentrations and temperatures. The experimental errors are 0.03, 0.1 and 1 kJ mole-1 for DePC, DPC and TPC respectively.*

surfactant	c_{NaCl} mM	T °C	pre-cmc enthalpy shift (kJ mole^{-1})	post-cmc enthalpy shift (kJ mole^{-1})
DePC	0	6	0.0	?
		25	0.0	0.0
		45	0.2	0.3
	100	6	0.0	0.0
		25	0.0	0.0
		45	1.8	0.0
DPC	0	6	~0	0.0
		20	0.1	0.3
		30	~0	~0
		45	0.5	1.0
		60	1.0	1.0
	100	6	~0	0.5
		20	0.1	0.2
		30	~0	0.3
		45	1.0	0.8
		60	2.0	1.0
TPC	0	6	1.8	0.0
		25	1.2	0.9
		45	2.3	2.3
	100	6	0.9	0.0±1.5
		25	0.2	1.9
		45	6.4	9.0

CHAPTER 4

Adsorption of Cationic Surfactants on Homoionic–Kaolinite Surfaces

Abstract

The adsorption of two cationic surfactants, dodecylpyridinium chloride (DPC) and dodecyltrimethylammonium bromide (DTAB), on Na-kaolinite is studied by measuring adsorption isotherms and electrophoretic mobilities. For both surfactants, adsorption isotherms measured at different electrolyte concentrations show a common intersection point (cip) at a surfactant concentration which is close to the isoelectric point (iep) of the kaolinite particles in the presence of adsorbed surfactant. The adsorption of surfactants continues to rise beyond compensation of the surface charge, indicating that not only electrostatic interactions are involved. Our experimental data fit well into a bilayer model based on the Frumkin-Fowler-Guggenheim isotherm equation.
The different effect of the DPC adsorption on the (relative) surface charge of Na- and Cs-kaolinite, as determined by the potentiometric titration, is caused by specific adsorption of Cs^+. This is verified by electrophoresis.

4.1 Introduction

The main object of our investigations was to study the interaction of cationic surfactants with a clay mineral surface. The clay characteristics have been extensively described in Chapter 2, whereas several aspects of the micellization process of cationic surfactants were presented in Chapter 3. Now we discuss the behaviour of a mixture of a clay suspension and a cationic surfactant solution. We start with a brief review of the electrostatic interaction between a charged solid surface and ionic amphiphilic species in aqueous media and the aggregation behaviour of these amphiphiles at the surface. In Chapter 5 the emphasis will be on the effect of temperature on adsorption, whereas the thermodynamics of

the interaction between surfactants and kaolinite will be discussed in Chapter 6.

Adsorption of ionic surfactants on oppositely charged surfaces has been studied extensively. Due to the important role of anionic surfactants in industrial applications, the number of papers on anionics strongly exceed that on cationics, except in the case of clay minerals where the adsorption of organic cations has received much more attention than that of organic anions. Reviews have been given by Ginn[1] and by Rosen[2]. Very recently some reviews on the adsorption behaviour of cationic surfactants at air-liquid and solid-electrolyte interfaces were presented in "Cationic Surfactants. Physical Chemistry" (ed. D.N. Rubingh and P.M. Holland) by Ingram and Ottewill[3], and by Fuerstenau and Herrera-Urbina[4]. Below we will review some relevant aspects of the adsorption of cationics at oxide and clay mineral surfaces.

The adsorption of cationic surfactants on oxide surfaces has been studied mainly since the 1950's[5-15]. Fuerstenau[6] emphasized the importance of chain-chain interaction for the adsorption process at concentrations below the critical micelle concentration (cmc) and introduced the concept of 'hemimicelles' for the aggregates formed at the oxide surface. From electrokinetic experiments he concluded that reversal of the electrokinetic charge took place. Tamamushi and Tamaki[7] showed that the adsorption decreases with increasing temperature (over a range of 20-40°C) indicating that the adsorption is an exothermic process. They found S-shaped isotherms for the adsorption of a homologous series of alkylammonium chlorides which are congruent if the concentration is expressed relative to the critical micelle concentration (c/cmc) according to Traube's rule. At a certain adsorption density, the decrease in the equilibrium concentration caused by addition of a CH_2 is compensated by the decrease in the cmc. From the shift of the isoelectric point of alkylammonium ions on quartz Somasundaran et al.[16] calculated a contribution of 1.0 RT per CH_2-group to the adsorption free energy. For the adsorption of alkyltrimethyl-ammonium bromides Bijsterbosch[11] concluded that at low concentration a monolayer is formed as a result of electrostatic interaction whereas at higher concentration a bilayer is developed due to hydrophobic bonding. The formation of hemimicelles and that of bilayers is deriven by hydrophobic bonding. It

makes the surface more hydrophilic than that in the case of a monolayer coverage. Harrop[12] studied the adsorption of cetylpyridinium bromide on silica at different pH's. From the same characteristic shape of the bromide adsorption isotherms as that of the cationic isotherms at pH>6, he concluded that at higher pH values chemisorption (via an ion exchange mechanism) becomes increasingly important.

Adsorption of cationic surfactants on clay minerals is much more complicated than for simple inorganic oxides due to the intrinsic heterogeneity (presence of faces and edges) and the possibility of the presence of interlayers for some clays. As is the case for oxides, electrostatic interactions and hydrophobic bonding are important driving forces for adsorption. In the older (particularly the soil science) literature the importance of van der Waals forces in the case of large organic cations on clays was stressed[17-19]. However, it is unlikely that van der Waals forces are the dominating non-electrostatic forces. Probably the importance of hydrophobic bonding was not recognized in those days. Since the 1960's the adsorption of cationic surfactants has been studied by different investigators. Greenland and Quirk[19] measured the adsorption of n-alkylpyridinium bromides on montmorillonite. They found that if the alkyl chain length was longer than eight methyls, the adsorption exceeded the CEC value of the clay. Below the CEC the Na^+ ions were mainly exchanged at the surface for surfactant ions whereas above the CEC co-adsorption of the anion (Br^-) also took place in order to compensate the adsorbed surfactant charge. Adsorption of dodecyldimethylbenzylammonium chloride, distearyldimethylammonium chloride and cetylpyridinium chloride on kaolinite was investigated by Law and Kunze[20]. From X-ray diffraction measurements it was concluded that, unlike for swelling clays e.g. montmorillonite, no intercalation occurred with kaolinite. Recently Cases et al.[21] found that the adsorption of dodecyltrimethylammonium chloride on kaolinite continues beyond the CEC. These authors attributed this to the adsorption of the surfactant on the edges of the kaolinite. A similar suggestion was made by Xu et al.[22] for the adsorption of the same surfactant on kaolinite above the CEC.

In spite of the amount of work that has been done with respect to the adsorption of (cat)ionic surfactants on mineral surfaces, a lot of questions about the adsorption mechanism remain unanswered e.g.

-'What are the separate contributions of the edges and the faces to the adsorption?';
-'What is the nature of the bilayer or the hemimicelles at the surface?';
-'To what extent is the process enthalpically or entropically determined?';
-'How do we separate electrostatic and non-electrostatic contributions to the adsorption process?' etc.

In this chapter we demonstrate that a greater insight is obtainable by employing several techniques simultaneously under a number of different conditions. To that end we consider the surfactant adsorption to be directly related to the chemical potential of the individual surfactant molecules (monomers) in solution and to the nature of the structural groups on the solid surface as well as to the molecular structure of the surfactant being adsorbed. We consider the adsorption of the two cationic surfactants, dodecylpyridinium chloride (DPC) and dodecyltrimethyl-ammonium bromide (DTAB) on Na-kaolinite. The effects of indifferent electrolyte, pH and the nature of the counter ion on adsorption are determined. Potentiometric titrations of Na- and Cs-kaolinite in the presence of DPC are carried out in order to determine the mechanism of proton (and hydroxyl) charge formation for this homo-ionic clay. We also studied the effect of adsorption of DPC and DTAB on the electrophoretic mobilities of Na-kaolinite particles. Our data can be qualitatively well interpreted in terms of a model that we have developed for bilayer adsorption of ionic surfactants.

4.2 Experimental

4.2.1 Materials

Sigma Na-kaolinite was used in the powder form as is explained in Chapter 2. A pure sample of DPC was used as described in Chapter 3. DTAB 99% was obtained from Aldrich-Chemie and used without further purification. For DPC and DTAB the curves of surface tension (γ) against the logarithm of the concentration (ln c) show no dip, indicating that

these surfactants are surface chemically pure (see Figures 1 and 2). From NMR measurements no chemical impurities could be detected.

All solutions are prepared by weight. The indifferent electrolytes used were NaBr and NaCl for the systems including DTAB and DPC, respectively.The quality of the distilled water and all chemicals used in this work were the same as those described in Chapter 2.

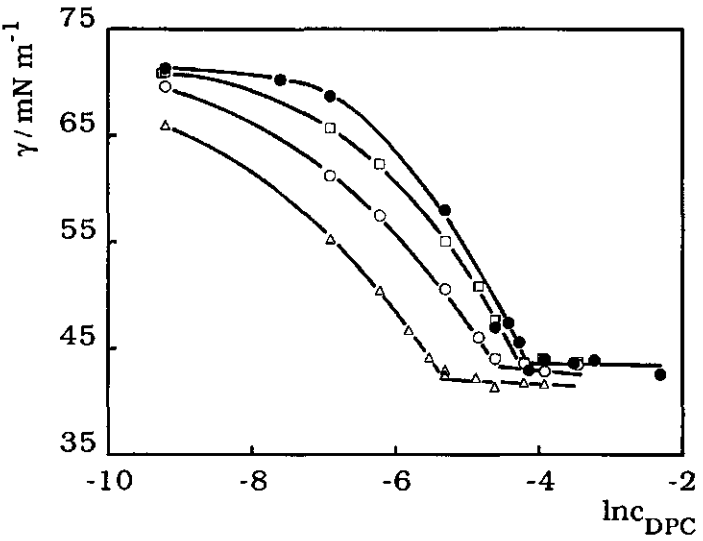

Figure 1. *γ / lnc curves for aqueous DPC solutions; c_{NaCl} 0 (Δ), 5 (o),20 (□) and 100 mM(●); T = 20°C.*

4.2.2 Methods

The surface tensions of surfactant solutions were determined by the static Wilhelmy plate method. Different solutions were made from 0.1 M DPC and 0.2 M DTAB stock solutions. All measurements were performed at room temperature.

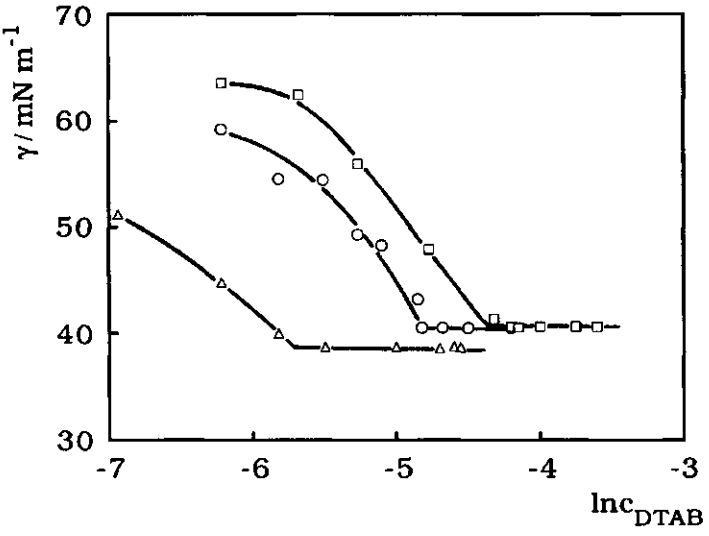

Figure 2. *γ / lnc curves for aqueous DTAB solutions; c_{NaBr} 0 (Δ), 10 (o), and 100 mM (□); T = 20°C.*

Adsorption was determined batchwise by depletion measurements. About 2 g of Na-kaolinite powder was added to the indifferent electrolyte solution. The pH of the suspension was adjusted by addition of 0.05 M solution of NaOH or HCl. Thereafter a certain volume of surfactant solution was added and the suspension placed in a thermostatted shaker. The order of addition of the components had no significant effect on the results. Although adsorption equilibrium was rapidly obtained (within 15 min.) we continued shaking for 3 hours. In the meantime the pH was re-adjusted if necessary.

In order to perform adsorption measurements over a temperature range between 6 and 60°C, it was not easy to separate the clay from the solution by centrifugation without disturbing the adsorption equilibrium. Therefore, the suspension was filtered using a 100 ml double-walled thermostatted filter cell, see Figure 3. A Millipore filter membrane type GS (pore size 22 nm) was used. The equilibrium concentrations of DTAB and DPC were measured by complexation with bromothymol blue as will be described in Chapter 5.

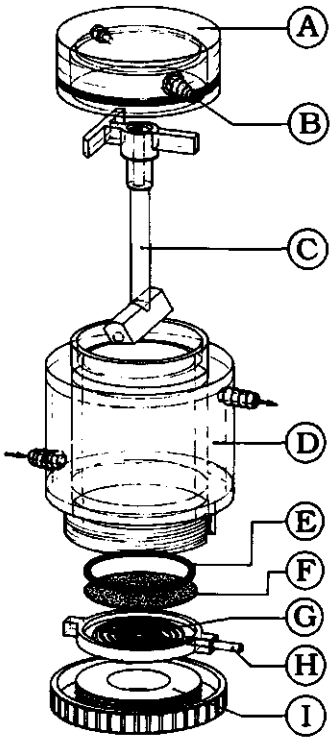

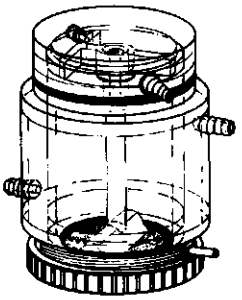

Figure 3. *Schematic presentation of the titration cell. (A) top plate, (B) N_2 stream inlet (C) stirring bar, (D) double-walled reservoir (E) O-ring, (F) filter membrane, (G) filter plate, (H) bottom plate and (I) filtrate outlet.*

The adsorbed amounts of surfactants were calculated from depletion of the adsorbate. The reversibility of the adsorption with respect to a temperature change was confirmed by measuring a few points of an adsorption isotherm in the following way. First, the temperature of the suspension in the presence of DPC was lowered to 5°C, at which it was kept for a few hours. After warming it up to 20°C the adsorption was measured. The same sample was heated to 60°C and kept for several hours again, then cooled down to 20°C and the adsorbed amount was measured. The adsorption of DPC on pre-cooled and pre-warmed clay suspensions did not show any significant difference from those measured in the usual way.

Potentiometric titrations of Na-kaolinite and Cs-kaolinite were first performed in the absence of DPC and then (on the same sample) in the presence of different amounts of DPC. Experimental details are explained in Chapter 2. The blanks were indifferent electrolyte solutions containing the same amounts of DPC as in the suspensions but with no clay. The position of the titration curves with respect to each other were checked by addition of DPC to a kaolinite suspension at a certain pH. We recall

here that there is hysteresis in the titration curves (see Chapter 2); in this chapter we present the same curves as in Chapter 2, viz. the base-titration curves.

Electrophoretic mobilities of kaolinite sols were determined by a microelectrophoresis Zetasizer II (Malvern, Instruments Ltd.) apparatus. A volume of 6 cm^3 of the Na-kaolinite suspension (1.3% by mass) as is discussed in Chapter 2, was added to about 90 cm^3 of a surfactant solution at a desired concentration of indifferent electrolyte (NaCl or NaBr for DPC or DTAB, respectively). The pH was adjusted using 0.05 M HCl, HBr or NaOH standard solutions and the final volume was adjusted to 100 cm^3. The suspension was then sonicated in an ultrasonic bath for 20 min. Afterwards the pH was rechecked and the electrophoretic mobility measured.

4.3 Results and Discussion

4.3.1 Molecular Cross-Section of the Surfactants

In order to analyse adsorption phenomena of surfactants at interfaces on a molecular scale, knowledge of the molecular area of the surfactant is essential. However, for (asymmetric) amphiphilic molecules with flexible chains this property cannot be unambiguously determined. For the interpretation of adsorption phenomena at solid-liquid interfaces the effective molecular area of a surfactant, which has been adsorbed perpendicular to the surface in a densely packed monolayer, is most relevant. This area can be estimated by three independent methods. First, it can be obtained by calculating the geometrical cross-section from a molecular model. Second, one can estimate the effective molecular area at the air-liquid interface near the critical micelle concentration using γ/lnc curves according to the Gibbs equation. Finally, the molecular area can be directly determined from adsorption experiments at the solid-liquid interface from the estimated monolayer coverage and the effective specific surface area of the adsorbent.

In Figures 1 and 2 the surface tension of DPC and DTAB solutions is presented as a function of lnc at various electrolyte concentrations. The

cmc is identified as the break in the γ/lnc curves (Table 1). The results are in a good agreement with the cmc's measured by conductometry. The difference between the two methods are within experimental error.

The adsorption at the air-water interface can be derived from the Gibbs equation[23,24]:

$$d\gamma = -s^{\sigma}dT - \sum_{i}\Gamma_i d\mu_i \qquad (1)$$

In (1) γ is the surface tension, T is the temperature, s^{σ} is the surface excess entropy, μ_i is the chemical potential of component i and Γ_i is its surface concentration. For a completely ionized surfactant in aqueous electrolyte at constant temperature we can write:

$$d\gamma = -RT\left(\Gamma_{Na^+}\frac{dc_{Na^+}}{c_{Na^+}} + \Gamma_{A^-}\frac{dc_{A^-}}{c_{A^-}} + \Gamma_{L^+}\frac{dc_{L^+}}{c_{L^+}}\right) \qquad (2)$$

Where A^- is the common anion (Cl^- or Br^- in our experiments) and L^+ is the organic cation, dodecylpyridinium and dodecyltrimethylammonium respectively. Electroneutrality implies that:

$$\Gamma_{A^-} = \Gamma_{Na^+} + \Gamma_{L^+} \qquad (3)$$

At constant indifferent electrolyte concentration $d\,c_{NaA} = d\,c_{Na^+} = 0$, $dc_{LA} = dc_{A^-}$ and $dc_{LA} = dc_{L^+}$, hence,

$$-\frac{1}{RT}\left(\frac{\partial\gamma}{\partial \ln c_{LA}}\right)_{c_{NaA}} = \Gamma_{A^-} \times \frac{c_{LA}}{c_{LA} + c_{NaA}} + \Gamma_{L^+} \equiv x \qquad (4)$$

For constant surfactant concentration experiments $d\,c_{LA} = d\,c_{L^+} = 0$, $dc_{NaA} = dc_{Na^+}$, $dc_{NaA} = dc_{A^-}$, so that

$$-\frac{1}{RT}\left(\frac{\partial\gamma}{\partial \ln c_{NaA}}\right)_{c_{LA}} = \Gamma_{A^-} \times \frac{c_{NaA}}{c_{NaA} + c_{LA}} + \Gamma_{Na^+} \equiv y \qquad (5)$$

From Equations 3, 4 and 5 we can derive Equations for the adsorption of the three ionic components in our system.

$$\Gamma_{L^+} = \frac{x}{2}\left[1 + \frac{c_{NaA}}{c_{LA} + c_{NaA}} - \left(\frac{y}{x} \times \frac{c_{LA}}{c_{LA} + c_{NaA}}\right)\right] \qquad (6a)$$

$$\Gamma_{A^-} = \frac{x + y}{2} \qquad (6b)$$

$$\Gamma_{Na^+} = \frac{y}{2}\left[1 + \frac{c_{LA}}{c_{LA} + c_{NaA}} - \left(\frac{x}{y} \times \frac{c_{NaA}}{c_{LA} + c_{NaA}}\right)\right] \qquad (6c)$$

In order to determine the adsorbed amount the surface tension γ is plotted against surfactant concentration at constant electrolyte concentration or against the electrolyte concentration at constant surfactant concentration. From these plots x and y are obtained by interpolation. Γ_{max} at a given indifferent electrolyte concentration is equal to the value of Γ_{L^+} near the cmc and the molecular cross-section is

Table 1. *cmc, Γ_{max} and molecular cross-section a_s for DPC and DTAB. All values are at 20°C, except those between parentheses which are at 25°C.*

LA	c_{salt} mM	This work			Literature			
		cmc mM	Γ_{max} µmol m^{-2}	a_s nm^2	cmc mM	Γ_{max} µmol m^{-2}	a_s nm^2	Ref.
DPC	0	15.4	2.59	0.64	(14.6-15.0)	2.7	(0.62)	*
	5	15.1	3.14	0.53				
	20	11.2	3.21	0.52				
	100	5.6	3.35	0.50		3.0	0.55	30
DTAB	0	14.0	3.34	0.50	15.4-15.9			**
	10	10.8	3.58	0.46				
	100	4.0	3.76	0.44	(4.5)			30

* ref. 25-31.

** ref. 28 and 32.

$1/N_{Av}\Gamma_{L+}$. In Table 1 the molecular areas together with some literature data are presented.

The decrease in the molecular area on increasing the electrolyte concentration is clearly due to charge screening which reduces the repulsion between the surfactant head groups located at the air/water interface.

From the geometry of the molecules molecular cross sections of DPC and DTAB are calculated as follows. We consider the pyridinium group as a regular hexagon whose plane is parallel to the surface. The length of the hexagon side is calculated from the C—C and the C—H bond lengths and the H atomic radius (being 0.1395 nm, 0.1084 nm and 0.037 nm respectively). The area is calculated from the formula for the area of a regular polygon with n sides each of length l: *(area =1/2 nl^2 cot (180/n))*. For our hexagonal group the area is 2.6l^2. From the geometry of the molecules a cross-section of 0.21 nm^2 is calculated for the head groups of DPC.

The effective molecular area of trimethylammonium head group is defined as area of a circle which encloses its projection onto the (horizontal) plane of adsorption. The radius of this circle is calculated from the sum of the projections of C—N, C—H bonds and the H atomic radius, being 0.106 nm (sin 37.5°), 0.147 nm (sin 72°) and 0.037 nm, respectively, 37.5° being the angle between C—H and the vertical plane and 72° the angle between C—N and C—H bonds. The radius of the circle amounts to 0.242 nm and its area to 0.18 nm^2.

On inspection of the adsorption isotherms, it is seen that at the isoelectric point, (iep) the charged head groups compensate the surface charge. Therefore the adsorption at the iep may also be compared with the cation exchange capacity (CEC). The CEC as determined by the silver-thiourea method (57 mmole kg^{-1}) more or less represents the total number of sites on the plates and on the edges. However, the ammonium acetate method (at a fixed pH of 7) only enables the measurement of the cation exchange of the plates (30 mmole kg^{-1}). Another method for the estimation of the CEC is to measure the adsorption of paraquat (1,1'-dimethyl-4,4'-dipyridinium chloride) which mainly adsorbs on the plates[33]. According to de Keizer[33] the plateau value of the adsorption

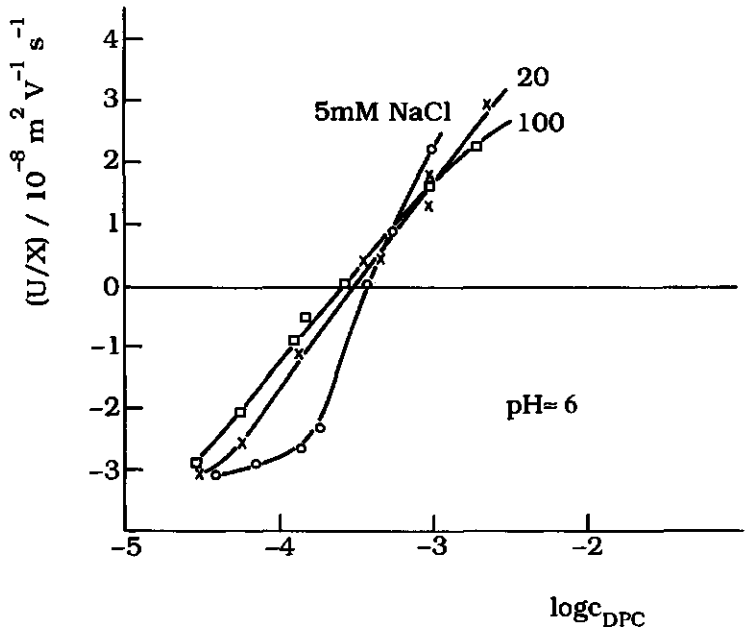

Figure 4. *Electrophoretic mobility of Na-kaolinite as a function of DPC concentration for three NaCl concentrations, pH = 6, T = 20°C.*

isotherm of paraquat on Sigma kaolinite amounts to 16 mmole g^{-1} which is very close to the iep we measured. The fact that at the iep the adsorption is comparable with the ammonium acetate CEC and the paraquat CEC values indicates that the surfactant adsorption essentially takes place on the plates.

From our adsorption data at the iep (see Figures 4, 5, 6 and 8) an area of about 0.4 nm^2 for each molecule of DPC or DTAB is obtained.

The discrepancy between the three above mentioned molecular areas is not surprising. Considering the entropy of the surfactant molecules and the electrostatic repulsion between the head groups, we do not expect a close packing at the solid-liquid interface. The geometrical surface area is therefore not a realistic estimation of the area covered by one molecule at the interface. The area calculated from the γ/lnc curves refers to the air/water interface where the repulsion between the charged head groups and the dissociation of the counterions, which is an entropically driven process, both lead to a larger molecular surface area than at the clay interface. Because of the electrostatic attraction exerted by clay particles,

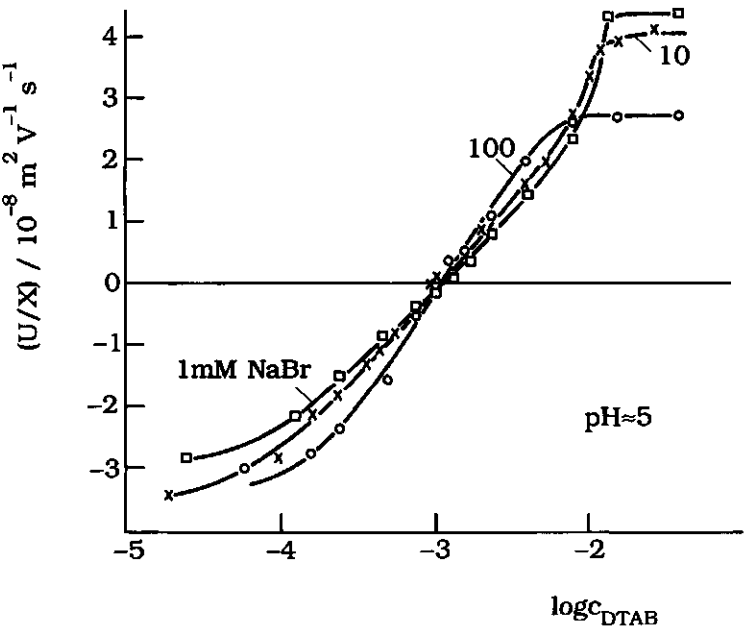

Figure 5. *Electrophoretic mobility of Na-kaolinite as a function of DTAB concentration for three NaBr concentrations, pH = 5, T = 20°C.*

the packing at a clay surface will be denser than that at the air-water interface. Hence the effective molecular area must remain different from any of those computed on the basis of a model.

4.3.2 Adsorption Isotherms and Electrophoretic Mobilities

Adsorption isotherms of the cationic surfactants DPC and DTAB on kaolinite are measured at different electrolyte concentrations, at pH = 5. For kaolinite, edges are present with a pzc of 6.8, (see Chapter 2) in addition to the permanently (negatively) charged planar faces. Thus at a solution pH of 5 the edges are slightly positive. Therefore, it is likely that the adsorption behaviour is dominated by the faces. This will be discussed in more detail in Chapter 5.

Adsorption isotherms at 20 and 60°C are presented in Figures 6 to 9. The strong surfactant-surface interaction is reflected by the initial steep

rise. The adsorption of the surfactants reaches a pseudo saturation value at the critical micelle concentration (cmc) of the surfactant.

As we presented elsewhere[34], for DPC an (unsharp) common intersection point is detected near $\log c_{DPC} = -3.3$ independent on the temperature.

The intersection point for DTAB is located at $\log c_{DTAB} = -3.0$. The occurrence of a more or less well-defined common intersection point (cip) in adsorption isotherms of organic ions at different electrolyte concentrations is a general feature of organic ion adsorption at an oppositely charged interface[35]. At low adsorbate concentrations the adsorption decreases with increasing electrolyte concentration, while at high adsorbate concentration the effect is reversed. An indication of the presence of such a cip was given by Chander et al.[36] who have reported adsorption isotherms of dodecyl sulphate on alumina at different salt concentrations (c_S) which deviate at low c_S, but merge at high c_S. The point were the isotherm start to coincide corresponds with the iep. Brownawell et al.[37] also found an intersection point for the adsorption of DPC on a soil sample.

The presence of a cip in a series of adsorption isotherms at different values of c_S can be qualitatively described by assuming that the organic ions adsorb with their centres of charge in a plane at a small distance from the surface, whereas outside this adsorption plane the double layer is purely diffuse. At low surfactant concentration the adsorption potential ψ_a in the plane of adsorption of the organic ions has a sign equal to that of the surface charge and opposite to that of the organic ions. Increasing the electrolyte concentration compresses the double layer and reduces ψ_a. Consequently, the attractive part of the adsorption energy is decreased and the adsorbed amount will be lower at higher electrolyte concentration. At some degree of adsorption the adsorbate charge compensates the surface charge and ψ_a, is zero. Adding indifferent electrolyte at this

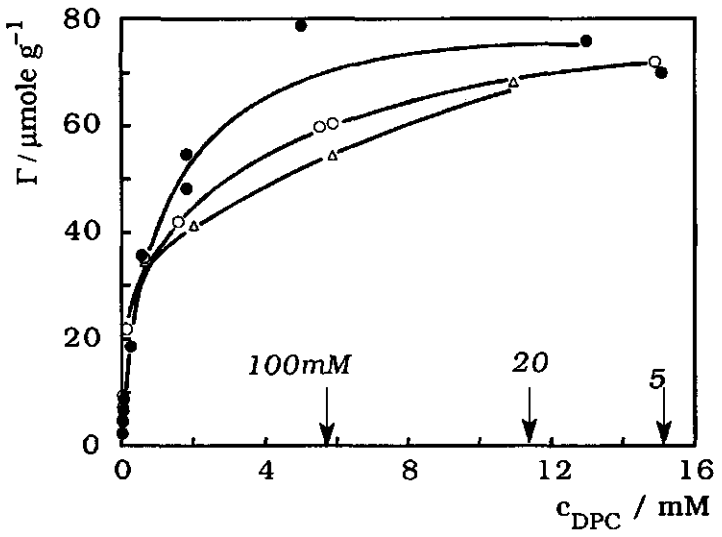

Figure 6. *Adsorption isotherms of DPC on Na-kaolinite at 5(Δ), at 20 (o) and at 100 mM (●) NaCl; T = 20°C, pH = 5.0. The arrows show the cmc's of the aqueous DPC solutions.*

point has no effect on ψ_a and the adsorption of the surfactant is independent on the electrolyte (ionic) strength: the cip corresponds with zero adsorption potential. At high adsorbate concentrations the surface charge is overcompensated by the adsorbate charge and ψ_a has the same sign as the organic ion. The electrostatic repulsion now contributs to the adsorption free energy. Increasing the electrolyte concentration decreases this repulsion and the adsorption increases. The above reasoning applies both to variable charge surfaces and to surfaces with a permanent charge. A thermodynamic analysis of the cip will be given below.

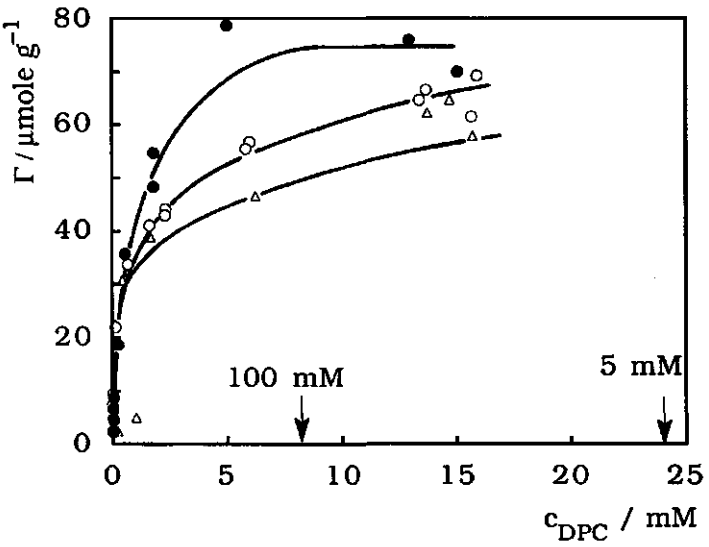

Figure 7. *Adsorption isotherms of DPC on Na-kaolinite at 5 (Δ), at 20 (o) and at 100 mM (●) NaCl; T = 60°C, pH = 5.0. The arrows show the cmc's of the aqueous DPC solutions.*

Electrophoretic mobilities of kaolinite particles in the presence of DPC and DTAB have been measured at pH = 6 and pH = 5, respectively. The results at 20°C are given in Figures 4 and 5 for DPC and DTAB, respectively. The electrokinetic charge changes from negative to positive at monolayer coverage. At the isoelectric point the surface charge is compensated and the diffuse double layer is absent. For DPC the iep is only slightly dependent on c_S and ranges from $\log c_{DPC} = -3.56$ for 10^{-1} M NaCl to −3.42 for 5.10^{-3} M NaCl. The iep occurs at a slightly lower concentration than the cip although the difference is hardly beyond experimental error. For DTAB the intersection point ($\log c_{DTAB} = -3.0$) and the iep coincide exactly. In principle one would expect a small difference between the iep and the cip. As the edges are slightly positive at the experimental pH, no adsorption at the edges is expected. Thus, the iep will be present if the small positive charge at the edges is compensated by the effect of a small negative electrokinetic charge at the faces, i.e. just before compensation of the plate charge. However, the cip will occur if the charge on the plates has been compensated, i.e.

indifferent electrolyte does not affect adsorption at this point and, hence, the local electrostatical potential is zero. Thus in general it is concluded that the iep occurs at a slightly lower concentration than the cip. This trend seems to be met for DPC, but for DTAB a difference is absent within experimental error. Anyhow, the conclusion seems to be justified that at the pzc of the edges the cip and the iep will coincide.

The effect of pH on the adsorption of DPC on Na-kaolinite is given in Figure 10. The adsorption increases slightly with pH. This potential change is due to the variation of the specific adsorption of the protons at the faces. To get a rough idea of the latter we can correlate the shift of the adsorption isotherm at a fixed value of the adsorbed amount to the surface potential. To this end we neglect non-electrostatic lateral interactions and adopt a general isotherm according to Equation 7.

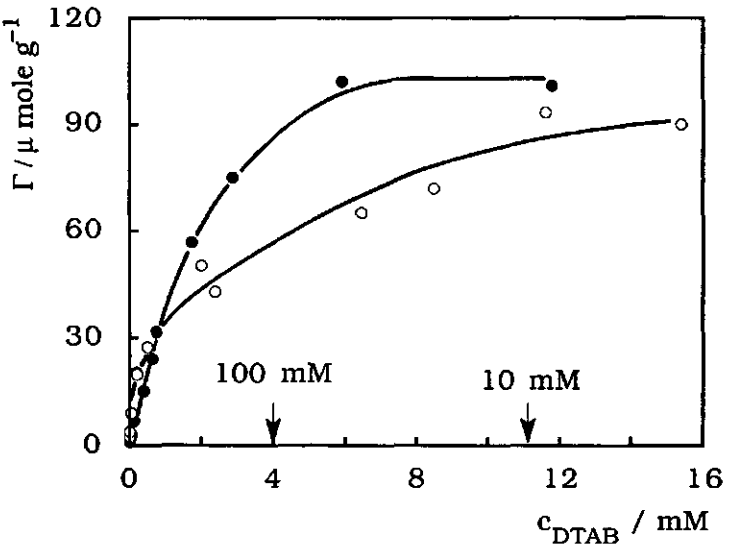

Figure 8. *Adsorption isotherms of DTAB on Na-kaolinite at 10 (o) and at 100 mM (●) NaBr; T = 20°C, pH = 5.0. The arrows show the cmc's of the aqueous DTAB solutions.*

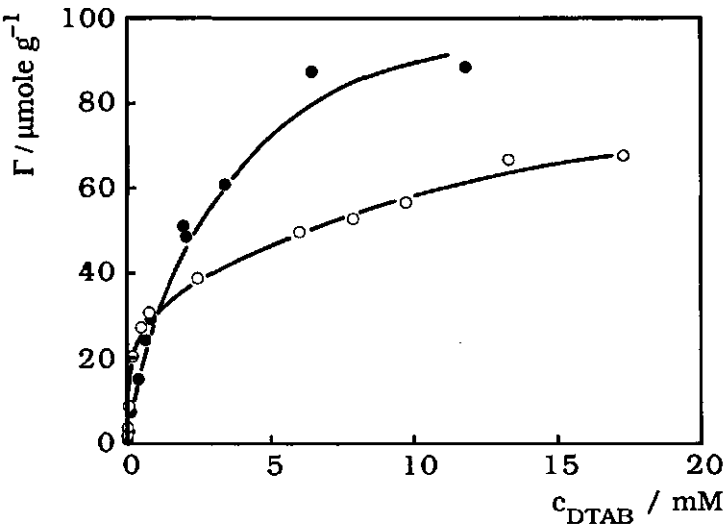

Figure 9. *Adsorption isotherms of DTAB on Na-kaolinite at 10 (o) and 100 mM (●) NaBr; T = 60°C, pH = 5.0.*

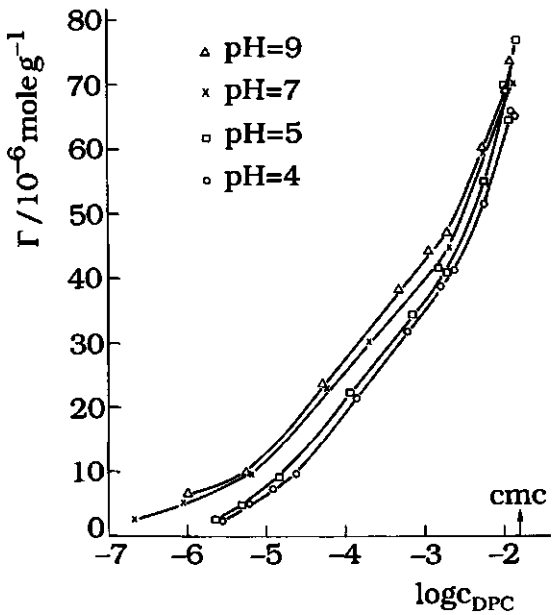

Figure 10. *Adsorption of DPC on Na-kaolinite, as a function of pH at c_{NaCl} = 5 mM, T = 20°C*

$$f(\theta) = k_{eq} c_{DPC} \exp(-F\psi_a / RT) \qquad (7)$$

where ψ_a is the potential at the plane of adsorption and the other symbols have their usual meaning. At a constant degree of coverage of surfactant θ we can write:

$$\Delta\psi_a = \frac{RT}{F} \Delta \ln c_{DPC} \qquad (8)$$

The calculated $\Delta\psi_a$ values per pH unit are presented in Table 2. The potential ψ_a corresponds effectively to the potential at the adsorption plane of the faces. Apparently the variation of the potential ψ_a is relatively large up to about half the saturation value (Γ = 40) and becomes much smaller for higher coverages. This behaviour is fully in line with an adsorption of the charged head groups close to the surface, whereas the head groups of the second layer are much further removed from the surface and consequently the potential in the second adsorption plane is less effected by specific adsorption of protons. The variation of the potential change with pH in the adsorption plane can be compared with the change of the ζ-potential of the bare kaolinite particle with pH. The ζ-potentials are calculated from the electrophoretic mobility data using the computer program MOBZET[38], which is based on the work of O'Brien and White[39]. For the radius of the particles an average of 500 nm was chosen. The results expressed as a potential change per pH unit are also given in Table 2.

Assuming that the adsorption takes place only at the plates, then ψ_a is merely a potential due to the faces, whereas ζ is some average of the effect of the faces and the edges. We also assume, for the sake of simplicity, that the edge-face area ratio is 1 and the ζ-potential is a simple average of the faces and the edges: $\zeta_{(total)} = (\zeta_{(edge)} + \zeta_{(plate)})/2$. The effect of pH on the edge potential is much higher between pH 4-5 (22 mV) than around the point of zero charge of the edges (6 mV) which is in accordance with a simple Gouy-Chapman model. The potential change of the faces with pH is lowest at pH 7 as is expected because there are mainly protons (and not hydroxyls) which change the surface charge at the faces. We are aware that the O'Brien and White model is not a perfectly suitable model for our kaolinite particles, nevertheless it gives

Table 2. *Estimated surface potential and ζ-potentials from the adsorption isotherms and from the mobility measurements respectively. amount adsorbed* (Γ) *is in μmole* g^{-1}.

Γ	($\Psi_{a(pH=5)}-\Psi_{a(pH=4)}$) (mV)	$0.5(\Psi_{a(pH=7)}-\Psi_{a(pH=5)})$ (mV)	$0.5(\Psi_{a(pH=9)}-\Psi_{a(pH=7)})$ (mV)
5	7	20	7
10	9	12	5
20	9	11	5
30	6	9	5
40	7	6	5
50	6	4	2
60	2	5	1
70	2	0	1
0 (Δζ)	15	9	6

a rough indication about the magnitude of the potential in the plane of shear. Although the above reasoning is rather qualitative, it is evident that the shift of the adsorption isotherms with pH correlates with the shift of the ζ-potential with pH.

The charge reversal of the kaolinite particles due to the adsorption of DPC or DTAB is reflected in the colloidal stability of the kaolinite particles. The maximum stability occurs in the absence of the surfactant ions. During addition of the surfactant the sol becomes increasingly unstable (it can be easily filtered). At the iep the suspension is almost completely coagulated, and further addition of the surfactant restabilizes the suspension. Apparently the stability is a consequence of the repulsion between the diffuse double layers of the particles. Generally speaking, at a constant surfactant concentration, addition of indifferent electrolyte decrease the colloidal stability of the suspension.

Information about the configuration of the amphiphilic molecules at the solid-liquid interface can be deduced from the wetting properties. Fuerstenau[40] reported that the hydrophobicity of a hematite surface increases with the addition of anionic surfactants. Around the iep the hydrophobicity passes through a maximum. The surfactant cations first

adsorb with their (hydrophilic) head groups adjacent to the surface, their tails are oriented towards the bulk. Therefore, the surface becomes more hydrophobic. Formation of the second layer takes place with the surfactant head groups oriented towards the bulk; hence the interface becomes hydrophilic again.

4.3.3 Potentiometric Titrations in the Presence of DPC

The effect of the adsorption of DPC on the surface charge of Na- and Cs-kaolinite in the presence of 0.02 M NaCl and CsCl respectively, as

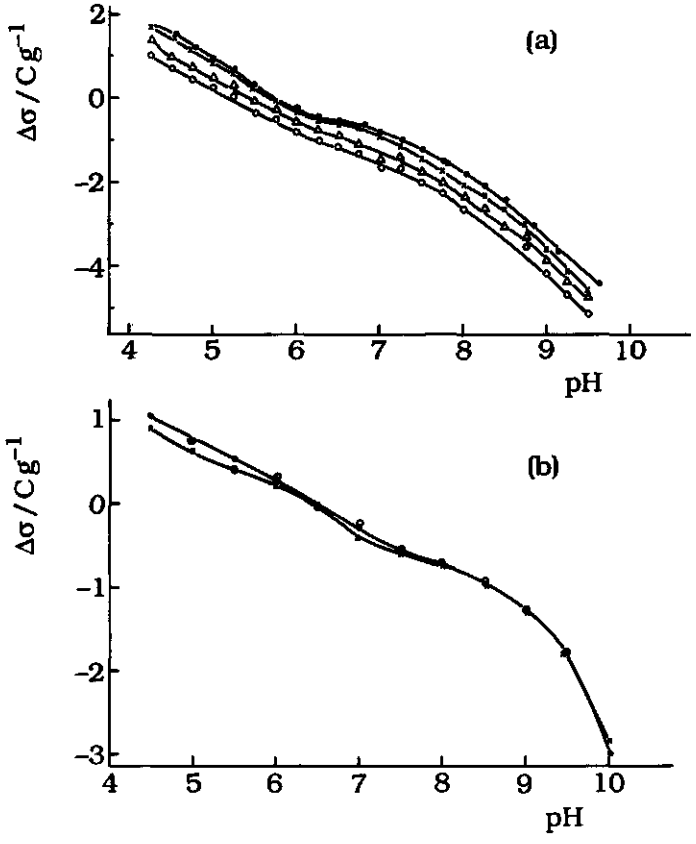

Figure 11. *Charge potential curves of (a) Na-kaolinite, (b) Cs-kaolinite.* •*0,* ×*0.1,* △*0.3 , and* ○ *0.5 mmole DPC is added.* c_{NaCl} *= 20 mM, T = 20°C.*

obtained by potentiometric titration, are presented in Figures 11a and 11b.

In the case of Na-kaolinite the surface charge decreases with increasing adsorption of DPC. Brownawell et al.[37] and Greenland and Quirk[41] also reported a decreasing surface charge for the adsorption of alkylpyridiniums on kaolins and a montmorillonite clay. In our case the amount of desorbed protons is slightly dependent on pH and ranges from 6 to 9 μmole/ g or 0.6 to 0.9 C/g for the highest surfactant concentration. The number of exchanged protons is small compared to the adsorption of DPC molecules and ranges from about 5% below the cip till 15-20% above the cip. The minimum desorption of protons is near the point of zero charge of the edges, epzc, (pH = 6-7) and we assume that the proton exchange mechanism is different below and above the epzc. Below the epzc the charge decrease is caused by the exchange of adsorbed protons due to adsorption of DPC molecules at the plates. Above the epzc, adjustment of the variable charge at the edges becomes significant as soon as charge reversal takes place at the plates i.e. as the plates become positive due to DPC adsorption. However, it can not be completely excluded that above the epzc some adsorption of DPC at the edges also occurs leading to a relative large proton exchange, although this is certainly only a fraction of the adsorption above the cip.

In the case of Cs-kaolinite addition of DPC had hardly any effect on the surface charge suggesting that the Cs^+ ions adsorb more strongly and specifically replace protons and dodecylpyridinium ions. Substantial adsorption of Cs^+ on the plates is also evident from our potentiometric titration results as indicated in Chapter 2.

Cases et al.[21] and Xu et al.[22] attributed the overcompensation of the CEC to the adsorption of the surfactant on the edges of kaolinite and not to the formation of a bilayer. Generally speaking adsorption of cationic surfactants on silica is pH dependent[8,12], so that the maximum adsorption increases roughly 3 times when the pH rises from 4 to 9. This suggests that the surfactants have a relatively low affinity to a positively charged surface. The edges of kaolinite are positively charged when pH ≤ 6.8. In our opinion the affinity of a cationic surfactant for the positively charged adsorption sites located at the hydrophilic edges is very low as is the case for oxides. This is also supported by the fact that no abrupt change in the

adsorbed amount around pH=7 is observed. These conclusions are confirmed by the temperature dependence of the adsorption and direct enthalpy measurements, to be presented in Chapter 5. The temperature dependence of the adsorption enthalpy has the same trend as that of micellization indicating that beyond monolayer coverage bilayers or surfactant aggregates are formed at the plates rather than monolayers at the edges.

4.3.4 Thermodynamic Analysis of the Common Intersection Point

The interfacial thermodynamics of adsorption of ions from an aqueous electrolyte solution can be evaluated on the basis of the Gibbs adsorption equation which in a rather general form has been given before (Equation 1). We will present a more sophisticated analysis of the Gibbs equation than in section 4.3.1, but in principle a similar detailed analysis could have been also given for the analysis of the Gibbs equation at the air water interface.

We will apply Equation (1) to the system described above, which contains an NaCl concentration c_s, potential or charge determining ions H^+ and OH^- and a strongly specifically adsorbing organic ion L^+, at constant temperature. First $\Gamma^{\sigma}_{H_2O}$ can be eliminated using the Gibbs-Duhem equation for the bulk phase so that Gibbs' equation for such a system reads:

$$d\gamma = -\Gamma^{(s)}_{H^+} d\mu_{H^+} - \Gamma^{(s)}_{OH^-} d\mu_{OH^-} - \Gamma^{(s)}_{Na^+} d\mu_{Na^+} - \Gamma^{(s)}_{Cl^-} d\mu_{Cl^-} - \Gamma^{(s)}_{L^+} d\mu_{L^+} \quad (9)$$

The relative surface excess concentration of i, $\Gamma^{(s)}_i$, or briefly the adsorption of i is defined as:

$$\Gamma^{(s)}_i \equiv \Gamma^{\sigma}_i - \frac{x_i}{x_{H_2O}} \Gamma^{\sigma}_{H_2O} \quad (10)$$

where x_i is the mole fraction of i. To simplify the notation we will drop the superscript (s) of the excess quantities. Equation (9) can be worked out by considering the following conditions.

1) The chemical potentials of H^+ and OH^- are related by the dissociation product of water, so that (at constant T) $d\mu_{H^+} = -d\mu_{OH^-}$.

2) It is assumed that the salt concentration c_s determines the ionic strength. This is a good approximation because c_s is always much higher than the concentrations of charge determining and organic ions. The activity coefficients of Na^+ and Cl^- are then equal and:

$d\mu_{Na^+} = d\mu_{Cl^-} \approx 0.5 d\mu_s$.

3) The surface excess concentrations are related by the electroneutrality condition:

$$\Gamma_{H^+} - \Gamma_{OH^-} + \Gamma_{Na^+} - \Gamma_{Cl^-} + \Gamma_{L^+} = 0 \qquad (11)$$

For the given conditions the surface charge, σ_0, the charge due to L^+, σ_{L^+}, and the indifferent components of charge, σ_{Na^+} and σ_{Cl^-}, can be defined by Equations (12) - (15):

$$\sigma_0 \equiv F(\Gamma_{H^+} - \Gamma_{OH^-}) \qquad (12)$$

$$\sigma_{L^+} \equiv F\Gamma_{L^+} \qquad (13)$$

$$\sigma_{Na^+} \equiv F\Gamma_{Na^+} \qquad (14)$$

$$\sigma_{Cl^-} \equiv -F\Gamma_{Cl^-} \qquad (15)$$

where F is the Faraday constant. Equation (9) can now either be written as

$$d\gamma = \frac{-\sigma_0}{F} d\mu_{H^+} - \left(\frac{\sigma_{Na^+} - \sigma_{Cl^-}}{2F} \right) d\mu_s - \Gamma_{L^+} d\mu_{L^+} \qquad (16a)$$

or as

$$d\gamma = \frac{\sigma_0}{F} d\mu_{OH^-} - \left(\frac{\sigma_{Na^+} - \sigma_{Cl^-}}{2F} \right) d\mu_s - \Gamma_{L^+} d\mu_{L^+} \qquad (16b)$$

Cross-differentiation between the μ_{L^+} and μ_s terms can be carried out in (16a) or (16b). From (16b) we have:

$$\left(\frac{\partial \Gamma_{L^+}}{\partial \mu_s} \right)_{T,\mu_{H^+},\mu_{L^+}} = \frac{1}{2F} \left(\frac{\partial \left(\sigma_{Na^+} - \sigma_{Cl^-} \right)}{\partial \mu_{L^+}} \right)_{T,\mu_{H^+},\mu_s} \qquad (17)$$

The conditions specified in (17) are rather awkward. In order to render Equation (17) applicable we rewrite the LHS using the extended chain rule:

$$\left(\frac{\partial\Gamma_{L^+}}{\partial\mu_s}\right)_{T,\mu_{H^+},\mu_{L^+}} = \left(\frac{\partial\Gamma_{L^+}}{\partial\mu_s}\right)_{T,\mu_{H^+},c_{L^+}} - \left(\frac{\partial\Gamma_{L^+}}{\partial\mu_{L^+}}\right)_{T,\mu_{H^+},\mu_s} \times \left(\frac{\partial\mu_{L^+}}{\partial\mu_s}\right)_{T,\mu_{H^+},c_{L^+}} \qquad (18)$$

Substitution of (18) into (17) leads to:

$$\left(\frac{\partial\Gamma_{L^+}}{\partial\mu_s}\right)_{T,pH,c_{L^+}} = \frac{1}{2RTF}\left(\frac{\partial\left(\sigma_{Na^+}-\sigma_{Cl^-}\right)}{\partial\ln c_{L^+}}\right)_{T,pH,c_s} + \left(\frac{\partial\Gamma_{L^+}}{\partial\ln c_{L^+}}\right)_{T,pH,c_s} \times \left(\frac{\partial\ln f_{L^+}}{\partial\mu_s}\right)_{T,pH,c_{L^+}} \qquad (19)$$

where it is assumed that $d\mu_{L^+} = RTd\ln f_{L^+}c_{L^+} = RTd\ln f_{L^+} + RTdc_{L^+}$.

Below it will be shown that $\Gamma_{L^+}(\ln c_{L^+})$ isotherms, measured at different values of the indifferent electrolyte concentration, show a cip. The condition for the cip is

$$\left(\frac{\partial\Gamma_{L^+}}{\partial\mu_s}\right)_{T,pH,c_{L^+}} = 0 \qquad (20)$$

Schematically the situation is illustrated by de Keizer et al. in reference 35. Below the cip the adsorption decreases with increasing electrolyte concentration, whereas above the cip it increases. From the adsorption isotherms we are able to derive $(\sigma_{Na^+}-\sigma_{Cl^-})$ as a function of c_{L^+} by integration of (19):

$$\left(\sigma_{Na^+}-\sigma_{Cl^-}\right)-\left(\sigma_{Na^+}-\sigma_{Cl^-}\right)^* = 2RTF\int_{\ln c_{L^+}{}^*}^{\ln c_{L^+}}\left\{\left(\frac{\partial\Gamma_{L^+}}{\partial\mu_s}\right)_{T,pH,c_{L^+}} + C\right\}d\ln c_{L^+} \qquad (21)$$

where the second term on the RHS of Equation (21) is abbreviated to C. If we neglect for this moment the correction term C, it can be argued that

$(\sigma_{Na^+} - \sigma_{Cl^-})$ as a function of c_L^+ passes through a minimum. As Na^+ and Cl^- ions only adsorb in the diffuse layer, the minimum value of $(\sigma_{Na^+} - \sigma_{Cl^-})$ must correspond with a diffuse charge zero, i.e. $\sigma_{Na^+} = \sigma_{Cl^-} = 0$ and the cip corresponds with the iep.

Deviations can arise for heterogeneous surfaces with different charging mechanisms as is the case for clay minerals as we discussed in Chapter 2. Deviations between the position of the cip and the minimum in $(\sigma_{Na^+} - \sigma_{Cl^-})$ can also arise if the correction term C is not negligible any more. Hence, for intermediate values of the electrolyte concentration ($c_s > 10^{-2}$ M) the cip gives only a rough indication of the iep.

Finally, it has been assumed that the cations and anions of the background electrolyte adsorb only in the diffuse layer. Activity effects and specific adsorption may be assumed to be negligible for low electrolyte concentrations so that the cip coincides with the iep. At moderate or high indifferent electrolyte concentrations specific adsorption may occur. For cation adsorption the potential in the plane of adsorption becomes more positive, so that the adsorption of the organic cations is counteracted. To obtain the same adsorption as at the cip of the curves at low salt concentration a larger value of $\log c_L^+$ is required. Hence the intersection point shifts to higher $\log c_L^+$. This tendency might partly explain the shift of the intersection points observed for DPC, see Figure 4.

Specific adsorption will also affect the iep's. Due to specific adsorption of Na^+, the surface potential ψ_a becomes more positive, so that Γ_L^+ is lower at a given value of $\log c_L^+$. However, in order to reach the iep less adsorption of L^+ is required (Na^+ is also adsorbed within the plane of shear). The iep is therefore less sensitive to specific adsorption than the cip.

Our conclusion in accordance with the thermodynamic analysis is that a cip may occur for the adsorption of organic ions at different electrolyte concentrations. This has been experimentally observed. The occurrence of a cip which is located very close to the iep seems to be a general property for adsorption of organic cations on a surface with an opposite charge[35].

4.3.5 A Model for the Bilayer Adsorption of Surfactants

Our study of adsorption isotherms of DPC and DTAB on kaolinite in combination with electrophoresis measurements and microcalorimetry has shown the occurrence of two distinguished regions, one below and the other above the iep (see also Chapters 5 and 6). These data together with acid-base titration results for the clay (given above and in Chapter 2) suggest that:

(a) the adsorption of surfactants occurs mainly on homogeneous plates

(b) the adsorption extends beyond monolayer coverage.

A powerful approach to model surfactant adsorption is a self-consistent field lattice theory for two-block copolymers as performed by Böhmer et al[42]. In our work we prefer to apply a more simple bilayer model based on a Frumkin-Fowler-Guggenheim (FFG) model modified for charged adsorbates. In this model we start with a homogeneous surface on which surfactant molecules adsorb, neglecting the different conformations of the surfactant molecules at the surface. Each adsorbed molecule forms an adsorption site for the formation of a second layer similar to that in the BET model. The affinity for the second layer is different from that for the first layer. Due to the amphipolar character of the surfactant molecules formation of more than two layers is forbidden.

In this model the fraction of sites which are occupied by the surfactant molecules θ consists of two parts (a) a fraction θ_1 of the sites which is occupied in the first layer and (b) a fraction θ_2 of the sites occupied in a second layer (θ_2). Maximum amount of θ_1 and θ_2 being 1, $\theta = \theta_1 + \theta_2$ and θ_2 is always smaller than θ_1. For the first layer we can write:

$$\frac{\theta_1 - \theta_2}{1 - \theta_1} = x e^{-\left(\Delta G_1^0 + \theta_1 \Delta G_1^{lat}\right)/RT} \qquad (22)$$

and for the second layer:

$$\frac{\theta_2}{\theta_1 - \theta_2} = x e^{-\left(\Delta G_2^0 + \theta_2 \Delta G_2^{lat}\right)/RT} \qquad (23)$$

In (22) and (23) ΔG_1^0 and ΔG_2^0 are the standard adsorption Gibbs energies for the formation of the first and the second layer respectively, ΔG_1^{lat} and

ΔG_2^{lat} are the lateral interaction Gibbs energies for the first and the second layer formation, respectively. The parameter x is the mole fraction of the surfactant in the solution. From (22) and (23) using $\theta = \theta_1 + \theta_2$ we derive

$$\frac{\theta}{1-\theta}.\frac{1}{x} = e^{-\left(\Delta G_1^0+\theta_1\Delta G_1^{lat}\right)/RT} + xe^{-\left(\Delta G_1^0+\theta_1\Delta G_1^{lat}+\Delta G_2^0+\theta_2\Delta G_2^{lat}\right)/RT}\left(\frac{2-\theta}{1-\theta}\right) \qquad (24)$$

Our analysis of the bilayer model is based on the last equation. If the saturation value for adsorption is directly estimated from the adsorption isotherms then this equation contains four unknowns which can be solved from the adsorption isotherms. From the extrapolated experimental adsorption isotherms Γ_{max} was estimated to be 90 and 110 μmole/g for DPC and DTAB, respectively.

We start with the analysis of the adsorption at the highest electrolyte concentration. For this case we may neglect the lateral interactions between the adsorbed surfactant molecules in the first layer ($\Delta G_1^{lat}=0$). The term ($\theta_2\Delta G_2^{lat}$) is negligible with respect to the other terms in the exponential part for low surface coverage. Plotting the left hand side of the Equation (24) against $\left(x\frac{2-\theta}{1-\theta}\right)$ for DPC and DTAB at 0.1M electrolyte gives a reasonably linear curve. From the slopes and the intercepts ΔG_1^0 and ΔG_2^0 are obtained. These last parameters are used to fit the complete isotherms to the best value of ΔG_2^{lat} at 0.1M electrolyte.

The parameters at the other electrolyte concentrations are obtained as follows. We used the region of low surface coverage of the isotherms at different electrolyte concentrations to obtain ΔG_1^0 relative to its value at 0.1M. At low coverage $\theta_2 \approx 0$ and θ_1 is very small which gives $RT\delta\ln x = -\delta\Delta G_1^0$. Adsorption isotherms at different electrolyte concentrations show a cip. At the cip the right hand sides of Equations (23) and (24) are independent of the electrolyte concentration. As at the cip θ_2 is much smaller than θ_1, ΔG_1^{lat} can be easily deduced and ΔG_2^0 and ΔG_2^{lat} are obtained by fitting the isotherm, applying the properties of the cip mentioned above.

At the cip the calculated θ_2 was 0.04 for DPC both at 20 and 60°C. For DTAB, θ_2 was 0.12 and 0.06 at 20 and 60°C respectively.

The adsorption Gibbs energy parameters (in RT units) for the adsorption of DPC and DTAB on Na-kaolinite at 20 and 60 °C and various indifferent electrolyte concentrations are given in Table 3. These parameters are used to calculate the adsorption isotherms from our bilayer model. Experimental and calculated semilogarithmic isotherms are compared in Figures 12-15.

The model fits the experimental data very well at all temperatures and electrolyte concentrations. Small deviations at the lowest salt concentration may arise from experimental errors in the values measured for very low equilibrium concentrations.

Some interesting trends are obtained from the thermodynamic parameters shown in Table 3.

Comparison of the ΔG_1^0 for DPC and DTAB shows that DPC has slightly more affinity for the surface than DTAB (see column 4 of Table 3). The same conclusion has been drawn elsewhere[34] on the basis of the fact that the iep for DPC occurs at a lower surfactant concentration than for DTAB. This is also illustrated by calculated values of θ and θ_1 at 20°C which are presented in Figure 16. At 60°C the same trend is observed both for DPC and DTAB. The origin of the higher affinity of DPC compared to DTAB may be due to differences in the behaviour of the head groups or to those of the counterions. If the latter were the dominating factor we would expect the difference in ΔG_1^0 between DPC and DTAB to increase with electrolyte concentration. Since this is not the case we conclude that the head group difference is the most important factor. Probably the pyridinium ring with its π electrons has more affinity for the kaolinite surface the trimethylammonium.

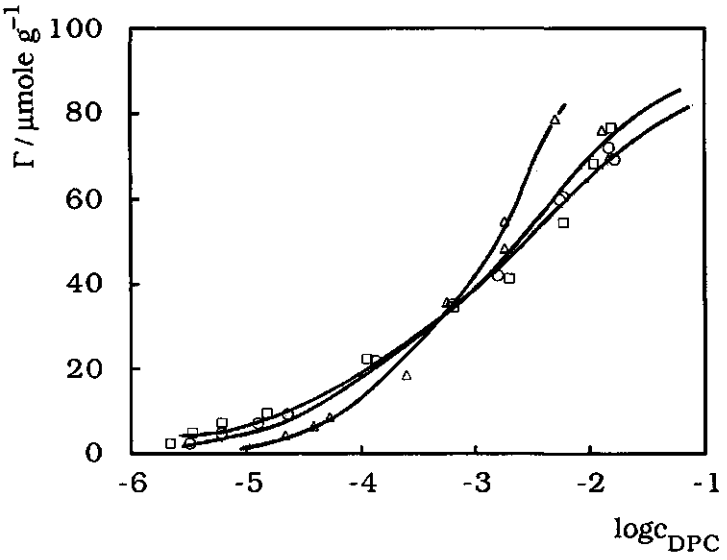

Figure 12. *Experimental and calculated adsorption isotherms for the adsorption of DPC on Na-kaolinite. The solid curves are the calculated isotherms. The experimental results at 5, 20 and 100 mM NaCl are indicated by (□), (o) and (Δ) respectively. T = 20°C, pH = 5.*

The decrease of ΔG_1^0, for both surfactants, upon increasing electrolyte concentration is due to the screening of the charge by the background electrolyte. For the first layer, salt addition decreases the attractive electric potential which is reflected in the decrease of (negative) ΔG_1^0. The change in ΔG_1^0 due to the increasing electrolyte concentration is almost equal for DPC and DTAB, showing that the charged groups of the surfactants are adsorbed at the same distance from the surface. The effect

Table 3. *Thermodynamic parameters calculated from our bilayer adsorption model for the isotherms measured at different electrolyte concentrations and temperatures.*

LA	T (°C)	c_{salt} (mM)	ΔG_1^0 / RT	ΔG_1^{lat} / RT	ΔG_2^0 / RT	ΔG_2^{lat} / RT
DPC	20	5	-13.8	3.0	-9.0	1.0
		20	-13.4	1.8	-8.9	0.0
		100	-12.3	0.0	-8.8	-2.3
	60	5	-14.4	3.0	-9.0	4.0
		20	-13.6	1.8	-9.0	2.0
		100	-12.3	0.0	-8.9	-2.0
DTAB	20	10	-12.7	3.7	-10.1	2.0
		100	-10.9	0.0	-10.0	0.0
	60	10	-12.7	3.1	-9.4	8.0
		100	-11.1	0.0	-9.0	0.0

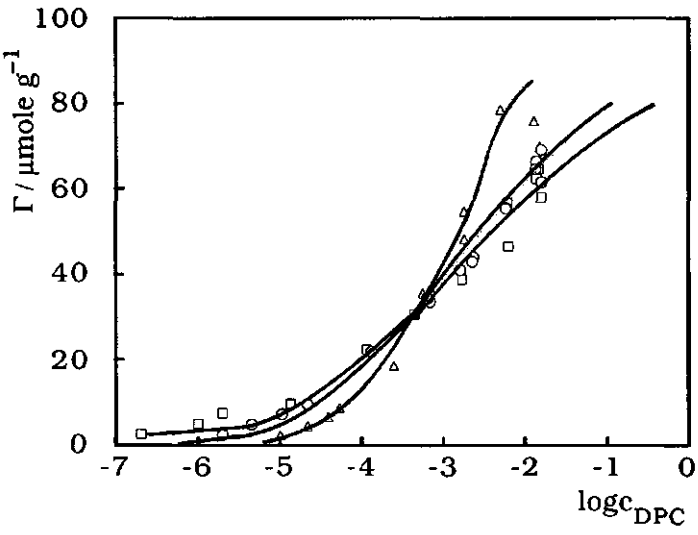

Figure 13. *Experimental and calculated adsorption isotherms for the adsorption of DPC on Na-kaolinite. The solid curves are the calculated isotherms. The experimental results at 5, 20 and 100 mM NaCl are indicated by (□), (o) and (Δ) respectively. T = 60°C, pH = 5.*

of salt addition on ΔG_1^0 is opposite to that on ΔG_1^{lat} as is shown in columns 4 and 5 of Table 3. The salt effect on the former is unfavourable whereas on the latter it is favourable (the presence of electrolyte decreases the repulsion between the surfactants head groups). These two effects compensate each other at the cip. The ΔG_2^0 's are hardly dependent on the salt level, suggesting that the second layer adsorption indeed occurs when the surface potential is very small (~zero). Salt addition causes a decrease of ΔG_2^{lat} for both surfactants at both temperatures and as a result of a decrease in the repulsion between the head groups the adsorption is promoted, see column 7 of Table 3.

For DPC and DTAB, the sum of $(\Delta G_1^0 + \Delta G_1^{lat})/RT$ is not temperature dependent, showing that the effect of the temperature on the adsorption at the first layer is negligibly small, i. e. according to the Gibbs Helmholtz equation $\Delta H_1^0=0$. On the other hand, $(\Delta G_2^0 + \Delta G_2^{lat})/RT$, is smaller at 20°C than at 60°C, implying that the process is exothermic within this temperature range.

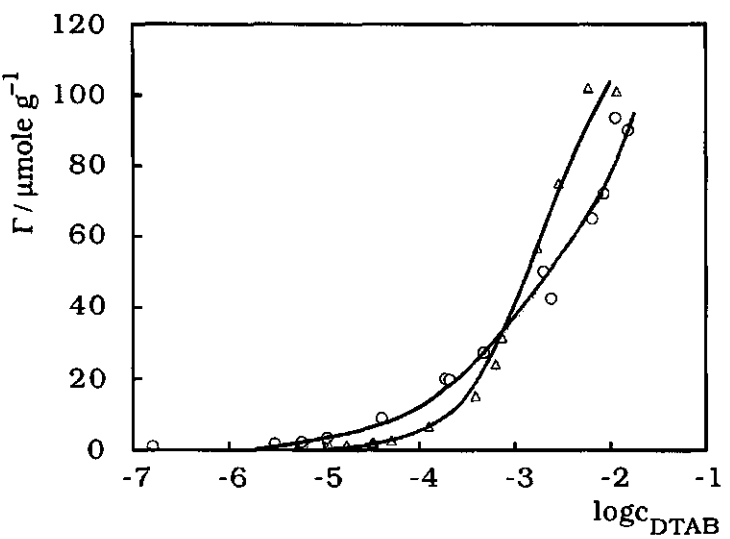

Figure 14. *Experimental and calculated adsorption isotherms for the adsorption of DTAB on Na-kaolinite. The solid curves are the calculated isotherms. The experimental results at 10 and 100 mM NaBr are indicated by (o) and (Δ), respectively. T = 20°C, pH = 5.*

Since the formation of the double layer around kaolinite particles involves electrical and chemical contributions, generally the change in the Gibbs energy can be written as: $\Delta G_1^0 = \Delta G_{1(el)}^0 + \Delta G_{1(chem)}^0$. As we mentioned above, the formation of the second layer begins when the surface potential $\psi_a \sim 0$, hence to a good approximation it follows that at the cip: $\Delta G_2^0 = \Delta G_{2(chem)}^0$. For the adsorbed molecules in the first as well as in the second layer, ΔG^{lat} can be divided into two terms as follows: $\Delta G^{lat} = \Delta G_{hydroph}^{lat} + \Delta G_{el}^{lat}$, where the first term on the right hand side refers to the attraction between the hydrophobic tails and the second one is attributed to the repulsion between the head groups. The sum of the adsorption Gibbs energy parameters of the second layer formation for the DPC is slightly higher (about one kT) than that of DTAB, both at 20 and at 60°C. Since the surfactants have the same tail this difference is either due to the difference in the hydrophilic part or due to the different counterions. From our data we can not point out whether the head group or the counterion is more important.

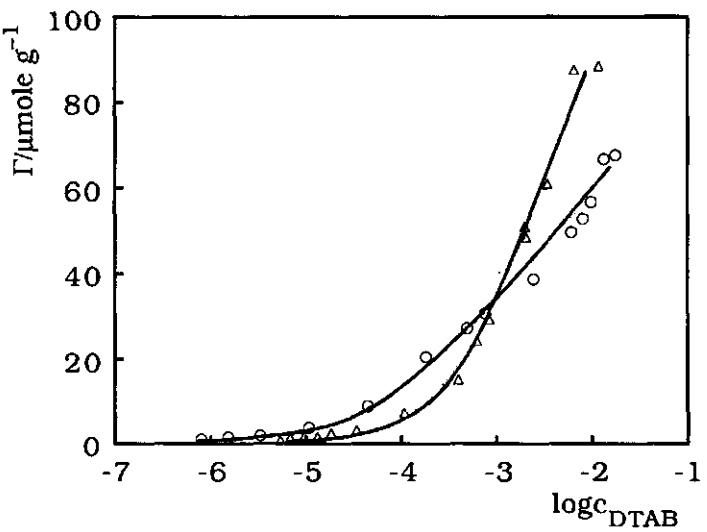

Figure 15. *Experimental and calculated adsorption isotherms for the adsorption of DTAB on Na-kaolinite. The solid curves are the calculated isotherms. The experimental results at 10 and 100 mM NaBr are indicated by (o) and (Δ), respectively. T = 60°C pH = 5.*

4.4 Conclusions

Cationic surfactants, DPC and DTAB, are specifically adsorbed on Na-kaolinite. The evidence obtained from our experimental results is as follows:

(a) within a certain pH range, the increase in proton adsorption sites, as calculated from the potentiometric titration results exceeds than that of DPC adsorption sites, showing that DPC does not occupy all the available sites on the kaolinite surface.

(b) comparison of the acid/base titrations in the presence of DPC with the titrations performed in its absence, shows that the adsorption of the surfactant molecules takes place mainly on the plates. Interactions of the cationic head group with the (negatively) charged sites and of the hydrophobic tail on previously adsorbed molecules both contribute to the adsorption mechanism. The adsorption of both surfactants extends beyond compensation of the surface charge. The closeness of the iep in the presence of the surfactants to the cip of the isotherms at different electrolyte concentrations suggests that under our experimental conditions, pH = 5, the contribution of the edges to the total surface potential is small. Specific adsorption of Cs^+ ions on the kaolinite surface deduced from the potentiometric titrations of Cs-kaolinite (see Chapter 2 of this thesis) is confirmed by acid/base titrations of Cs-kaolinite in the presence of DPC.

Our experimental results fit well into a simple bilayer model developed on the basis of the FFG equation. From this model the degrees of occupancy of the first and the second layer can be estimated at any point of the isotherm. The slightly higher affinity of DPC than that of DTAB for the surface is reconfirmed by the comparison of the calculated θ_1's.

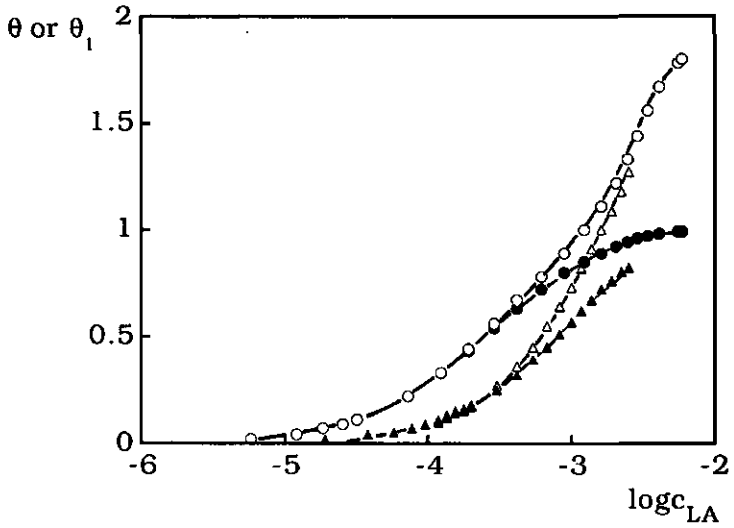

Figure 16. *Calculated θ (empty symbols) and θ_1 (full symbols) for the adsorption of (o) DPC and (Δ) DTAB on Na-kaolinite; T = 20°C, pH = 5* $c_{electrolyte}$ *= 100mM.*

4.5 Acknowledgements

The contributions of Mr. B. van der Wal in the analytical work and Mr. A. J. van der Linde in writing the computer program for the model calculations are gratefully appreciated.

4.6 References

(1) Ginn M. E. In "*Cationic Surfactants*"; Ed. Jungermann E.; Marcel Dekker, Inc.,: New York, **1970**; Vol. 4, p 369-415.

(2) Rosen M.J. In "*Surfactants and Interfacial Phenomena*"; Ed. Rosen M.J.; John Wiley & Sons: Toronto, **1989**; p 431.

(3) Ingram B.T., Ottewill R.H. In " *Cationic Surfactant Physical Chemistry*", Ed. Rubingh B. N. and Holland P. M., Marcel Dekker, Inc: New York and Basel, **1991**; Vol. 37, p 87-140.

(4) Fuerstenau D. W., Herrera-Urbina R. In " *Cationic Surfactants, Phsical Chemistry.*"; Ed. Rubingh B.N. and Holland P.M., Marcel Dekker: New York and Basel, **1991**; Vol. 37, p 407-447.
(5) deBruyn P. L. *Trans. AIME.*, **1955**, *202*, 291-295.
(6) Fuerstenau D. W. *J. Am. Chem. Soc.*, **1956**, *60*, 981-985.
(7) Tamamushi B., Tamaki K., Proceedings: *"Second International Congeress of Surface Activity"*, Ed. Schulman J. H., London, **1957.**
(8) Tadros Th. F. *Colloid Interface Sci.*, **1974**, *46*, 528-540.
(9) Jaycock M. J., Ottewill R. H. *Bull. Inst. Mining Met.*, **1963**, *73*, 497-503.
(10) Patzko A., Szanto F. *Colloids and Surfaces*, **1987**, *25*, 173-182.
(11) Bijsterbosch B. H. *J. Colloid Interface Sci.*, **1974**, *47*, 186-198.
(12) Harrop R. *Surface Technology*, **1978**, *7*, 81-90.
(13) Vilcu R., Oleanu M. *Revue Roumaine de Chimie*, **1975**, *20*, 1041-1050.
(14) Somasundaran P., Fuerstenau D. W. *J. Phys. Chem.*, **1966**, *70*, 90-112.
(15) Dobiås B. *Tenside*, **1972**, *6*, 322-330.
(16) Somasundaran P., Healy T. W., Fuerstenau D. W. *J. Phys. Chem.*, **1964**, *68*, 3562-3566.
(17) McAtee J. L., Hackman J. R. *Am. Miner.*, **1964**, *49*, 1569-1577.
(18) Greenland D. J., Quirk J. P. *Clays Clay Minerals*, **1964**, *15*, 178-191.
(19) Greenland D. J., Quirk J. P. *Clays Clay Minerals*, **1962**, *9*, 484-499.
(20) Law J.P., Kunze G. W. *Soil Sci. Soc Amer. Proc.*, **1966**, *30*, 321-327.
(21) Cases J. M., Cunin P., Grillet Y., Poinsignon C. , Yvon J. *Clay Minerals*, **1986**, *21*, 55-68.
(22) Xu Q., Vasudevan T. V., Samasundaran P. *J. Colloid Interface Sci.*, **1991**, *142*, 528-534.
(23) Overbeek J. Th. G. In "*Colloid and Surface Chemistry. A Self-Study Course.*"; Centre for Advance Engineering Study, Massachusetts Institute of Technology: Massachusett, **1974**.
(24) Lyklema J. In " *Fundamentals of Interface and Colloid Science*"; Vol. 1. Academic Press: London San Diego New York Boston Sydney Tokyo Torronto, **1991**.
(25) Ford W. P. J., Ottewill R. H., Parreira H. C. *J. Colloids Interface Sci.*, **1966**, *21*, 522-528.

(26) Kelvens H. B. *J. Am. Oil Chemists Soc.*, **1953**, *30*, 74-76.

(27) Haydon D. A., Phillips, J. N. *Trans. Faraday Soc.*, **1958**, 54, 1958-62.

(28) Evans D. F., Allen M., Ninham B. W. *J. Solution Chem.*, **1984**, *13*, 87-91.

(29) Rosen M. J., Dahanayaka M., Cohen A. W. *Colloids Surfaces*, **1982**, 5, 159-172.

(30) Schick M. J. *J. Am. Oil. Chemists Soc.*, **1966**, *43*, 1926-1930.

(31) Schick M. J. *J. Phys. Chem*, **1963**, *67*, 1796-1799.

(32) Anacker E. W., Rush R.M., Johnson J.S. *J. Phys. Chem.*, **1964**, *68*, 81-86.

(33) de Keizer A. *Progr. Colloid Polym Sci.*, **1990**, *83*, 118-126.

(34) Mehrian T., de Keizer A., Lyklema J. *Langmuir*, **1991**, *9*, 3094-3098.

(35) de Keizer A., Böhmer M. R., Mehrian T., Koopal L. K. *Colloids Surfaces*, **1990**, *51*, 339-357.

(36) Chander S., Fuerstenau D. W., Stigter D. In " *Adsorption From Solution*", Ed. Ottewill R. H., Rochester C. H. and Smith A. L., Academic Press: London, **1983**; p 478.

(37) Brownawell B. L., Chen H., Collier M. J., Westall J. C. *Environ. Sci. Technol.*, **1990**, *24*, 1234-1241.

(38) de Keizer A. Program:" MOBZET ": Wageningen Agricultural University, **1981**.

(39) O'Brien R. W., White L. R. *J. Chem. Soc. Faraday Trans. II*, **1978**, *74*, 1607-1626.

(40) Fuerstenau D. W., Colic M., Proceedings: *"7 ICSCS"*, Ed. Clausse M and Solans C., Compiégne, **1991.**

(41) Greenland D. J., Quirk J. P., Proceedings: " *Ninth National Conference on Clays and Clay Minerals.*", Ed. Swineford A., Adelaide, **1962.**

(42) Böhmer M. R. *"Adsorption and Micellization of Surfactants. Comparison of Theory and Experiment"*, Ph. D. Thesis, Wageningen Agricultural University, **1991.**

CHAPTER 5

Effect of Temperature on the Adsorption of Organic Cations on Charged Surfaces

Abstract

A study has been made of the adsorption of tetrabutylammonium nitrate (TBAN) on silver iodide and of dodecylpyridinium chloride (DPC) and dodecyltrimethylammonium bromide (DTAB) on Na-kaolinite. Our goal was to identify the Coulombic and non-Coulombic contributions to the driving force. Investigation of the temperature dependence is very suitable for that, besides studying the effects of indifferent electrolytes.
All adsorption isotherms have in common that, if measured at different salt concentration, a common intersection point (c.i.p.) develops, which almost or exactly coincides with the isoelectric point. Before this point adsorption is reduced by electrolyte addition; beyond it, electrolytes promote adsorption. On the hydrophobic AgI, adsorption of TBAN proceeds until monolayer coverage, exhibiting a maximum as a function of temperature. For the amphiphilic molecules DPC and DTAB adsorption on Na-kaolinite is not or not much dependent on temperature before the c.i.p., whereas beyond the c.i.p. adsorption again passes through a maximum as a function of temperature. This second part is driven by hydrophobic bonding; the effect of temperature on the enthalpy shows the same trend as that for micellization of these surfactants.

5.1 Introduction

Adsorption of small organic molecules on mineral surfaces is besides of the pure scientific importance, of much industrial interest such as oil recovery, mineral processing, paper, food, pharmaceutical and cosmetics

industry. Considering the agricultural point of view, ionic surfactants can modify the physical soil properties such as water permeability.

The adsorption of charged organic molecules at the interface between a solid and an aqueous solution is as a rule determined by electrostatic and non-electrostatic interactions. Only the sum of these is observed and there is no unambiguous way to break it down into the constituent parts. However, by studying the influence of indifferent electrolytes and temperature, some unraveling may be achieved. Typically, electrolytes screen Coulombic attraction and repulsion; hence the variation of the amount adsorbed with c_{salt} is a diagnostic tool to obtain information about the electrostatic part of the interaction. From the temperature dependence, insight into the driving force is obtainable (i.e. is the process exothermal or endothermal?) and, indirectly, into the roles played by electrostatic and non-electrostatic interactions. In addition, electrophoresis can provide the charge accumulated within the surface of shear.

In the present paper we illustrate these principles by studying the adsorption of tetrabutylammonium nitrate (TBAN) on silver iodide and of dodecylpyridinium chloride (DPC) and dodecyltrimethylammonium bromide (DTAB) on the clay mineral Na-kaolinite. Adsorption of the spherically symmetrical tetrabutylammonium ions can proceed until monolayer coverage, whereas the amphiphilic ions, DP^+ and DTA^+, are able to form bilayers or surface aggregates. Notwithstanding the differences between these systems, some interesting analogies are observed in the adsorption behavior which, in turn, provide useful information about the mechanism. We note that AgI is more hydrophobic than Na-kaolinite. As will be shown below, adsorption of quaternary ammonium ions on the hydrophobic AgI surface is to some extent similar to the formation of a second layer of amphiphilic molecules on Na-kaolinite.

Hereafter we shall, for easy reference, call all non-electrostatic interactions "chemical", although obviously dispersion forces, hydrophobic bonding, hydrogen bridging etc, basically have an electrical origin.

5.2 Materials and Methods

A silver iodide suspension has been prepared by the slow addition of 0.1 M $AgNO_3$ to a solution of 0.1 M KI in the dark under vigorous stirring . The washed-aged-suspension has a specific surface area of 0.56 m^2 g^{-1} based on methylene blue adsorption [1].

A well-crystallized sample of Sigma (98%) Na-kaolinite has been repeatedly washed with 1M NaCl. The cation exchange capacity (CEC) amounted to 57 meq kg^{-1} as measured by the silver-thiourea method[2] and 30 meq kg^{-1} according to the Schofield (ammonium acetate) method[3]. In de adsorption measurements the Na-kaolinite was added in powder form. The particle diameters range between 0.1 - 4 μm and the BET (N_2) surface area amounts to 12 m^2 g^{-1}. In the electrophoresis measurements a kaolinite sol has been used in which the particles have a diameter smaller than 1 μm. After freeze-drying of the sol the BET surface area of the particles is about the same as that of the original kaolinite powder.

Tetrabutylammonium nitrate (TBAN) was prepared from tetrabutylammonium iodide (Fluka, for polarography) as described elsewhere[1]. Dodecylpyridinium chloride (DPC) has been synthesized from 1-chlorododecane and pyridinium, both of PA grade, and purified according to the method of Colichman[4].

Dodecyltrimethylammonium bromide 99% (DTAB) was obtained from Aldrich-Chemie and used without further purification. The curves of surface tension (γ) against the logarithm of the concentration (ln c) show no dip, indicating that both surfactants are surface chemically pure. From NMR measurements no chemical impurities could be detected. The critical micelle concentrations (c.m.c.) at 20°C in the absence of electrolyte were estimated as 0.0158 M (from γ-log c) and 0.0146 M (from γ-log c and conductometry) for DPC and DTAB, respectively. Literature values of 0.0146 M (25°C)[5] and 0.0159 M (20°C)[6] were reported for DPC and DTAB, respectively.

Water has been pre-purified by reverse osmosis and subsequently passed through a Millipore Super-Q system, and before use boiled for 30 minutes to remove the dissolved gases, especially CO_2. All other chemicals were of pro analyse quality and used without further purification.

Adsorption measurements on AgI have been performed at fixed pAg = 11.6 at different concentrations of TBAN and total volume of 50 ml indifferent electrolyte (KNO_3) solution in volumetric flasks. The amount of AgI was ca. 4 gram. The flasks were rotated end-over-end at the desired temperature for at least 15 hours. In the case of kaolinite adsorption experiments at different surfactant concentrations and pH = 5.00±0.01 have been carried out using about 2.00 gram of kaolinite powder and about 50 ml of indifferent electrolyte solution (NaCl in the case of DPC and NaBr in that of DTAB). The suspensions were shaken for three hours at the desired temperature. During the shaking the pH was checked and readjusted .

In our temperature dependent measurements the DPC and DTAB equilibrium concentrations have been taken up to the c.m.c. In the AgI case, the suspensions settled readily, so that the supernatant could be easily sampled by pipetting; in the clay case, filtering was necessary; it was carried out in a thermostatted filtration cell using a Millipore filter membrane type GS, pore size 22 nm.

The equilibrium concentrations of TBAN, DPC or DTAB in the supernatant or filtrate have been determined by complexation with bromothymol blue[1,7,8] at pH = 9.2. The concentrations of organic cations were measured spectrophotometrically at λ = 419 nm for TBAN and at 422 nm for DPC or DTAB. The adsorbed amounts of organic cations are calculated from the depletion of the adsorptive. Since at low surfactant concentration and T>20°C the amount of the surfactant adsorbed on the filter membrane is not negligible, the data had to be corrected.

Electrophoresis measurements of a silver iodide sol in the presence of TBA^+ ions have been performed in a Rank Bros MK II electrophoresis apparatus, as described by two of us before [1,8]. For kaolinite the mobilities have been determined using a Malvern Zetasizer II instrument.

5.3 Results and Discussion

5.3.1 Electrostatic characterization of the adsorbent surfaces; review of some previous results.

For the present purpose, the electrostatic characterization of the surfaces is important. Two kinds of surface charge (density) have to be distinguished, the real surface charge σ^o and the electrokinetic charge σ^{ek}.

For AgI the two are relatively easily accessible. From potentiometric titrations with KI and $AgNO_3$, σ^o is obtainable as a function of $pAg = \log c_{Ag^+}$[1,13]. From σ^o (pAg) curves at different concentrations of electrolytes and/or organic adsorptives, much information on the adsorption of the two has been obtained. Regarding most organic substances, including organic cations as TBA^+, it was deduced that the adsorption passes through a maximum as a function of pAg[8,13]. This information could be obtained without actually measuring the adsorption, but later this trend was confirmed for TBAN by direct analytical determination. One striking inference of this maximum is that to the right of it an increase of the negative surface charge leads to a *de*crease of the organic cation adsorption. This "counterelectrostatic" trend indicates that the adsorption is certainly not solely driven by purely Coulombic attraction of the organic cation. The origin of this second electrostatic force was attributed to the interaction of water dipoles with the surface. The latter are exchanged against specifically adsorbed TBA^+ ions.

In the present study, the pAg was kept at 11.6. Then the surface is negatively charged, but σ^o may vary as a function of c_{TBAN}, c_{salt} and T; these variables modify the double layer capacitance. However, near the c.i.p. in the σ^o-pAg curves the effect of c_{TBAN} is only small.

At given pAg, upon adsorption of TBAN, the electrokinetic potential of AgI particles first becomes less negative then passes through a zero point that we shall also call isoelectric point (i.e.p.), to become positive. It was shown[8] that in the i.e.p. the surface charge is almost exclusively compensated by specific adsorption of TBA^+.

Proton titrations on kaolinite are more difficult to interpret in view of the different charging mechanisms of the plates (constantly negative due

to isomorphic substitution, but exchange of cations, including protons, possible) and on the edges (variable charge as on amphoteric oxides). We intend to discuss this in some detail elsewhere[9]. Electrophoretic mobilities reflect the sum of the electrokinetically found charges on the plates and on the edges. As illustrated by Figure 1a, U/X is negative over the entire pH range. This trend has also been found by Williams and Williams[10] for Na-kaolinite and by Cases et al.[11] for K-kaolinite . At very low pH the curve extrapolates to a zero point below pH=2, but it is difficult to indicate the precise position of this point because at low pH the clay lattice may decompose somewhat under uptake of additional protons. At any rate, at this zero point the surface has a mosaic charge with compensating contributions of the plates (–) and edges (+). Addition of NaCl reduces the mobility (Figure 1b), due to double layer compression at the plates and edges. Quantitatively, the NaCl effect is much less pronounced than that of the pH. As could be expected, adsorption of DPC or DTAB also leads to electrokinetic charge reversal[12]. The isoelectric points were located at $-\log c_{DPC} = 3.4\text{-}3.6$, slightly dependent on c_{NaCl} (pH≈6), and at $-\log c_{DTAB} = 3.0$ (pH≈5), respectively. As judged from the concentration of surfactant needed to attain the iep, DPC adsorbs with a slightly higher affinity than DTAB.

5.3.2 Adsorption of organic cations: influence of surface charge and indifferent electrolyte concentration

Data regarding the adsorption of TBAN on AgI will be presented in the next section in connection with its temperature dependence.

Adsorption isotherms of DPC on Na-kaolinite are given in Figures 2 and 3. The amount adsorbed increases progressively with $\log c_{DPC}$ and the steep slope close to the c.m.c. suggests some kind of association on the surface when the c.m.c. is approached. The maximally attained adsorption is about 80-85 μmole g^{-1}. Given the specific surface area of our kaolinite sample (12 m^2 g^{-1}) this corresponds with an average cross-section of 0.25-0.24 nm^2 per molecule. This value must be considered with some reservation, realizing that the edges and the plates both

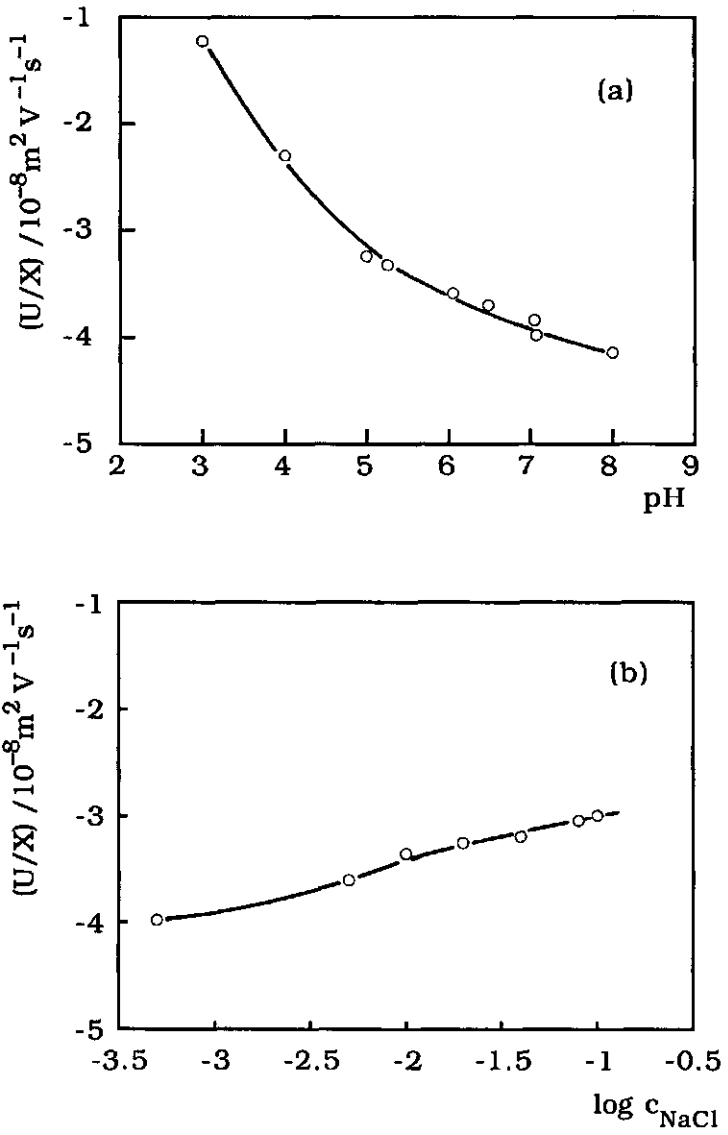

*Figure 1. Electrophoretic mobility of Na-kaolinite particles. T = 25°C. (a) as a function of pH at c_{NaCl} = 5*10^{-3} M; (b) as a function of c_{NaCl} at pH = 6.*

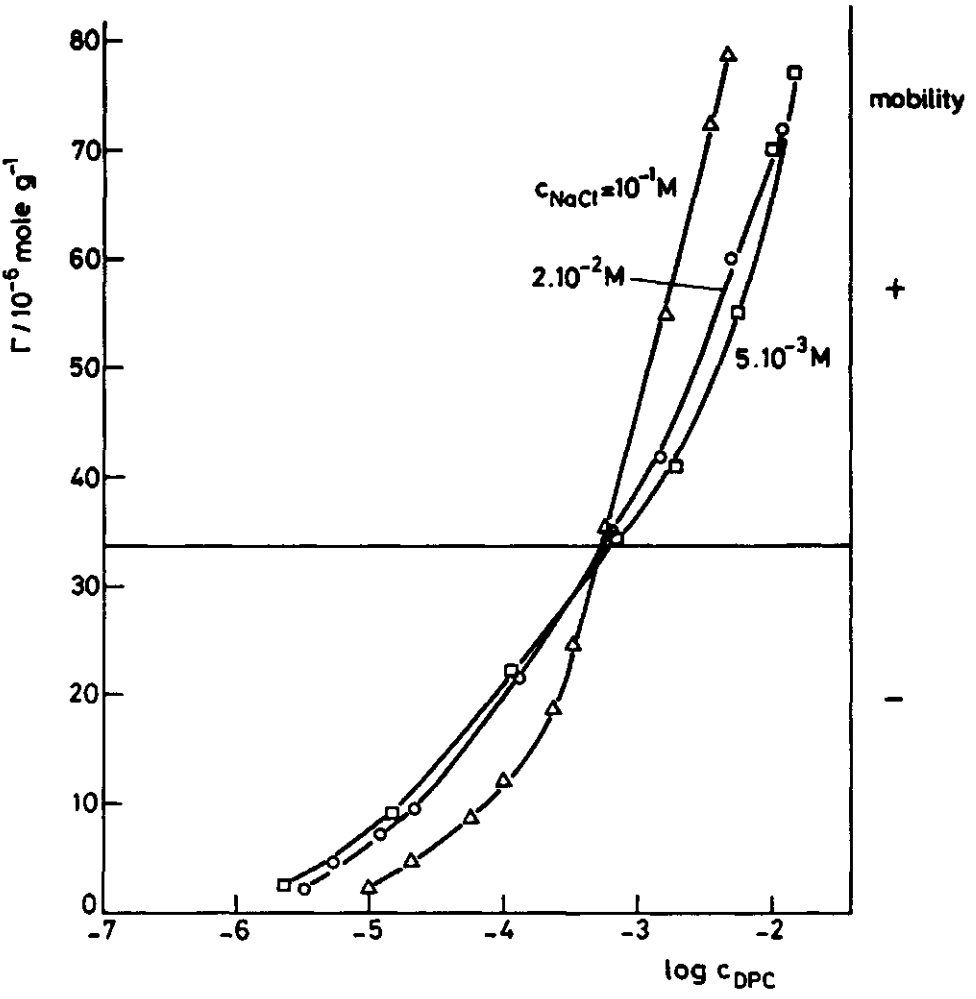

Figure 2. *Adsorption of DPC on Na-kaolinite; T = 20°C, as a function of* c_{NaCl} *at pH = 5.00.*

contribute to the total specific surface area but probably have a strongly different affinity for DPC. In the following we propose major contribution to the adsorption is on the plates.

The influence of electrolyte (Figure 2) shows a common intersection point (c.i.p.) at about Γ_{DPC} = 32 μmole g^{-1}. This point coincides very well with the value of Γ_{DPC} where the covered kaolinite particle becomes isoelectric. To the left of this point NaCl compresses the electrical double

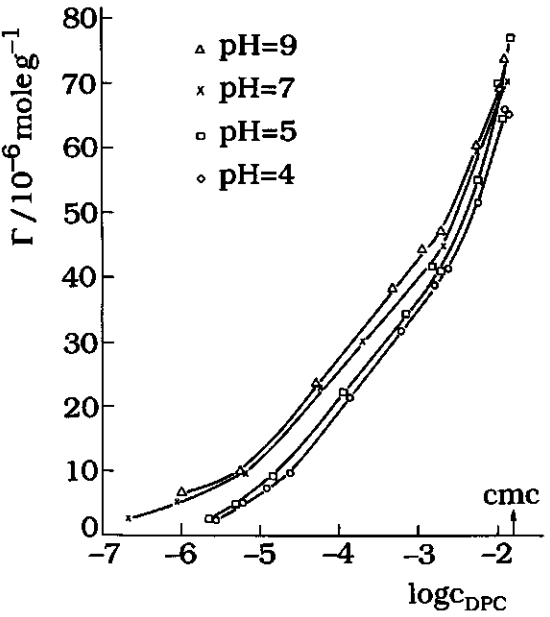

Figure 3. *Adsorption of DPC on Na-kaolinite; T = 20°C, as a function of pH at* $c_{NaCl} = 5*10^{-3}$ *M.*

layer, leading to a decreasing electrical potential in the plane of adsorption and a lower affinity, hence $\partial\Gamma_{DPC}/\partial\log c_{NaCl}<0$. To the right, the DPC adsorption is superequivalent; probably association between parallel oriented cations plays an important role.

This process proceeds against lateral repulsion between the charged pyridinium groups; as this repulsion is screened by Cl^--ions, $\partial\Gamma_{DPC}/\partial\log c_{NaCl}$ is now positive. The second mechanism starts to take over at Γ_{DPC} = 32 μmole g^{-1}, roughly 40% of the maximally attained value. The presence of a c.i.p. and the correspondence with the i.e.p. seems to be a general property for adsorption of organic cations on a surface with an opposite charge[12].

In the i.e.p. the charged pyridinium groups just compensate the surface charge. Therefore the above value for Γ_{DPC} may also be compared with the cation exchange capacity(CEC). The CEC according to the silver-thiourea method (57 μeq g^{-1}) more or less represents the total number of sites on the plates and on the edges, whereas the ammonium acetate method at pH≈7 (30 μeq g^{-1}) measures only the cation exchange on the

plates. The fact that in the i.e.p. Γ_{DPC} is comparable with the latter value is evidence that DPC adsorption takes place essentially on the plates.

From the pH-dependence (Figure 3) the same suggestion may be inferred. If DPC mainly adsorbed on the edges, Γ_{DPC} ought to rise strongly with pH above the p.z.c. of the edges (pH≈7) because σ^o (edges) becomes more negative, whereas below the p.z.c. DP^+ would be electrostatically repelled. However between pH 4 and 9, a smooth increase of Γ_{DPC} is observed, which amounts only to about 20% of the corresponding increase of σ^o as will be presented in Ref. 9. Thus, it is not likely that this increase is caused by the edges and we suggest that the pH effect is mainly due to the exchange of organic cations against the specifically adsorbed protons on the plates. This conclusion is also supported by the fact that no abrupt change in the adsorbed amount around pH=7 is observed.

It may thus be concluded that adsorption of DPC on Na-kaolinite takes place mainly on the plates. Below Γ=32 μmole g^{-1} charge compensation is the main driving force, thereafter hydrophobic bonding between the alkyl chains takes over and association between DPC molecules is the driving force. Assuming a molecular cross-section of 0.35 nm^2/molecule and neglecting adsorption on the edges we can estimate that the relative contribution of the plates to the total surface area is about 0.65. We found from electron microscopic photographs a corresponding ratio of 0.60. This ratio is not far from the CEC (ammonium acetate) / CEC (Ag-thiourea) ratio, amounting to 0.55. This similarity suggests that indeed the former measures only the plates whereas by the latter the entire clay surface is "seen".

Similar features are observed for DTAB. These have been discussed by some of us before[12].

5.3.3 Adsorption of organic cations: Temperature dependence

For the adsorption of TBAN on AgI, (Figure 4) a small but undeniable temperature influence is observed: over the entire range Γ_{TBAN} passes through a maximum as a function of T. This feature is shown in more

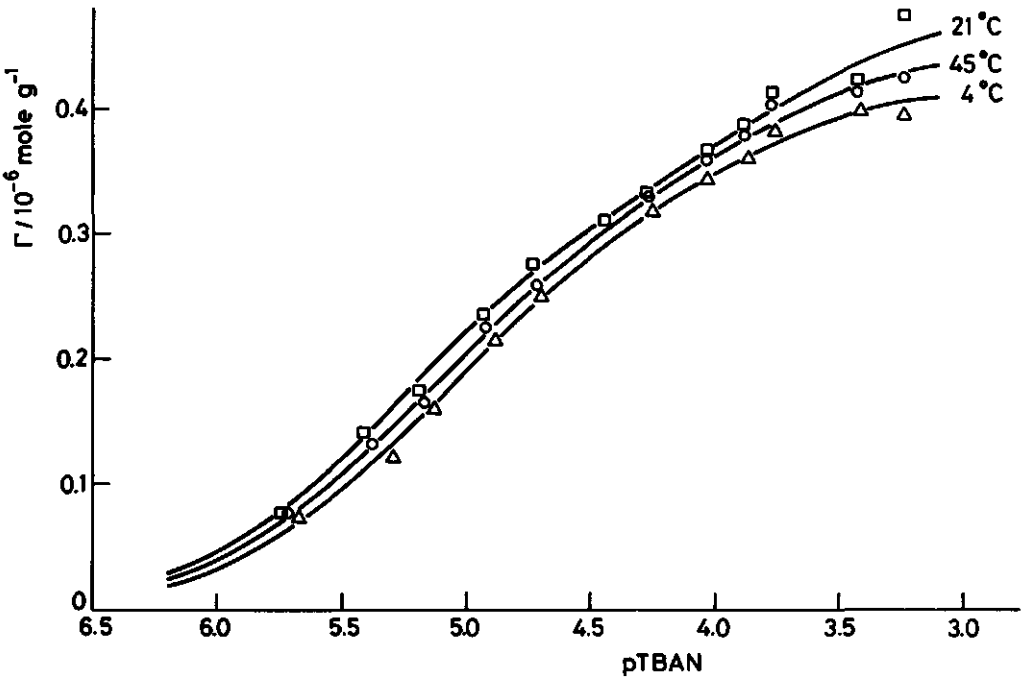

Figure 4. *Adsorption of TBAN on AgI, pAg = 11.6, $c_{KNO_3}=10^{-1}$ M. The temperature is indicated.*

detail in Figure 5, where the salt (KNO_3) effect is also included. Beyond the i.e.p. (pTBAN = 4.02) the adsorption of TBAN is strongly promoted by the salt. Near the i.e.p. (pTBAN=4.95) only a minor effect of salt on the adsorption is observed except at lower temperature. Below 20°C adsorption *de*creases with increasing salt concentration. Apparently we are just below the i.e.p., which means that the surface charge would be higher at lower temperatures.

Silver iodide is a hydrophobic substance[14] and TBAN adsorbs due to electrostatic attraction and hydrophobic bonding. This picture is supported by the observations of Figures 4 and 5 together with the results presented in ref. 12:

(i) Before the i.e.p. electrolyte inhibits the TBAN adsorption because the electrolyte compresses the electrical double layer and lowers the potential in the plane of adsorption. See Figures 2, 7, 8 and reference 12.

(ii) Beyond the i.e.p. electrolyte promotes TBAN adsorption because of screening of the repulsion between the organic cations.

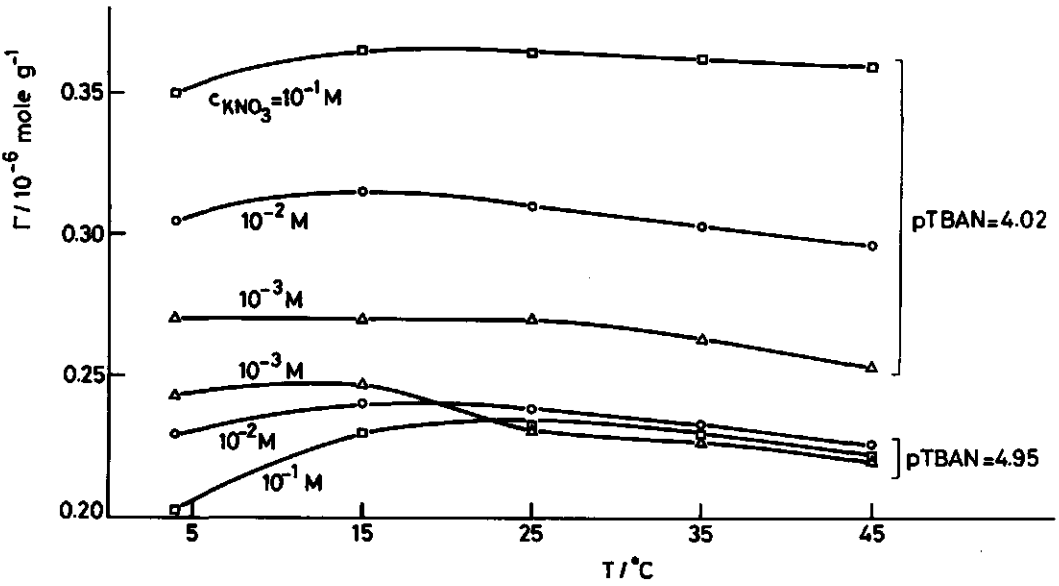

Figure 5. *Adsorption of TBAN on AgI, pAg =11.6. Influence of temperature for different values of* c_{KNO_3} *and pTBAN = – log* c_{TBAN} *.*

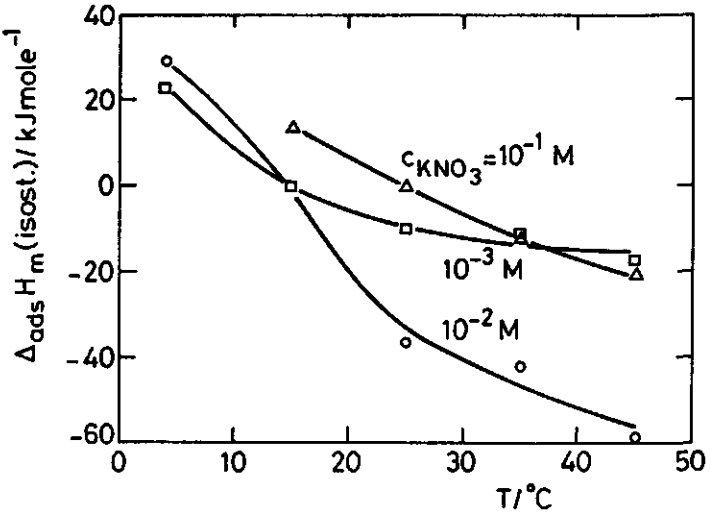

Figure 6. *Isosteric enthalpy of TBAN adsorption on AgI, pAg = 11.6. The concentration of* KNO_3 *is indicated.*

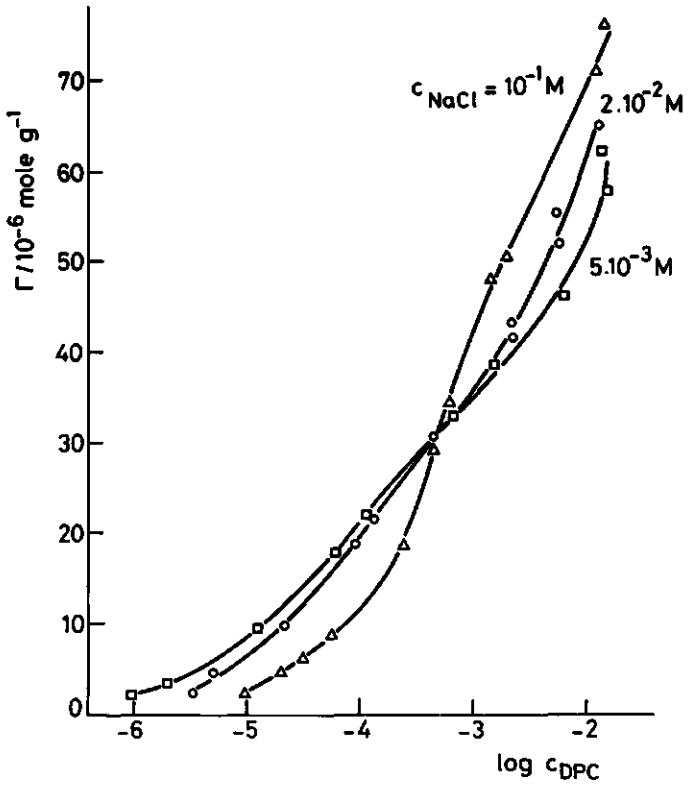

Figure 7. *Adsorption of DPC on Na-kaolinite at T = 60°C. pH = 5.00. The NaCl concentration is indicated.*

These two features have also been found for DPC and DTAB on Na-kaolinite.

(iii) The strength of hydrophobic bonding passes through a maximum as a function of temperature[15]. The position of this maximum, henceforth called T_{max}, depends on the nature of the interacting organic molecules and on their degrees of freedom, i.e. T_{max} may be different for free and adsorbed molecules.

From the adsorption data for TBAN on AgI at different temperatures and electrolyte concentrations the isosteric molar enthalpy of adsorption can be estimated using

$$\left[\frac{\partial \ln c_{TBAN}}{\partial (1/T)}\right]_{pH,c_{KNO_3}} = -\frac{\Delta_{ads}H_m(\text{isost.})}{R} \qquad (1)$$

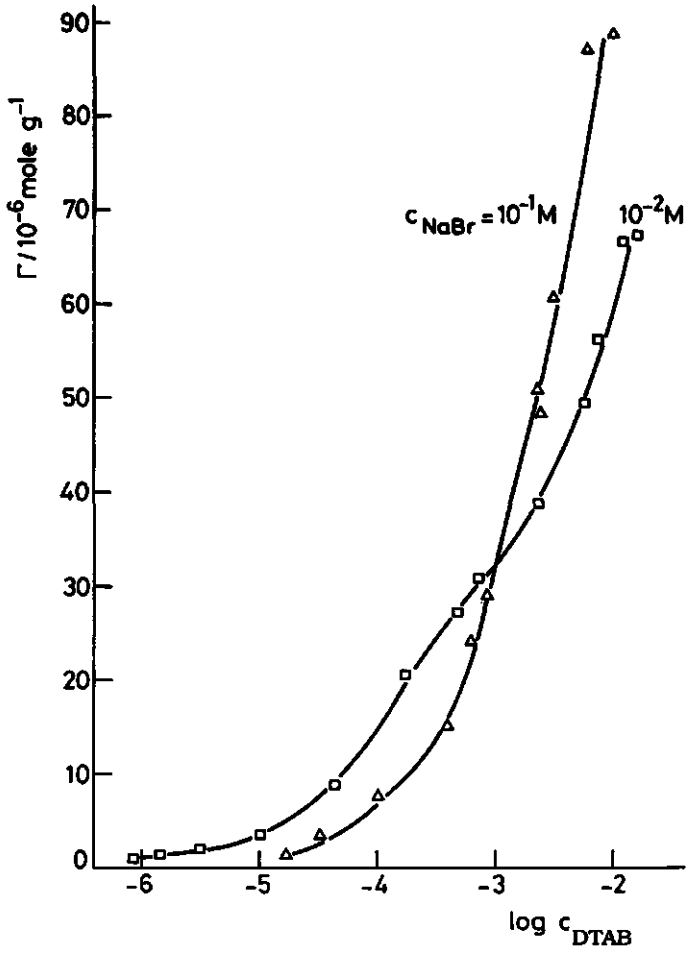

Figure 8. *Adsorption of DTAB on Na-kaolinite at T = 60°C. pH = 5.00. The NaBr concentration is indicated.*

Results are presented in Figure 6. Near 20°C the enthalpy is almost zero. It is deduced that the $\Delta_{ads}H_m$ values are up to 15 kT for a molecule containing 16 CH_2 groups, on the average less than 1 kT per such a group. At lower temperatures the adsorption is endothermic (up to 12 kT per molecule in our temperature range), hence here this process must be entropically driven. At higher T the enthalpic contribution becomes increasingly negative, down to -24 kT per molecule, whereas the entropic contribution decreases because of the increasing randomization of the water structure. In another paper de Keizer and Fokkink[16] calculated a Gibbs adsorption energy of about -43 kJ/mol, corresponding

to 1.1 kT per CH_2 (Traube's rule) which corresponds well with our results.

Figures 7 and 8 give adsorption isotherms of DPC and DTAB at different electrolyte concentrations on Na-kaolinite at 60°C. Qualitatively the trends are the same as at 20°C, compare Figure 2 and ref. [12]. The c.i.p's at 20°C and 60°C are also almost identical which is in line with our interpretation of adsorption on the plates because for the plates (unlike for the edges), the surface charge is virtually temperature independent. Consequently, the mechanism, proposed for the driving force and the influence of electrolytes on it, remains valid at elevated temperatures.

We interpret the adsorption below the i.e.p. as caused by exchange of DP^+ or DTA^+ cations against Na^+ and H^+. The enthalpy change of this process is small. In fact, if the exchange takes place at a given potential, the driving force is of a purely entropical (configurational) origin and $\Delta_{ads}H_m = 0$. If Na^+ or H^+ ions are exchanged by organic cations that, because of their sizes have to remain a bit further away from the surface, and hence adsorb at a slightly lower potential, enthalpies of a few kT per exchanged ion may be encountered. All of this indicates that the (electrical) adsorption enthalpy is zero or small. Similar results were obtained by two of us for the adsorption of protons and cadmium ions on a (high capacitance) oxide surface[17,18]. Hence, by virtue of (1) none or little temperature dependence of the adsorption of the organic cation should be expected. This is entirely corroborated by the experiment; below the i.e.p. no significant trend as a function of T has been observed. Compare the left parts of Figures 2 and 7. The same was found for DTAB.

Adsorption beyond the i.e.p. was attributed to association of the organic cations. Hydrophobic bonding is the driving force of this process. As was the case with TBAN adsorption on AgI, a maximum of Γ as a function of T must be anticipated. Figures 9 and 10, giving more detailed data for these conditions, fully support this. T_{max} is about 25°C for DTAB and 20-23° for DPC.

Using (1), from the temperature dependence of the adsorption of the organic cations the isosteric enthalpy of adsorption can be estimated (Figures 11 and 12). As was the case for TBAN on AgI (Figure 6), $\Delta_{ads}H_m$ (isost.) changes sign at T_{max}. For the sake of comparison the enthalpies of

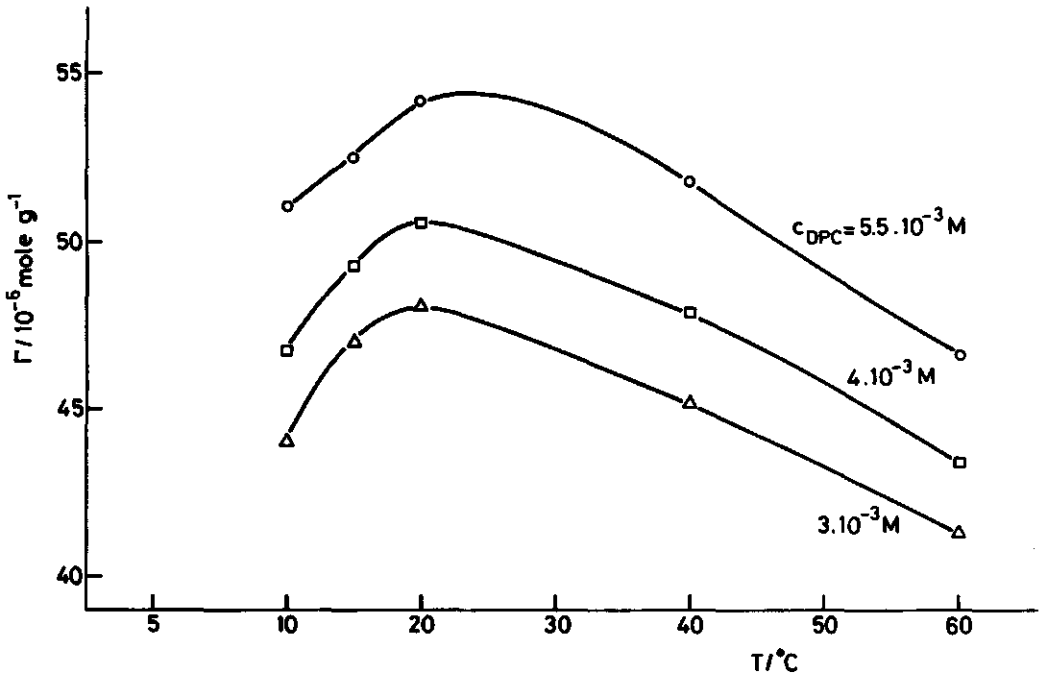

Figure 9. *Adsorption of DPC on Na-kaolinite as a function of temperature. Region beyond the i.e.p. pH = 5.00, c_{NaCl} = 5*10^{-3} M, concentration of DPC indicated.*

micellization of DPC and DTAB are also included[19,20]. Of course, micelle formation of several tens of monomers in aqueous solution and association at interfaces are not identical processes, and the conditions (e.g. nature of counter-ion) may also differ. However, a certain analogy may be expected and, in fact, is observed, both with regard to the order of magnitude, the temperature dependence and the reversal of sign. This similarity underscores the mechanism that we proposed and confirms the consistency of our model.

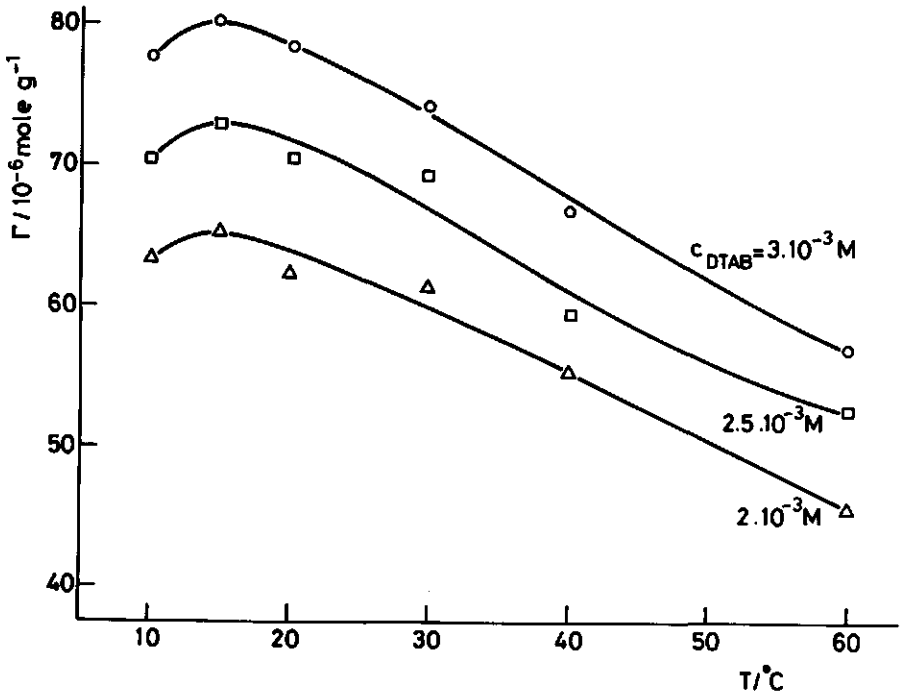

Figure 10. *Adsorption of DTAB on Na-kaolinite as a function of temperature. Region beyond the i.e.p., pH = 5.00, c_{NaBr} = 10^{-1} M, concentration of DTAB indicated.*

5.4 Conclusion

The present study illustrates the potentialities of investigating the temperature dependence of adsorption equilibria as a diagnostic tool to obtain mechanistic information.

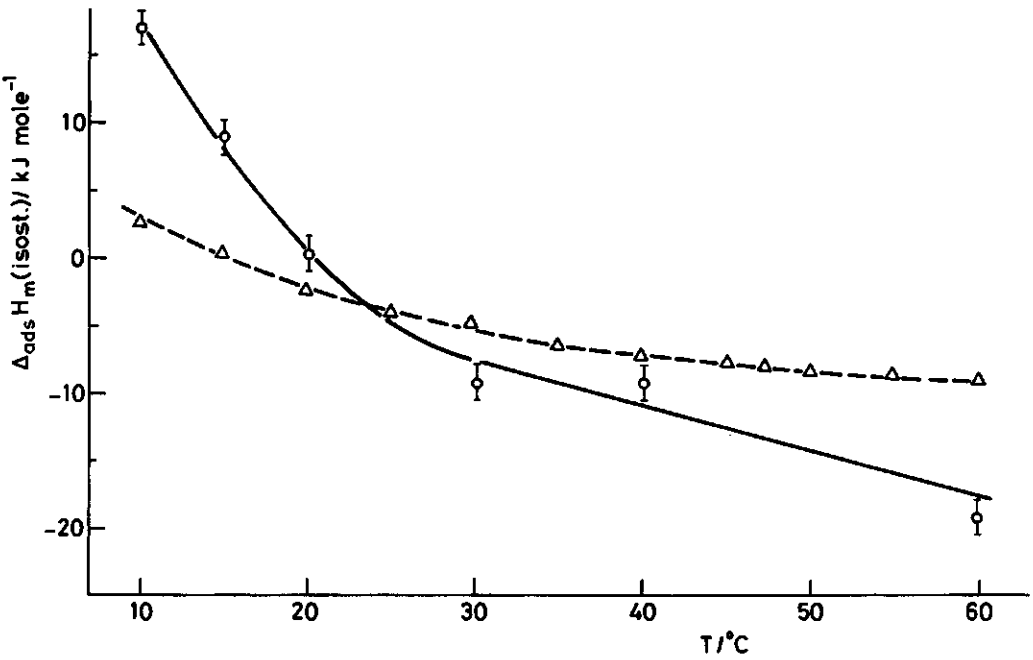

Figure 11. *Isosteric enthalpy of the adsorption of DPC on Na-kaolinite. Region beyond the i.e.p., pH = 5.00,* $c_{NaCl} = 5*10^{-3}$ *M. Dashed curve: molar enthalpy of micellization of DPB. Absence of salt*[19].

5.5 Acknowledgements

The contributions of Mr. A. Korteweg and Mr. B. van der Wal in the analytical work and Mr. M. Bakkenes for synthesizing DPC are gratefully appreciated.

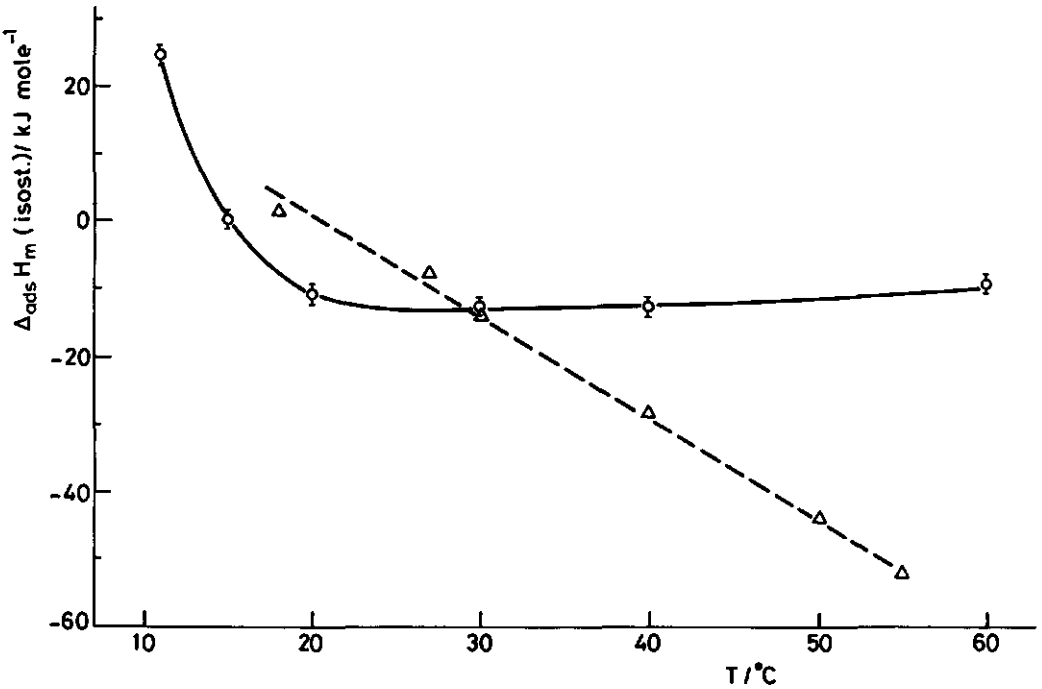

Figure 12. *Isosteric enthalpy of the adsorption of DTAB on Na-kaolinite. Region beyond the i.e.p pH = 5.00,* $c_{NaBr} = 10^{-1}M$. *Dashed curve: molar enthalpy of micellization of DTAB. Absence of salt*[20].

5.6 References

(1) de Keizer A., Lyklema J. *J. Electroanal. Chem.* **1986**, 199, 395.
(2) Chabra, R., Pleysier J., Cremers A. *Proc. Intern. Clay Conf.* **1975**, 439.
(3) Schofield R.K. *J.Soil Sci.* **1949**, 1, 1.
(4) Colichman E. L. *J. Am. Chem. Soc.* **1950**, 81, 1834.
(5) Ford W. P. J., Ottewill R. H., Parreira H. C. *J. Colloid Interface Sci.* **1966**, 21, 522.
(6) Haydon D. A., Phillips J. N. *J. Chem. Soc.,Trans. Faraday Soc.* **1958**, 54, 698-704.
(7) Ballard, C. W., Isaacs J., Scott P. G. W. *J. Pharm. Pharmacol.* **1954**, 6, 971.

(8) de Keizer A., Lyklema J. *J. Colloid Interface Sci.* **1980**, 75, 171.
(9) Mehrian T., de Keizer A., Lyklema J. in preparation.
(10) Williams D. J. A., Williams K.P. J. *Colloid Interface Sci.* **1978**, 65, 79.
(11) Cases J., M. Touret-Poinsignon C., Vestier D. C. R., *Acad. Sci. C* **1971**, 272, 728.
(12) de Keizer A., Böhmer M. R., Mehrian T., Koopal L. K. *Colloids Surfaces* **1990**, 51, 339.
(13) Bijsterbosch B. H., Lyklema, J. *Advan. Colloid Interface Sci.* **1978**, 9, 147.
(14) Billett D. F., Hough D. B., Ottewill R. H. *J. Electroanal. Chem.* **1976**, 74, 107.
(15) Némethy G., Scheraga H. A. *J. Chem. Phys.*, **1962**, 36, 3382.
(16) de Keizer A., Fokkink L. G. J. *Colloids Surfaces* **1990**, 51, 323.
(17) Fokkink L. G. J., de Keizer A., Lyklema J. *J. Colloid Interface Sci.* **1990**, 135, 118.
(18) de Keizer A., Fokkink L. G. J., Lyklema, J. *Colloids Surfaces* **1990**, 49, 149.
(19) Adderson J. E., Taylor H. *J. Colloid Interface Sci.* **1964**, 19, 495-500.
(20) Barry B.W., Russell G. F. J. *J. Colloid Interface. Sci.* **1972**, 40, 174.

CHAPTER 6

Enthalpy of Adsorption of DPC on Na-Kaolinite

Abstract

A study has been undertaken of the influence of temperature and electrolyte concentration on the adsorption enthalpy of DPC on Na-kaolinite. Enthalpies are measured using an isothermal microcalorimeter by titration of a kaolinite suspension with a concentrated surfactant solution at 6, 20 and 60°C.
Curves of cumulative adsorption enthalpies against amount adsorbed show a break around half surface coverage. The break is almost identical with the iep of kaolinite particles in the presence of DPC, implying that a different adsorption mechanism for the first and the second layer formation takes place. The above mentioned curves are almost linear both below and above the iep, resulting in partial molar adsorption enthalpy values which are hardly dependent on the surface coverage.
In both regions, beyond or below the iep, the adsorption enthalpy changes the sign between T ~ 2 -30°C. Therefore, the formation of the second layer, and to a lesser extent that of the first layer, are similar to micellization. For the formation of the second layer, the isosteric heat of adsorption and the directly measured heats are identical within experimental error, but there is some discrepancy between the isosteric heats of adsorption and the directly measured heats of the formation of the first layer.
From this study and the results presented in Chapters 2 and 4 we conclude that the adsorption process is driven by, (i) direct interactions of DPC molecules with the oppositely charged kaolinite surface. (ii) interactions between hydrophobic parts of the surfactant.
The enthalpies of adsorption are maximally some tens of kJ/mole, implying physical adsorption.

6.1 Introduction

Thermodynamics is a diagnostic tool to understand the fundamentals of adsorption. In particular, heats of adsorption can reveal some interesting features about the adsorption mechanism. There exist two methods for estimating such heats of adsorption, viz. (a) from the temperature dependence of the adsorption and (b) calorimetrically.

It has become clear from the previous chapters that the adsorption of ionic surfactants on clay minerals is a complex phenomenon, due to the intrinsic heterogeneity of clay minerals, the amphiphilic character of the adsorptive, the possibility of bilayer formation, changes in the hydrophobicity of the surface as a result of the adsorption and, last but not least, the complex electrostatic interactions. From the temperature dependence of adsorption it was shown that the enthalpy of adsorption of the first layer is different from that of the second layer. In Chapter 5 it was indicated that the temperature dependence of the enthalpy of micellization and that of the adsorption process at the second layer resemble each other. Therefore it is logical to complete our thermodynamic study of the behaviour of cationic surfactants on clay minerals by calorimetric measurements. There are only a few papers on the temperature dependence of the adsorption of organic compounds on kaolinite[1-3]. The adsorption of some dyes (crystal violet, malachite green, methylene blue) and a drug (drotaverine hydrochloride) on kaolinite in a temperature range between 30 and 50°C gave rise to endothermic enthalpies, whereas the enthalpy of adsorption of cetylpyridinium bromide, cetyltrimethylammonium bromide and dodecylpyridinium bromide, on a H-kaolinite in the same temperature range was exothermic. From these studies adsorption of organic ions on charged adsorbents resulted in enthalpies with different signs. As far as we are aware no explanation has been given for the different sign of enthalpies.

The early ideas about the mechanism of adsorption of surfactants on alumina stems from Fuerstenau, Somasundaran and co-workers[4-7]. They introduced the term "hemimicelles", for a micelle-like aggregate adsorbed on the surface when the surfactant concentration exceeds the so-called hemimicelle concentration. In their work, they obtained information on the adsorption of anionic surfactants on minerals by

studying ζ–potentials, adsorption isotherms, contact angle and sedimentation rates.

Only over the last decades sensitive calorimetric techniques have been developed for the adsorption from solution. Adsorption of the anionic surfactants decyl-, dodecyl- and sodium p-(2-decyl)-benzenesulfonates on various sand samples and on silica gel was studied by Noll and co-workers[8,9], Rouquerol and Partyka[10] and by van Os and Haandrikman[11]. Except for the work of Noll, Berg and co-workers, where the experimental temperature was not mentioned, the others worked at 30°C. All of these investigators found exothermic adsorptions. Vilcu and Olteanu[12] studied the heat of adsorption of some alkylpyridinium and alkyloxyethylene pyridinium chlorides at the silica-alumina interface. They found an exothermic process at room temperature. Partyka et al.[13] found an exothermic process with different enthalpic values depending on the surface coverage of some anionic surfactants on alumina. Rouquerol and Partyka[10] also studied the adsorption of three nonionics and one anionic surfactant on kaolin, a natural kaolinite. They found a very small (though not constant) exothermic adsorption enthalpy of –5 to –17 mJ m^{-2} at 30°C. From the variation in the enthalpy they concluded that the adsorbent had a heterogeneous surface and reported the transformation of two-dimensional into three-dimensional aggregates. Partyka et al.[14] studied the adsorption of sodium dodecylsulfate and dodecyltrimethylammonium bromide on alumina and silica. They found exothermic processes in all cases (at a temperature of 25 and 35°C), the adsorption enthalpy being three times larger than that of micellization. Denoyel and Rouquerol[15] studied the adsorption of nonionic and anionic surfactants onto silica, kaolin and alumina. They confirmed that micelle-like aggregates are formed. These authors found a reasonable agreement between the isosteric heats of adsorption and the directly measured heats for the nonionic surfactants. According to both methods the adsorption of nonionics, on three kinds of silicas and a kaolin sample, was exothermic at low surface coverage and became endothermic at high surface coverage. Wierer[16] studied the adsorption of n-alkylpyridinium chlorides on a kaolinite clay at 25°C. He found a small exothermic adsorption enthalpy for DPC. The adsorption became more exothermic with increasing chain length. From this literature review it becomes clear that

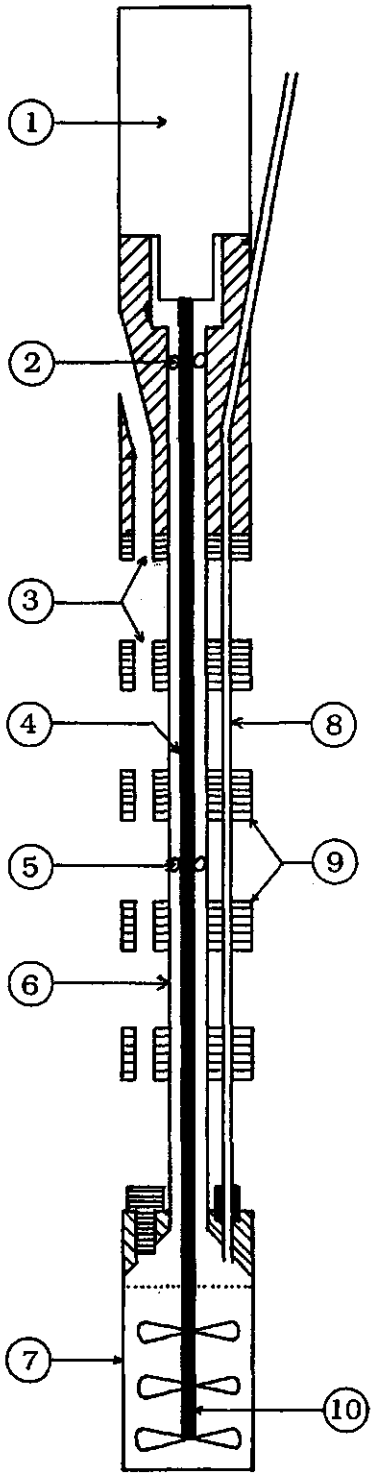

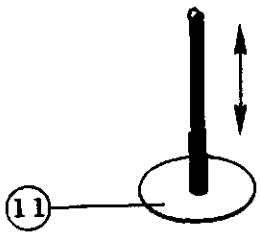

1 *Stirrer motor*
2 *O-ring seal*
3 *Lead-through for electrode cable*
4 *Stirrer shaft*
5 *Bearing*
6 *Main tube*
7 *Titration vessel*
8 *Titration addition tube*
9 *Heat exchangers*
10 *Stirrer*
11 *Stirrer we used*

Figure 1. *Schematic presentation of the calorimetric cell and the stirrer.*

the amount of work on this problem is neither large nor systematic. For example, as far as we are aware, adsorption calorimetry has never been studied over a sufficiently wide temperature range.

In this chapter we present the use of microcalorimetry as a tool to understand the mechanism of the adsorption of a surfactant (DPC) from aqueous electrolyte solutions on a Na-kaolinite. To that order a concentrated surfactant solution is added stepwise in the measuring cell containing a clay suspension. The dilution enthalpy of a concentrated surfactant solution may outweigh the adsorption enthalpy, i.e we are measuring small changes of a large signal. In this respect the experiment is technically difficult and such experiments require a lot of skill.

6.2 Experimental

All solutions and suspensions are prepared gravimetrically. The quality of the distilled water, DPC, Na-kaolinite and all chemicals used in this work is the same as that discussed in Chapters 2 and 3 of this thesis.

The details about the microcalorimetric technique are explained in Chapter 3. In the presence of a suspension, the choice of the stirring speed and direction is very crucial. A compromise must be achieved, to get a sufficiently homogeneous suspension and at the same time a minimum mechanical heat produced from the mixing process. In this respect different stirring systems were checked using the surfactant solutions with and without clay suspensions. The stirrer blades were two- or three-blade and a plate stirrer. It was possible to place them separately, as a pair or as a group of three on the stirrer bar. The position of the blades could be changed along the bar. The mixing could be performed either by rotation or by up and down movements. The best stirring method for our system turned out to be a circular-horizontal disk moving up and down with a frequency of 0.1 s^{-1}. See Figure 1.

The details concerning the experimental performance especially the advantage of the reference cell are described in Chapter 3. The adsorption enthalpies of DPC on Na-kaolinite were measured in 5 and 100 mM NaCl at 6, 20 and 60°C. About 1.0 g of Na-kaolinite powder was

suspended in about 17.0 g of an electrolyte solution in the calorimetric cell. The suspension was sonicated for 10 min. Afterwards the cell was brought into the calorimeter. The cell was placed in the cylinder. The cylinder was then lowered into the equilibrium position. In this position the cylinder was in direct contact with the thermostat water. The cylinder was kept in the equilibrium position until at least 3 hours, then the burette capillary was introduced into the titration cell and the cell was lowered to the measuring position. This was the starting point for the baseline recording. At this stage the content of the titration cell was stirred and equilibrated in the cylinder for at least 3 hours until the baseline obtained from the measuring channel and the reference channel were stable. After thermal equilibrium was obtained, a certain amount of DPC 0.25 M (10 - 100 μl) was injected into the cell. The dilution enthalpies of DPC, described in Chapter 3, were used for the blank corrections for calculating adsorption enthalpies from the overall heat effect.

The partial molar adsorption enthalpy ($\Delta_{ads}H_m$) at a given surface coverage was calculated according to the following procedure. The measured heat per titration step (q_{total}) is the sum of a dilution enthalpy of the stock solution, as obtained from Chapter 3, and the heat of adsorption q_{ads}.

$$q_{total} = q_{ads} + q_{dil} \qquad (1)$$

The value of $\Delta_{ads}H_m$ simply follows from Equation 2.

$$\Delta_{ads}H_m = \partial q_{ads} / \partial \Gamma_{DPC} \qquad (2)$$

In the calorimetric cell, the adsorption is not directly measured but we have obtained Γ_{DPC} and c_{DPC} from the adsorption isotherms presented in Chapters 4 and 5. For each step in the calorimetric experiments only the total amount of surfactant in the cell (adsorbed at the interface + remained in the bulk) is known, from which it was possible to calculate Γ_{DPC} and c_{DPC} as follows. Semilogarithmic adsorption isotherms were fitted to a 4th degree polynomial. The total amount of DPC added is only a function of c_{DPC} and can be solved using a Newton iteration (see Appendix). The dilution enthalpy of the stock solution (q_{dil}) follows from interpolation of the dilution data given in Chapter 3. Usually, the error in

the interpolation is negligible. Only around the cmc the slope of the q_{dil}/c curves changes drastically and then the error could become significant. The partial molar enthalpies of adsorption ($\Delta_{ads}H_m$) were calculated from the slope of the q_{ads}/Γ curves. Upon approaching the cmc, the value of q_{ads} per step becomes very small but as $\Delta\Gamma_{DPC}$ (per step) is also small, the error in $\Delta_{ads}H_m$ becomes larger. Therefore we have omitted the calorimetric results around and above the cmc.

At T ≥ 45°C the experiments were sometimes perturbed by the random appearance of an exothermic peak of unknown origin. Such a peak could occur either during the experimental procedure or when no experiment was running, quit at random. Probably some parts of the instrument do not function continuously and properly at high temperatures. The perturbing peaks could be clearly detected from the

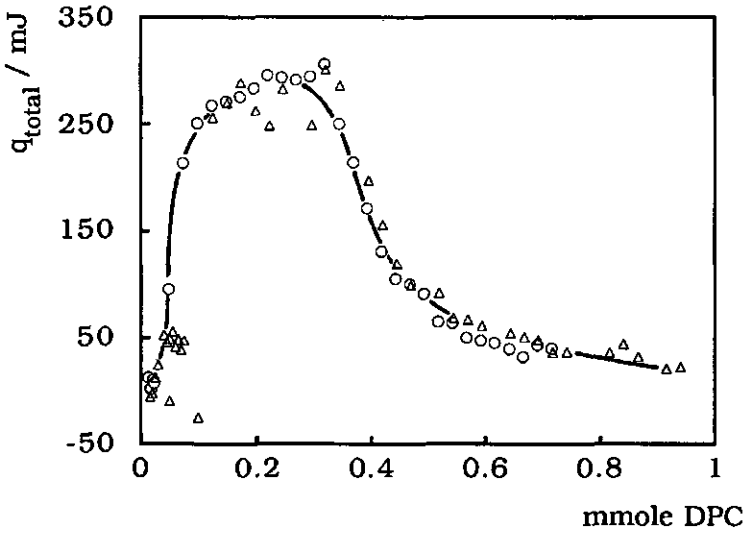

Figure 2. *Calorimetric titrations with different titration steps T = 60°C, c_{NaCl} = 5 mM, pH = 7, ΔV_{DPC} = 10 µl (Δ), ΔV_{DPC} = 20 µl (o), $m_{kaolinite}$ = 1g, V = 17 ml.*

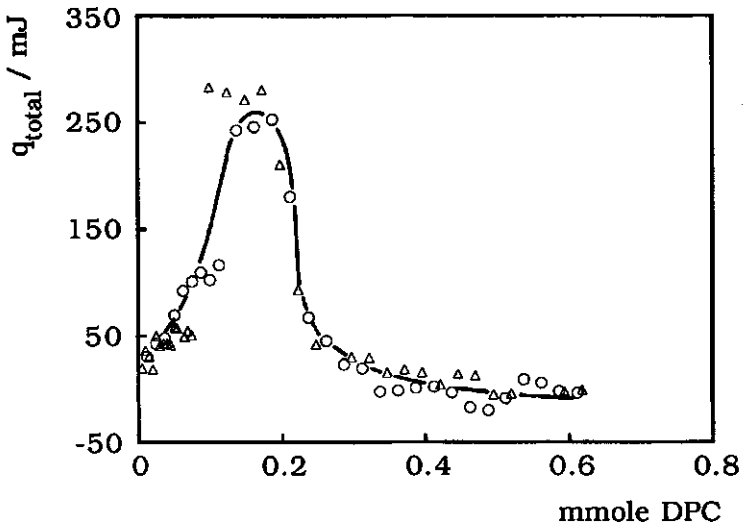

Figure 3. *Calorimetric titrations with different titration steps T = 60°C, c_{NaCl} = 100 mM, pH = 7, ΔV_{DPC} = 50 µl (Δ), ΔV_{DPC} = 20 µl (o), $m_{kaolinite}$ = 1g, V ≈ 17 ml.*

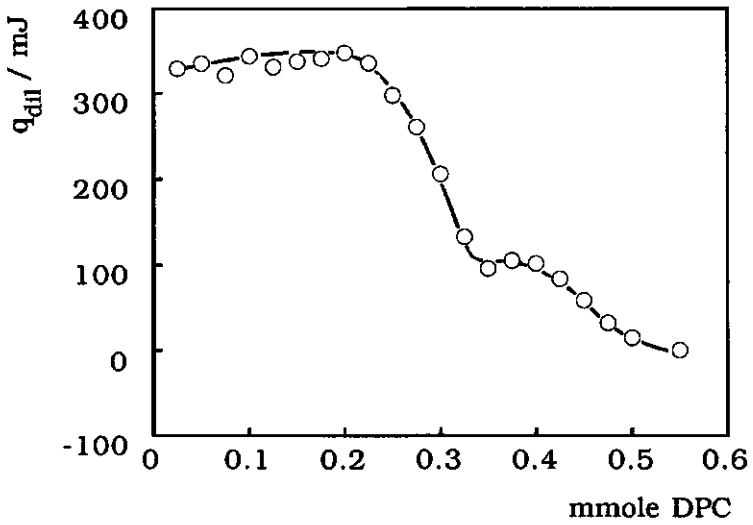

Figure 4. *Heat of dilution of 0.25 M DPC in 5 mM NaCl, T = 60°C, ΔV_{DPC} = 100 µl, V ≈ 17 ml.*

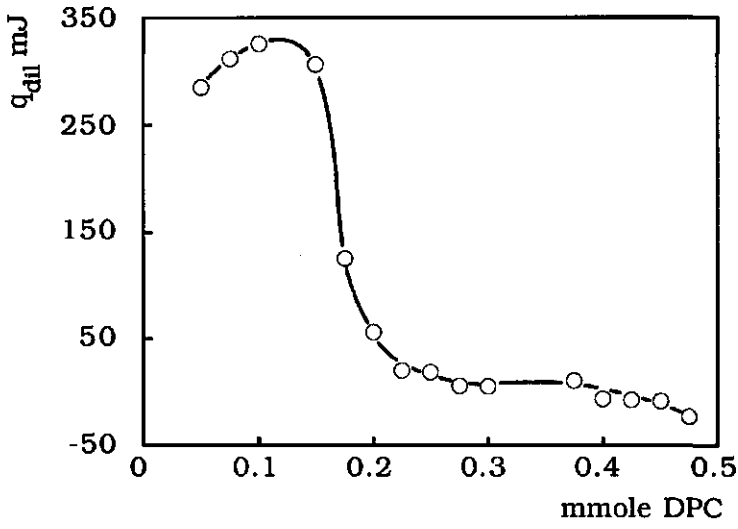

Figure 5. *Heat of dilution of 0.25 M DPC in 100 mM NaCl, T = 60°C, ΔV_{DPC} = 100 µl, V ≈ 17 ml.*

unprogrammed change and the unexpected enthalpies observed and the irreproducibility at certain points. During the experiment, the occurrence of such a peak affected one or two real (experimental) neighbouring peaks. We neglected those undesired peaks which were less than 10% of the total titration steps.

An indication of the reproducibility of the adsorption enthalpy measurements is given in Figures 2 and 3. The molar adsorption enthalpy is accurate within a maximum error of ± 0.7 kJ/mole. The blanks corresponding with Figures 2 and 3 are shown in Figures 4 and 5.

6.3 Results and Discussion

6.3.1 Calorimetric Adsorption Enthalpy

The cumulative heats of adsorption, q_{ads}(cum), at different electrolyte concentrations and temperatures are presented in Figures 6 - 8.

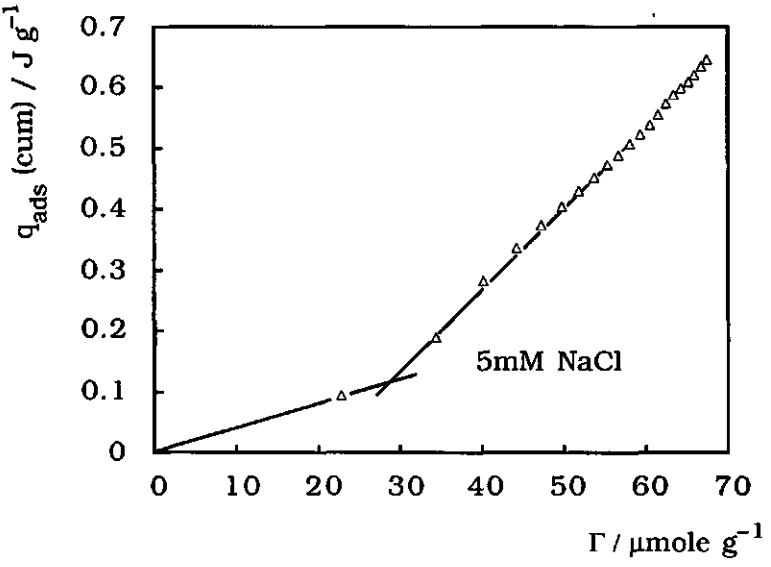

Figure 6. *q_{ads}(cum) of DPC on Na-kaolinite; T = 6°C.*

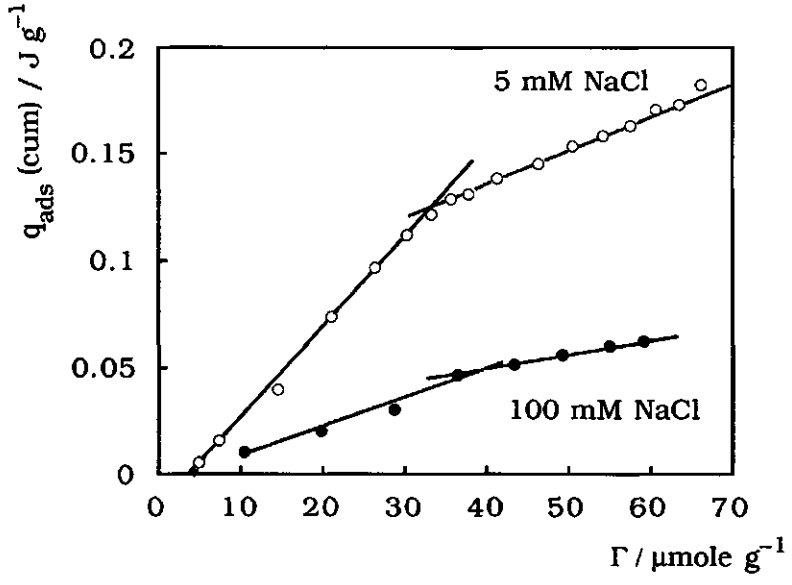

Figure 7. *q_{ads}(cum) of DPC on Na-kaolinite; T = 20°C.*

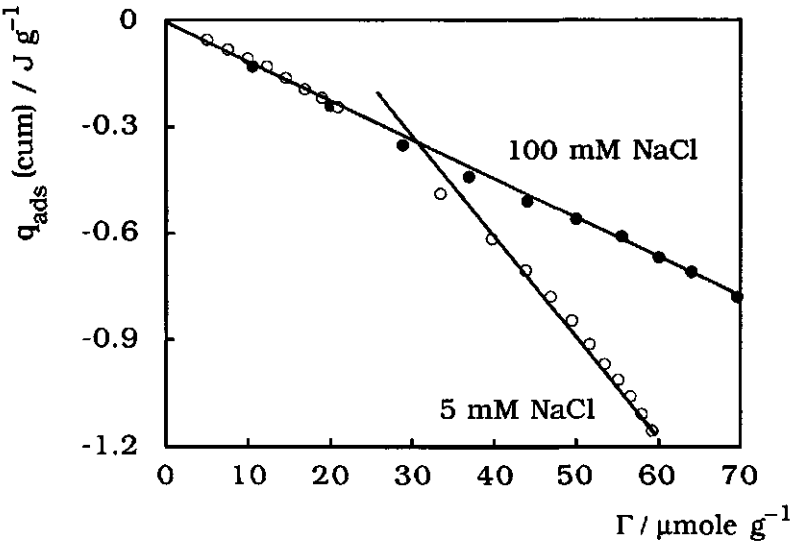

Figure 8. *q_{ads}(cum) of DPC on Na-kaolinite; T = 60°C.*

At zero coverage the cumulative enthalpy should be zero. Extrapolation of the curves to zero amount added do indeed give very small values.

Adsorption is endothermic at 6 and 20°C, but exothermic at 60°C. At 20°C as well as at 60°C the adsorption enthalpy decreases (in absolute value) with increasing electrolyte concentration. Due to substantial coagulation of the clay at 6°C and 0.1 M salt level, the experimental results at these conditions were not reliable. As is mentioned earlier, the only work in the literature which is comparable with ours is the investigation of Wierer who found two significant exothermic adsorption enthalpy peaks (of 0-10 kJ/mole) at 25°C for the adsorption of DPC on a kaolinite sample. He interpreted the second enthalpy peak as a result of surfactant aggregation at the interface.

The occurrence of a break is the most striking feature of the curves. The break appears around 35 μmole g^{-1} which corresponds with a degree of coverage of about 0.5, based on the information given in Chapters 4 and 5 (The adsorption sites are considered to be mainly the basal surfaces). Below and above the break the curves are fairly linear, indicating that the partial molar adsorption enthalpies in both regions are independent of the degree of coverage. At 60°C this picture is less pronounced than at

lower temperatures: at low salt concentration the curves below and above the break are not perfectly linear, whereas at high salt concentration the break is hardly detectable. The reason for the deviations at 60°C is not completely clear to us. The fact that phase transitions are less sharp at higher temperature is probably a reason for those deviations.

The linearity of the q_{ads}/Γ curves below and above the break suggests that the surface is homogeneous with respect to DPC adsorption. From the calorimetric adsorption measurements of Ar and N_2, as is reported in Chapter 2, we concluded that the basal surface of the clay is macroscopically homogeneous. This emphasizes that adsorption is mainly limited to the basal surface.

From the slopes of the lines in Figures 6-8 partial molar adsorption enthalpies are calculated for $\Gamma < 35$ μmole g^{-1} and $\Gamma > 35$ μmole g^{-1} which are called $\Delta_{ads1}H_m$ and $\Delta_{ads2}H_m$, respectively. The results are given in Table 1. The partial molar micellization enthalpies of the DPC are also included.

The absolute value of $\Delta_{ads1}H_m$ is generally smaller than or equal to $\Delta_{ads2}H_m$ within experimental error.

The effect of electrolyte concentration seems hardly significant except for the value of $\Delta_{ads2}H_m$ at 60°C. This indicates that electrostatic effects do not have a large influence on the measured enthalpies which itself

Table 1. *Partial molar enthalpy of the adsorption of DPC on Na- kaolinite, for $\Gamma < 35$ μmole g^{-1} ($\Delta_{ads1}H_m$) and $\Gamma > 35$ μmole g^{-1} ($\Delta_{ads2}H_m$), the experimental errors amount to ±0.5 to ±0.7 kJ/mole. Micellization enthalpies of DPC are also presented.*

T (°C)	c_{NaCl} (mM)	$\Delta_{ads1}H_m$ (kJ mole^{-1})	$\Delta_{ads2}H_m$ (kJ mole^{-1})	$\Delta_{mic}H_m$ (kJ mole^{-1})
6	5	4.1	13.2	12.2
20	5	4.1	1.7	5.0
	100	1.1	0.7	4.1
60	5	-11.9	-30.0	-13.3
	100	-12.0	-10.6	-14.1

implies that the enthalpy of the double layer formation of the surfactant head groups is relatively small.

Both $\Delta_{ads1}H_m$ and $\Delta_{ads2}H_m$ are temperature dependent; they have the same sign but slightly different magnitudes except for the enthalpy of adsorptions at 100 mM salt concentration for which $\Delta_{ads1}H_m$ is very close to $\Delta_{ads2}H_m$. The adsorption is endothermic at low temperatures, hence entropically driven. The entropies of the release of water from the vicinity of the clay basal surface and from the proximity of the surfactant molecules are the main driving force for the adsorption process. Since at low temperature the water molecules are more structured, heat is required to break the so-called "iceberg" water. As the temperature increases the water iceberg becomes less rigid and the process becomes more and more exothermic. The temperature dependence of the enthalpies of $\Delta_{ads2}H_m$ shows clearly the same trend as that of the micellization. This is also given in Figures 9 and 10. From Figure 9 it is clear that the values of $\Delta_{ads1}H_m$ are much smaller than both $\Delta_{ads2}H_m$ and $\Delta_{mic}H_m$. The transition from an endothermic process to an exothermic one takes place around 24-30°C which is in the same range as the corresponding transition temperature for micellization (28-30°C). This temperature dependence of the adsorption enthalpy is a strong indication of the importance of hydrophobic bonding to the adsorption process, especially for the second layer. $\Delta_{ads1}H_m$ is relatively small, with the exception of the results at 60°C and it is to a lesser extent temperature dependent. In fact at 6 and 20°C the formation of the first layer is slightly endothermic.

As mentioned earlier, from our calorimetric results, in all cases with one exception, a rather well defined break in q_{ads}/Γ curves occurs. In Table 2 we compare the position of this break with the cip of the adsorption isotherms at different electrolyte concentrations and with the iep of the kaolinite particles in the presence of the DPC, measured by electrophoresis. (See Chapters 4 and 5.)

Table 2. *Adsorbed amount of DPC Γ, on Na-kaolinite in μmole/g, at various important points.*

T (°C)	c_{NaCl} (mM)	Γ_{cip}	Γ_{iep}	Γ_{break}
6	5	32	?	30
20	5	32	34	33
	100	32	34	33±2
60	5	31	?	33
	100	31	?	?

From the results presented in Chapters 4 and 5 it was concluded that adsorption continues up to a bilayer coverage. The second layer starts roughly at the iep, (around 35 μmole/g) and is enthalpically different from that for the formation of the first layer. Within experimental error Γ_{cip}, Γ_{iep} and Γ_{break} are identical and independent of temperature and ionic strength, see Table 2. This is strong evidence that the adsorption mechanism is different for the first and the second layers. With regard to the comparison of the enthalpy of micellization with $\Delta_{ads2}H_m$, one would expect some similarity between the formation of the second layer and micellization. Such a similarity is indeed found (see the last two columns of Table 1) except for the experiment performed at 5 mM and 60°C. However, a less pronounced correspondence between $\Delta_{ads1}H_m$ and $\Delta_{mic}H_m$ exists. It seems that the contribution of hydrophobic bonding to the first layer is low but undeniable. We will return to this point later.

Let us consider the different contributions to the total adsorption enthalpies for the first and the second layer. During the development of the first layer, surfactant molecules are exchanged with counterions in the diffuse layer and with the counterions and bound water nearest to the interface (in the Stern layer). We suppose that exchange of DP^+ in the diffuse double layer is mainly entropically driven with $\Delta_{exch}H_m \sim 0$. The total enthalpy of the first layer formation consists of: (i) the enthalpy of water desorption, (ii) the enthalpy of the adsorption of DP^+ (iii) the enthalpies of desorption of specifically adsorbed counterions, (iv) the enthalpy of repulsion between the charged head groups and (v) the enthalpy of hydrophobic bonding. Since the adsorption takes place mainly

at the plates, most desorbed cations are Na^+ ions and, to a lesser extent, specifically adsorbed protons (see Chapters 2 and 4). At the same time, a decrease in the negative adsorption of the co-ions occurs. We recall here that the adsorption of DPC on Na-kaolinite results in the desorption of protons from the surface. As we have discussed in Chapter 2 of this thesis, the adsorption of protons on Na-kaolinite is an exothermic process within our temperature range, hence proton desorption is endothermic. However the enthalpy involved in the proton desorption is very small compared to our calorimetric enthalpies. According to Bansal[17] exchange of Ni on kaolinite against Na^+ or Ca^{2+}, estimated from the temperature dependence of the adsorption, is an exothermic process. From calorimetric measurements Ewin reported that the exchange of Cs^+ against Na^+ on kaolinite and montmorillonite is exothermic[18]. Since DP^+ and Cs^+ both are specifically adsorbed on our kaolinite (see our

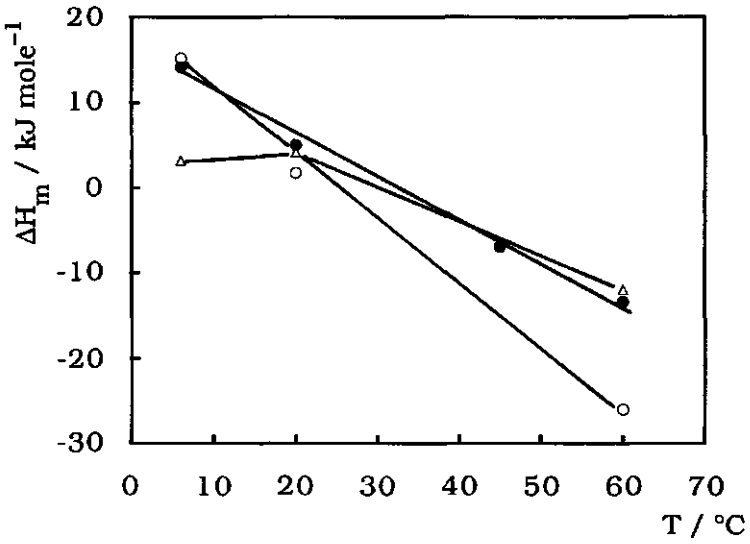

Figure 9. *Comparison of the temperature dependence of the enthalpies of adsorption $\Delta_{ads1}H_m$ (Δ) and $\Delta_{ads2}H_m$ (o) with that for the micellization enthalpy of DPC (●); at 5mM NaCl.*

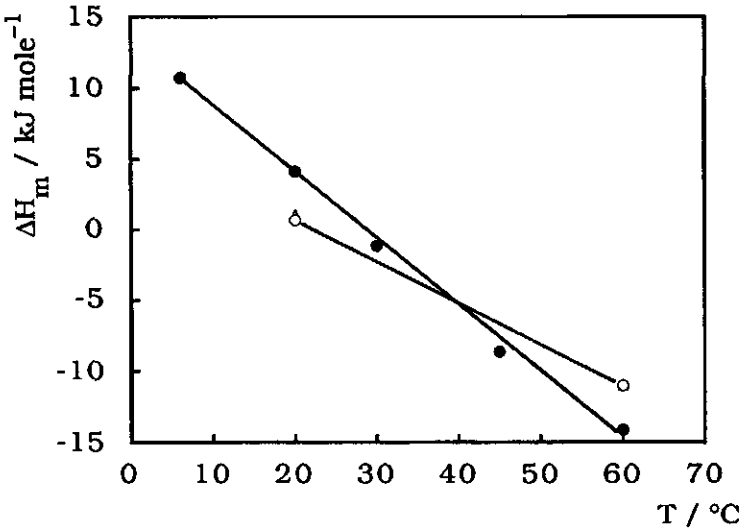

Figure 10. *Comparison of the temperature dependence of the enthalpies of adsorption, $\Delta_{ads1}H_m$ (Δ) and $\Delta_{ads2}H_m$ (o) with that for the micellization enthalpy of DPC (●) ; at 100 mM NaCl.*

conclusions on the Cs^+ adsorption in Chapters 2 and 4), it is likely that the nature of their exchange enthalpies against Na^+ is exothermic. Since at room temperature the desorption of water from the interface is an endothermic process[19], the sum of the endothermic enthalpy of the water desorption and that of the specific exchange must be exothermic. The repulsion between the charged head groups is endothermic and the hydrophobic bonding is a temperature dependent process. Generally speaking one may assume that the enthalpies other than that of hydrophobic bonding are not temperature dependent. In the formation of the second layer, (i), (ii) and (iii) are not contributing to the total enthalpy, therefore the endothermic enthalpy of double layer formation around the head groups remains as well as the enthalpy of hydrophobic bonding, i.e. we expect a strong contribution of hydrophobic bonding and a minor contribution for the formation of a diffuse layer between the bulk and the surfactant bilayer. Breaking the enthalpies of the first and second layer into their constituents is practically very difficult if not impossible. Nevertheless, our measured values of $\Delta_{ads1}H_m$ and $\Delta_{ads2}H_m$ satisfy our

expectations. Temperature dependence of the $\Delta_{ads2}H_m$ is much more pronounced than that of $\Delta_{ads1}H_m$. A relatively weak temperature dependence of $\Delta_{ads1}H_m$ is probably due to an unsharp transition between the formation of the first and the second layer.
It seems that the hydrophobic interactions between the adsorbate molecules starts even during the first layer formation but to a lesser extent than that of the second layer formation. Due to the existence of various compensatory enthalpic contributions in the formation of the first layer, interpretation of the results in this region is not easy.

6.3.2 Comparison of calorimetric enthalpies and isosteric enthalpies of the first and the second layer formation.

In Chapters 4 and 5, using isotherms measured at different temperatures we calculated the isosteric heat of adsorption according to the Clausius-Clapeyron equation:

$$\Delta_{ads}H_m(\text{isost}) = -RT^2\left(\frac{\partial \ln c_{DPC}}{\partial T}\right)_{\Gamma_{DP^+},\Gamma_{Na^+},\Gamma_{H^+},\Gamma_{Cl^-}}$$

$$= R\left(\frac{\partial \ln c_{DPC}}{\partial (1/T)}\right)_{\Gamma_{DP^+},\Gamma_{Na^+},\Gamma_{H^+},\Gamma_{Cl^-}} \qquad (3)$$

These values were negligibly small below the iep. However, beyond the iep, they depend on temperature and slightly on the surface coverage. Results obtained under the same experimental conditions as the calorimetric measurements are presented in Table 3, together with the calorimetric heat of adsorption for the first and the second layer formation.

In our interpretation we have to be aware that the adsorption of surfactants is a complex exchange process. The enthalpies obtained according to different procedures used are not necessarily identical.

Table 3. *Isosteric and calorimetric heat of formation of the first and second layer at various temperatures, c_{NaCl} = 5 mM, pH < epzc.*

T/°C	$\Delta_{ads1}H_m$(isost)	$\Delta_{ads1}H_m$	$\Delta_{ads2}H_m$(isost)	$\Delta_{ads2}H_m$
5-6	0	4.2	14 to 11	13.2
20	0	4.1	0	1.7
60	0	-11.9	-18 to -21	-28.0

If we take into account the experimental errors involved in these two very different techniques, then the isosteric enthalpies of the second layer formation show a reasonable agreement with the directly measured heats of adsorption. It follows that the process fulfils the condition of equilibrium thermodynamics. The enthalpies of the first layer formation deviate to some extent from the $\Delta_{ads1}H_m$. It has already been concluded that the calorimetric enthalpies of the first layer formation show also some temperature dependence, implying the presence of hydrophobic bonding for the formation of the first layer. This is not in complete agreement with the isosteric heats for the first layer. Up till now a strong thermodynamic argument for the above mentioned discrepancy has not been available. Nevertheless we can point out a few possible explanations. In our calorimeter we used a reference cell and the reproducibility was satisfactory. Therefore our directly measured heats are most reliable. On the other hand there are several uncertainties (approximations) in the estimation of the isosteric heat of adsorption: (a) Calculations of $\Delta_{ads}H_m$(isost) are performed by considering two isotherms measured at two temperatures and assuming that the composition of the adsorbed phase is the same as if the excess amount of DPC does not change. (b) It is assumed that the number of adsorption sites does not change with the temperature. (c) The activity coefficients in the liquid phase at various temperature are unknown. Thus we used concentrations instead of activities which causes an unreal estimation as has been explained by de Keizer et al.[20] (d) The logarithmic nature and the discrete characteristics of the adsorption isotherms which are used in calculations according to Equation (3) makes the isosteric adsorption enthalpy more prone to interpolating errors. Probably an important reason for the discrepancy

found between the two methods for the formation of the first layer, is the variation of Γ_{Na^+} and Γ_{H^+} with temperature. Since the formation of the second layer starts when the charge of the kaolinite is compensated, the values of Γ_{Na^+} and Γ_{H^+} at the interface are of minor importance. Therefore, beyond the iep a complete agreement between the two techniques is found.

6.4 Conclusions

The directly measured heats of adsorption of DPC on Na-kaolinite are temperature dependent, changing sign at a transition temperature of around 24-30°C. This transition temperature is very close to the T_{trans} of the micellization enthalpy.

All of the q_{ads}/Γ curves show a break which roughly corresponds to the iep of the kaolinite particles in the presence of surfactant. The curves are fairly linear below and above the break, confirming that the surface is homogeneous with respect to DPC adsorption. This is additional evidence that the surfactant is adsorbed on the edges to only a minor extent. The electrolyte concentration has a small effect on the adsorption enthalpies of the first and second layers. Our calorimetric results show that $\Delta_{ads2}H_m$'s are temperature dependent, suggesting that hydrophobic bonding is an important driving force for the formation of the second layer. $\Delta_{ads1}H_m$'s are also temperature dependent but this trend is not as strong as it is for the second layer formation. $\Delta_{ads1}H_m$'s differ somewhat from $\Delta_{ads}H_m$(isost), but $\Delta_{ads2}H_m$ is, within experimental error, identical with the isosteric heat of adsorption of the second layer. Generally, the values of $\Delta_{ads2}H_m$ are close to the micellization enthalpy, proving that surfactant aggregates are formed at the interface.

From this work we conclude that in order to investigate the thermodynamic parameters of complex processes, a study of the temperature dependence is useful although it is advisable to complement the measurements with other techniques such as electrophoresis and calorimetry.

6.5 Acknowledgement

The experimental contribution of Mr. A. J. Korteweg is highly appreciated.

6.6 References

(1) De D. K., Chakravati S. K., Mukherjee S. K. *J. Indian Soil Sci. Soc.*, **1968**, *45*, 566-575.
(2) Malik W. U., Srivastava S. K. , Gupta D. *Clay Minerals*, **1972**, *9*, 369-382.
(3) El-Mowafi M. A., Geneidi A. S. , Kassem A. A. *Egypt. J. Pharm. Sci.*, **1983**, *24*, 233-251.
(4) Somasundaran P., Fuerstenau D. W. *J. Phys. Chem.*, **1966**, *70*, 90-98.
(5) Fuerstenau D. W., Wakamatsu T. *Adv. Chem. Ser.*, **1968**, *79*, 161-170.
(6) Fuerstenau D. W., Wakamatsu T. *Trans. AIME*, **1973**, *254*, 123-128.
(7) Somasundaran P., Goddard E. D. *Mod. Aspects Electrochem.*, **1979**, *13*, 207-215.
(8) Noll L. A., Burchfield T. E., Good W. D., Proceedings: *"Fifth Annual DEO Symposium on Enhanced Oil & Gas Recovery & Improved Drilling Technology"*, Tusla OK, **1979.**
(9) Berg R. L., Noll L. A., Good W. D. *ACS Symp. Ser.*, **1979**, *91*, 87-102.
(10) Rouquerol J., Partyka S. *J. Chem. Tech. Biotechnol.*, **1981**, *31*, 584-592.
(11) van Os N. M., Haandrikman G. *Langmuir*, **1987**, *3*, 1051-1056.
(12) Vilcu R., Olteanu M. *Conf. Int. Thermodyn. Chim. (c.r.)*, **1975**, *4*, 116-125.
(13) Partyka S., Rudzinski W., Brun B. *Langmuir*, **1989**, *5*, 297-304.
(14) Partyka S., Keh E., Lindheimer M. , Groszek A. *Colloids Surfaces*, **1989**, *37*, 309-318.
(15) Denoyel R., Rouquerol J. *J. Colloid Interface Sci.*, **1991**, *143*, 555-572.

(16) Wierer K., *" Adsorption von H+/OH- Ionen und Tensiden an Mineralen, Kalorimetrische Untersuchungen"*, PhD Thesis, Regensburg University, **1987.**

(17) Bansal O. P. *J. Soil Sci.*, **1982**, *33*, 63-71.

(18) Ewin G. J., Erno B. P., Helper L. G. *Can. J. Chem.*, **1980**, *59*, 2927-2933.

(19) Conley R. F., Althoff A. C. *J. Colloid Interface Sci.*, **1971**, *37*, 186-194.

(20) de Keizer A., Fokkink L. G. J., Lyklema J. *Colloids Surfaces*, **1990**, *49*, 149-163.

APPENDIX TO CHAPTER 6

Calculation of Adsorption Enthalpy

The adsorbed amount Γ and the logc terms used in computing the heats of adsorption presented in chapter 6, are calculated using the data given in Tables A.1.2. A polynomial is drawn through the experimental points. In all cases a 4th degree polynomial fitted best. The relation between Γ and logc is therefore:

$$\Gamma = A + B(\log c) + C(\log c)^2 + D(\log c)^3 + E(\log c)^4 \qquad (1)$$

In (1) Γ is adsorption density in μmoles g^{-1} and A, B, C, D and E are constants. If Y moles DPC are added to a suspension in the calorimetric cell under the same experimental conditions as that of the isotherm measurements, then the following relationship must hold:

$$Y_n - 10^{-6}\left(A + B(\log c_n) + C(\log c_n)^2 + D(\log c_n)^3 + E(\log c_n)^4\right) + V_n \times c_n = 0 \qquad (2)$$

where V_n is the volume of the suspension in litre. Using Newton iteration the total moles of DPC used were related to a sum of amount adsorbed and the amount remained in the bulk.

In some cases (2) has more than one positive root, from which we could choose the proper one by checking both answers in the experimental adsorption isotherm. The values of A, B, C, D and E are shown in Table A1.1 The corresponding measured adsorption isotherms are given in Tables A1.2 and the calculated isotherms in Tables A1.3

Table A1.1 *Coefficients of Equation (1) at different salt concentrations and temperatures.*

T (°C)	c_{NaCl} (mM)	A	B	C	D	E	*R*
6	5	238.81	175.91	61.76	10.52	0.67	*0.9997*
20	5	374.89	315.19	112.87	18.55	1.13	*0.9993*
	100	-642.68	-943.87	-439.66	-83.79	-5.71	*0.9937*
60	5	155.94	81.91	21.09	2.88	0.16	*0.9940*
	100	-631.61	-943.87	-439.66	-83.79	-5.71	*0.9940*

Tables A1.2 *Adsorption isotherms of DPC on Na-kaolinite; pH = 5. The adsorption density Γ is in µmole/g, c_{equil}: equilibrium concentration*

Table A1.2.1 *T = 20°C*

c_{NaCl} = 5 mM		c_{NaCl} = 20 mM		c_{NaCl} = 100 mM	
Γ	$\log c_{equil}$	Γ	$\log c_{equil}$	Γ	$\log c_{equil}$
2.44	-5.66	2.40	-5.49	2.32	-5.00
4.91	-5.47	4.85	-5.22	4.47	-4.66
7.33	-5.21	7.18	-4.90	6.56	-4.41
9.66	-4.82	9.42	-4.64	8.68	-4.27
22.3	-3.95	21.80	-3.87	18.62	-3.60
34.5	-3.19	35.20	-3.20	35.71	-3.25
41.3	-2.70	42.00	-2.80	48.30	-2.74
54.50	-2.23	60.50	-2.23	54.71	-2.74
68.20	-1.96	59.80	-2.26	78.71	-2.30
50.50	-2.40	69.20	-1.78	76.00	-1.89
76.5	-1.81	72.00	-1.83	70.01	-1.82

***Table A1.2.2**; T = 60°C*

c_{NaCl} = 5 mM		c_{NaCl} = 20mM		c_{NaCl} = 100 mM	
Γ	$\log c_{equil}$	Γ	$\log c_{equil}$	Γ	$\log c_{equil}$
2.46	-6.10	2.45	-5.70	2.30	-5.05
4.98	-6.00	4.87	-5.35	4.48	-4.69
7.45	-5.70	7.28	-4.98	6.70	-4.49
9.67	-4.87	9.48	-4.66	8.67	-4.27
22.44	-3.94	21.91	-3.88	18.70	-3.59
30.75	-3.35	33.70	-3.16	34.80	-3.20
33.83	-3.17	41.00	-2.79	46.22	-2.85
38.83	-2.77	44.12	-2.63	49.80	-2.69
46.62	-2.20	56.71	-2.22	72.20	-2.28
62.31	-1.86	66.50	-1.86	76.80	-1.89
57.93	-1.80	69.21	-1.80	72.00	-1.88
		64.61	-1.87		
		34.41	-3.19		
		43.00	-2.64		
		55.40	-2.23		

***Table A1.2.3**; T = 6°C, c_{NaCl} = 5 mM*

Γ	$\log c_{equil}$	Γ	$\log c_{equil}$
2.46	-5.82	21.44	-3.88
4.81	-5.27	33.44	-3.19
7.22	-4.95	41.76	-2.65
9.40	-4.68	50.41	-2.22
21.44	-3.89	65.82	-1.80

Tables A1.3 *Calculated adsorption isotherms, enthalpies in J and Γ in μmoles g^{-1}, used for cumulative adsorption curves in chapter 6 (Figures 4–6).*

Table A1.3.1; *T = 6°C and c_{NaCl} = 5 mM.*

q_{ads}(cum)	$logc_{equil}$	Γ	q_{ads}(cum)	$logc_{equil}$	Γ
0.094	–3.88	22.76	0.473	–2.02	55.31
0.189	–3.04	34.3	0.489	–1.97	56.70
0.282	–2.70	40.2	0.507	–1.92	58.11
0.336	–2.49	44.2	0.522	–1.88	59.33
0.374	–2.35	47.2	0.538	–1.84	60.50
0.405	–2.24	49.7	0.555	–1.81	61.50
0.430	–2.16	51.84	0.574	–1.77	62.51
0.452	–2.09	53.67	0.588	–1.74	63.4
			0.599	–1.71	64.31

Table A1.3.2; *T = 20°C and c_{NaCl} = 5 mM*

q_{ads}(cum)	Γ	$logc_{equil}$	q_{ads}(cum)	Γ	$logc_{equil}$
0.005	4.91	–5.28	0.138	41.38	–2.71
0.016	7.35	–5.06	0.145	46.34	–2.51
0.040	14.51	–4.54	0.154	50.55	–2.37
0.074	21.07	–4.08	0.158	54.26	–2.26
0.097	26.37	–3.67	0.163	57.60	–2.18
0.112	30.26	–3.37	0.170	60.66	–2.11
0.121	33.23	–3.16	0.173	63.50	–2.04
0.129	35.66	–3.01	0.182	66.15	–1.99
0.131	37.77	–2.89	0.181	68.52	–1.95

***Table A1.3.3**; T = 20°C and c_{NaCl} = 100 mM*

$q_{ads(cum)}$	Γ	$\log c_{equil}$
0.01058	10.42	–3.94
0.02058	19.82	–3.54
0.03058	28.73	–3.31
0.04693	36.45	–3.12
0.05145	43.39	–2.97
0.0561	49.25	–2.84
0.06003	55.06	–2.74
0.06229	59.15	–2.64

Table A1.3.4; *T = 60°C*

c_{NaCl} = 5 mM			c_{NaCl} = 100 mM		
q_{ads}(cum)	Γ	$\log c_{equil}$	q_{ads}(cum)	Γ	$\log c_{equil}$
-0.027			-0.13	10.52	-3.94
-0.054	4.98	-5.86	-0.24	20.06	-3.54
-0.081	7.50	-5.48	-0.35	28.91	-3.31
-0.108	9.88	-5.00	-0.44	36.93	-3.12
-0.130	12.28	-4.89	-0.51	44.05	-2.97
-0.162	14.61	-4.65	-0.56	50.03	-2.84
-0.194	16.85	-4.42	-0.61	55.56	-2.74
-0.217	18.97	-4.22	-0.67	60.12	-2.64
-0.244	20.94	-4.04			
-0.489	33.48	-3.09			
-0.616	39.72	-2.72			
-0.705	43.84	-2.51			
-0.778	46.93	-2.36			
-0.847	49.50	-2.25			
-0.912	51.64	-2.17			
-0.969	53.50	-2.09			
-1.013	55.15	-2.03			
-1.059	56.63	-1.97			
-1.108	57.98	-1.93			
-1.154	59.22	-1.88			
-1.187	60.36	-1.84			

SUMMARY

The present work is aimed at understanding the interactions involved in the adsorption of cationic surfactants on heterogeneous surfaces. The relevance of the study derives from the environmental aspects of the adsorption of small organic molecules onto soil constituents. This thesis emphasizes the experimental aspects.

In order to achieve a better understanding of the driving forces involved in the adsorption process, classical equilibrium thermodynamics is used to estimate the energetic and entropic parameters of the system.

The main experimental systems were a homo-ionic kaolinite in an aqueous electrolyte solution which contained a cationic surfactant with a dodecyl tail and either a pyridinium chloride (DPC), or a trimethyl-ammonium bromide head group (DTAB).

In Chapter 2 a comprehensive study of the physico-chemical properties of the adsorbent has been carried out. Several techniques, such as X-ray diffractometry, electron microscopy, Ar/N_2 adsorption calorimetry, and BET gas adsorption have been used to characterize the kaolinite surface. The collected evidence shows that our kaolinite is free of 2:1 clay contaminants. Combination of electrophoresis measurements and potentiometric titration results gives information on the properties of our representative of the group of 1:1 clay minerals. Contrary to the idea of some soil scientists, about 50% of our kaolinite surface charge stems from isomorphic substitution which is mainly exposed to the basal surfaces. These surfaces are homogeneous with respect to Ar and surfactant adsorption. The particles posses a variable charge (pH-dependent) on the edges. The edges have a more heterogeneous character. Constant hysteresis observed between back- and forward potentiometric titrations confirm the binary nature of the surface charge and the possibility of edge-plate interactions resulting in a so-called card-house packing. The ratio found for the edge/plate surface area depends on the method used, viz. 0.35 from DPC adsorption, 0.55 from potentiometric titration, 0.20 from Ar adsorption calorimetry and 0.41 from electron microscopy. The CEC measured by the silver-thiourea method amounts to 57 μmole/g whereas that determined by using the ammonium acetate method is 30

μmole/g. Potentiometric titrations show that the clay surface is not covered by any oxide coating. Over the experimental pH range of 4 to 10, neither an isoelectric point (iep), nor a zero point of charge (pzc) has been found for the entire particles. Extrapolation of the electrophoretic data suggests a pzc of about 2. The zero point of charge of the edges (epzc) is estimated from the inflection point of charge-potential curves which is located in the region of minimum electrolyte effect. Of the three cations Li^+, Na^+ and Cs^+, Cs^+ adsorbs most strongly, resulting in a lower electrophoretic mobility and a slightly lower epzc for Cs-kaolinite. The epzc is 6.7 for Li- and Na-kaolinite and 6.0 for Cs-kaolinite.

Protons are specifically adsorbed, not only on the functional edge groups but also on the plates. Adsorption of protons on Na-kaolinite is exothermic, with the enthalpies increasing when the surface charge becomes more negative. The electrolyte effect on the proton adsorption enthalpy is very small. This suggests that the pH has a more pronounced effect on the surface potential than the indifferent electrolyte. From the fact that electrophoretic mobilities change more strongly with pH than with the electrolyte concentration we come to the same conclusion. The proton adsorption enthalpies at each pH show a qualitative similarity to that of oxides with similar pzc's.

Chapter 3 deals with the properties of the adsorbate. Here the thermodynamic properties of a homologous series of surfactants are studied. The micellization enthalpies of three surfactants with C_{10}, C_{12} and C_{14} tails and pyridinium head groups are directly measured as a function of electrolyte concentration and temperature. At a certain temperature and electrolyte concentration each surfactant has a characteristic critical micelle concentration (cmc) value, which is some 60-80, 10-20 and 5-10 mmoles per litre for C_{10}- C_{12}- and C_{14}-pyridinium chloride, respectively. Enthalpies of micellization of the surfactants ($\Delta_{mic}H_m$) are temperature dependent. They change sign at a certain temperature, T_{trans}. T_{trans} is dependent on the chain length and to a lesser extent on the electrolyte concentration. The (extrapolated) $\Delta_{mic}H_m(T)$ curves of the three surfactants cross each other at ~ −12°C. The enthalpy at this temperature is attributed to the head group contribution; here the enthalpic contribution of the tail is zero.

Increasing the temperature decreases the structuring of water around the tails and, consequently, the entropy rises upon association of tails, but this effect is more than compensated by the decrease in enthalpy.

An attempt has been made to break down the Gibbs energy, enthalpy and entropy of micellization into their electrical, hydrophobic and chemical constituents. Using the mass action model, Gibbs energies of micellization are estimated. In the presence of 0.1 M NaCl, the thermodynamic parameters of micellization of the surfactants expressed per CH_2 group are very close to the corresponding parameters of transporting a methyl group from water to a hydrophobic phase. According to our calculations, hydrophobic bonding contributes most to the micellization Gibbs energy. The electrical contribution is rather small and unfavourable. The constant chemical contribution is also unfavourable and can perhaps be attributed to a decrease in hydration forces of the solvent around the head group.

The enthalpy of adsorption may be derived from adsorption isotherms determined at different temperatures or may be directly measured by using a microcalorimetric technique. The former method is discussed in Chapters 4 and 5, the latter in Chapter 6.

More specifically, in Chapter 4 the adsorption of DPC and DTAB on Na-kaolinite is studied as a function of electrolyte concentration and pH at two temperatures. Adsorption isotherms have steep initial slopes reflecting the high affinity of the adsorptives for the surface. For both surfactants and at both temperatures, all isotherms, if measured at different salt concentrations, exhibit a common intersection point (cip) roughly around the iep. Below the cip adsorption is reduced by electrolyte addition; beyond it electrolyte promotes adsorption. Below the cip adsorption is to a large extent electrostatically driven; addition of salt reduces the attraction. However, beyond the cip association of adsorbed surfactant molecules takes place, which occurs despite the repulsion between the head groups; now electrolyte reduces this repulsion and hence promotes adsorption. The pyridinium head group shows a slightly higher affinity for the kaolinite surface than the trimethylammonium head group.

On kaolinite, adsorption of both surfactants takes place mainly on the plates. With increasing pH the (total) adsorption increases, but not so much that all adsorption sites on the edges become covered. On the plates adsorbed protons are, at least partly, exchanged against the surfactant molecules, as the pH is increased. A bilayer adsorption model has been developed on the basis of the Frumkin-Fowler-Guggenheim isotherm equation fits the adsorption data well.

Chapter 5 compares the temperature dependence of the adsorption of organic cations on Na-kaolinite with that on AgI. The former adsorbent is hydrophilic, the latter hydrophobic. On AgI the adsorption of tetrabutylammonium nitrate (TBAN) proceeds up to a monolayer, whereas on the hydrophilic kaolinite the adsorption of DPC and DTAB continues up to a bilayer. On AgI the adsorption of TBAN exhibits a maximum as a function of temperature. For amphiphilic molecules on kaolinite, the enthalpies of the formation of the first layer show hardly any temperature dependence, whereas those of the formation of the second layer again pass through a maximum as a function of temperature. The adsorption of surfactant molecules increases the hydrophobicity of kaolinite, hence, around the region of completion of the first layer, the surface becomes hydrophobic. Adsorption enthalpies on AgI and on the hydrophobic kaolinite show the same trend as those for the micellization of the surfactants used. This indicates that all these processes are determined by the same mechanism, viz. hydrophobic bonding.

Chapter 6 discusses the microcalorimetric measurements of the enthalpies of adsorption of DPC on Na-kaolinite at different salt levels and temperatures. Adsorption enthalpies are temperature dependent; they are positive at low temperatures, reduce to zero at about 24°C and turn to negative at $T > 24°C$. A break in the plots of the cumulative adsorption enthalpy as a function of adsorbed amount is detected under most experimental conditions. This break, the iep and the cip of the adsorption isotherms at different electrolyte concentrations are all identical within experimental error. Below and above the break, the adsorption enthalpies are fairly constant, suggesting that the surface is homogeneous. This is in accordance with the earlier conclusion that

adsorption takes place mainly on the basal surfaces. The change of the slope of the $\Delta H(\Gamma)$ curves upon completion of the first layer shows again the different adsorption mechanism for the first and second layer. This part of the study confirms that among the different contributions to the enthalpy the hydrophobic part is the most important for the second layer formation. However, for the first layer the head group affinity for the surface dominates.

Comparison of the isosteric adsorption enthalpy and the directly measured heat of adsorption leads to the next two conclusions: (a) For the formation of the first layer the isosteric heat of adsorption deviates somewhat from that measured by calorimetry. (b) For the formation of the second layer, good agreement has been found between the two. Both values are rather close to the enthalpy of micelle formation. Probably an important reason for the discrepancy found for the first layer is the variation of the concentrations of the other adsorbed cations at the interface as a consequence of a temperature change. Since the formation of the second layer starts when the charge of the kaolinite is compensated, the concentration of these ions at the interface is of minor importance. Therefore, beyond the iep a complete agreement between the two techniques is found.

With regard to the adsorption mechanism our results can be summarized as follows:

- Adsorption of cationic surfactants on charged clay surfaces takes place with a Gibbs energy of few tens of kJ/mole, implying a physical adsorption.
- Surfactants adsorb primarily on the basal surfaces of kaolinite which possesses a negative charge. Whether the adsorption also takes place on the edges is uncertain. On the plates first a monolayer is formed, then a bilayer. For the former, electrolytes act as competitors, for the latter, where hydrophobic bonding is the driving force, as promoters.
- Formation of the second layer is similar to micellization. The enthalpies of both processes have the same trend as a function of temperature. They are close to each other and their transition temperature agrees within a few degrees.

- The nature of the head group does not play a dominating role in micelle formation or in adsorption.

The adsorption of amphiphiles is sensitive to parameters such as the nature of the surface charge, electrolyte concentration, pH, and temperature. Therefore, in different climates one must expect different adsorption capacities of soils and hence, different rates of water pollution. For example, in natural systems consisting mainly of particles with a permanent charge, the adsorption capacity is probably much higher than in those systems which contain relatively large amounts of particles with variable charge. Hence, from this point of view, tropical soils may be more prone to pollution caused by the transport of organic compounds to ground water.

The adsorption of amphiphiles is not limited to charge compensation. Therefore the value of the CEC may underestimate the adsorption capacity of soils.

As the hydrophobic character of the charged particles changes with the amount adsorbed, there may be a large effect of soil pollution on the permeability of soils.

The overall conclusion is that the present study not only contributes to our knowledge about adsorption forces but may also be helpful in understanding and predicting processes which occur in natural systems.

SAMENVATTING

Thermodynamica van de Adsorptie van Organische Kationen aan Kaoliniet

Het doel van dit onderzoek was inzicht te krijgen in de drijvende krachten van de adsorptie van kleine geladen organische moleculen aan bodemmineralen met tegengesteld geladen oppervlak. De toepassing van dit onderzoek is te vinden in de milieuproblematiek van gewasbeschermingsmiddelen in de bodem. Deze stoffen kunnen o.a. het grondwater verontreinigen.

Met adsorptie aan een grensvlak bedoelt men, dat een stof zich ophoopt aan dat grensvlak. Een grensvlak is het overgangsgebied tussen twee fasen (in ons geval een waterfase en een vaste stof). Als er adsorptie uit een oplossing optreedt, is dit altijd ten koste van desorptie van het oplosmiddel en eventueel ook van andere stof indien die daar reeds aanwezig was.

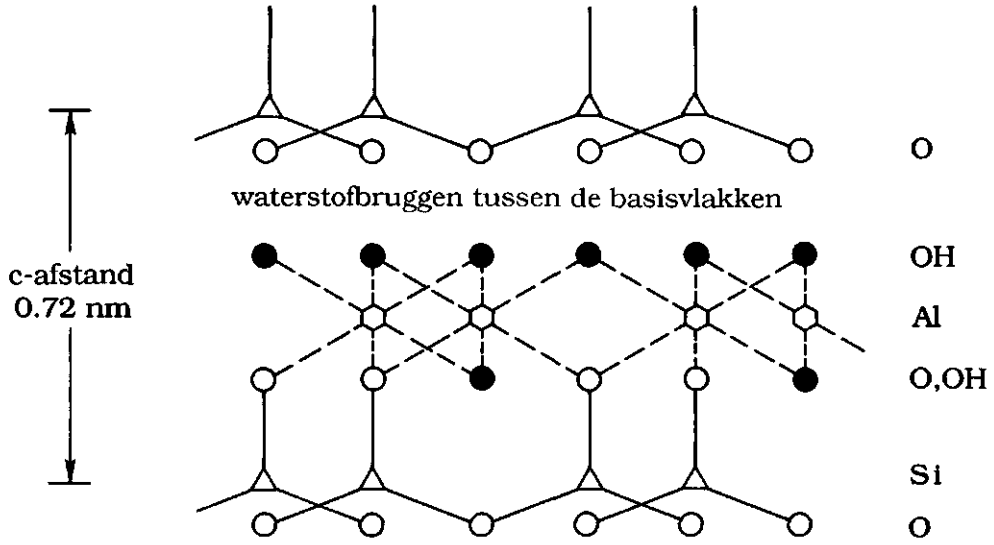

Figuur 1. *Schematische weergave van de stractuur van kaoliniet.*

Ons model systeem bestaat uit negatief geladen kaoliniet (een kleimineraal dat in de bodem voorkomt), een (indifferent) zout en meestal (één van) de positief geladen (kationogene) zepen dodecylpyridiniumchloride (DPC) of dodecyltrimethylamoniumbromide (DTAB).

Kaoliniet is een aluminiumsilicaat met $Si_4Al_4O_{10}(OH)_8$ als ideale struktuurformule. Dat betekent dat de elementaire kaolinietplaatjes uit een laag van aluminiumoxide en een laag van siliciumoxide bestaan. De zuurstof-atomen vormen de verbindende schakels tussen de Al en Si atomen. Hydroxylgroepen en de zuurstofatomen zorgen voor het juiste aantal covalente bindingen van Si en Al. De struktuur is schematisch in figuur 1 weergegeven.

Door de asymmetrie van kaolinietplaatjes, worden een stuk of 40 elementaire plaatjes aan elkaar verbonden door waterstofbruggen. De aldus ontstane kaoliniet deeltjes zijn hexaeders met een dikte van ongeveer 30 nm. Zie figuur 2. Men kan er de (oppervlakte) platen en de zijkanten aan onderscheiden.

Het oppervlak van kaoliniet is geladen door (a) isomorfe vervanging en (b) dissociatie of associatie van OH groepen. Isomorfe vervanging betekent dat tijdens het vormen van de klei een Si^{4+} ion door een driewaardige ion zoals Al^{3+} en/of een Al^{3+} door een tweewaardig ion zoals Mg^{2+} wordt vervangen. Dit resulteert in een positief ladingstekort oftewel in een

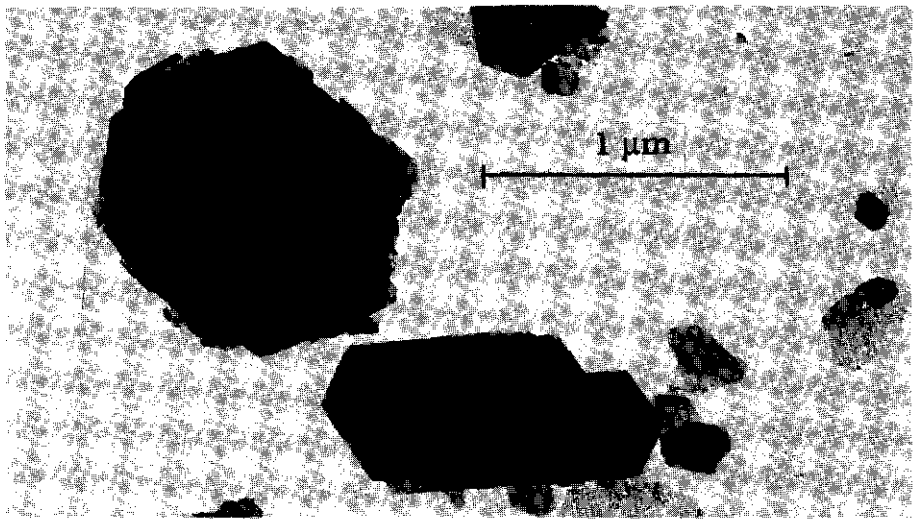

Figuur 2. *Electronenmicroscopie van Sigma Na-kaoliniet.*

negatief geladen deeltje. In de praktijk uit zich dat als een negatief geladen oppervlak. Deze negatieve lading wordt door positieve tegenionen gecompenseerd. Op de zijkanten van de deeltjes zit ook lading, maar die heeft een andere herkomst, namelijk dissociatie van OH groepen of binding van protonen daaraan. De lading door isomorfe vervanging is constant van grootte maar de lading door de dissociatie of associatie van OH groepen is variabel. Als maat van de grootte voor de lading op de kleien heeft men de kationenuitwisselingscapaciteit, in het engels: *cation exchange capacity*, (CEC) gedefiniëerd. De CEC is de maximale hoeveelheid van een vreemd kation dat uitgewisseld kan worden tegen de aanwezige tegenionen. De waarde die voor de CEC gevonden wordt, is afhankelijk van de experimentele methoden en experimentele omstandigheden. Verschillende methoden worden als standaard door bodemchemici gebruikt. Als het kleioppervlak neutraal is bij een bepaalde pH van de oplossing, wordt die pH het ladingsnulpunt (pzc) genoemd. Als de electroforetische beweeglijkheid van de deeltjes nul is, dan bevinden de deeltjes zich in het isoëlectrisch punt (iep).

Een kationogene zeep (de engelse term die ook vaak in het Nederlands gebruikt wordt is *cationic surfactant*) bestaat uit een hydrofobe of "watervrezende" staart en een hydrofiele of "waterminnende" kop die positief geladen is, zie figuur 3. Zeepmoleculen zijn daarom amfifiel en hebben de eigenschap zich op te hopen aan het hydrofiel-hydrofobe grensvlakken, zoals het water-lucht grensvlak. Belangrijke eigenschappen van zepen zoals het vermogen tot wassen en het mengbaar maken van water en olie zijn eveveens gevolgen van het amfifiele karakter. Als de concentratie van een zeep in een oplossing hoog genoeg is, associëren de zeepmonomeren tot grotere eenheden. Zo'n deeltje heet een micel en de concentratie die net hoog genoeg is om micellen te vormen is de kritische micelvormingsconcentratie, kmc. De grootte van de kmc is afhankelijk van de experimentele omstandigheden zoals de electrolyt-concentratie en de temperatuur. Bij adsorptie kunnen de staart en de kop verschillende wisselwerkingen hebben met het oppervlak. Soms treedt aggregatie van surfactantmoleculen aan het grensvlak op.

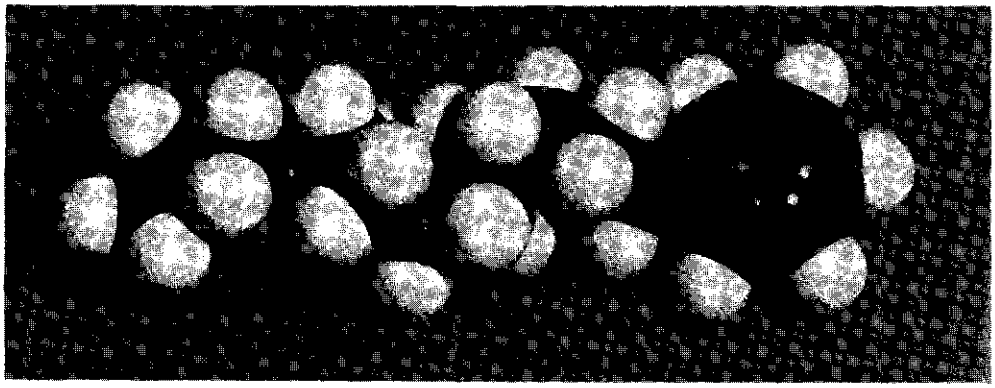

Figuur 3. *Model van een DPC molecuul.*

Door de kennis van de thermodynamica van de adsorptie, kan men de drijvende krachten van het proces leren en het gedrag van adsorberende moleculen beter kan begrijpen. De Gibbs energie; symbool G, enthalpie; symbool H en entropie; symbool S zijn thermodynamische parameters. De opgenomen of gevormde warmte van een reaktie bij constante druk heet enthalpie. Als warmte bij een proces wordt afgestaan (dat is zo in een exotherm proces) wordt volgens afspraak ΔH negatief geteld; in het omgekeerde geval (in een endotherm proces) is $\Delta H>0$. De entropie is een maat voor de wanorde van het systeem op een molekulaire schaal. De Gibbs energie is gedefineerd als H–TS. Voor een spontaan proces bij constante druk en temperatuur is de totale Gibbs energie van de produkten minder dan die van de reactanten. Met andere woorden, bij een spontaan proces moet bij konstant temperatuur en konstante druk, warmte (enthalpie) vrijkomen en/of de wanorde van het systeem groter worden. Men kan direkt of indirekt de waarde van ΔH van een proces bepalen. De waarden van ΔG kunnen met behulp van een model berekend worden. Als de waarden van ΔG en ΔH bekend zijn, kan voor reversibele processen daaruit de waarde van ΔS ook berekend worden.

Om ons systeem systematisch en grondig te kunnen behandelen, moeten we eerst de componenten er van zo goed mogelijk kennen. Daarom hebben we in de hoofdstukken 2 en 3 kaoliniet en kationogene zepen uitgebreid bestudeerd.

In hoofdstuk 2 zijn de eigenschappen van homo-ionogene kaolinieten experimenteel bepaald. In de natuur zijn verschillende tegenionen aanwezig om de oppervlaktelading te compenseren. In onze experimenten is de kaoliniet suspentie slechts met één bepaald tegenion (namelijk óf Li^+ óf Na^+ óf Cs^+) verzadigd. Zo'n klei noemt men homo-ionogeen.

Alle experimenten wijzen erop dat onze kaoliniet niet verontreinigd is met andere soorten klei. Zuur-base titraties tonen aan dat het plaat oppervlak van kaoliniet niet bedekt is met oxiden. Electroforese resultaten en zuur-base titraties bewijzen dat de lading op de platen ~50% van de totale lading is. De verhouding tussen het (specifiek) oppervlak van randen en platen is gemeten met verschillende methoden. Uit argon adsorptie volgt 0.2, uit DPC adsorptie 0.35, uit electronenmicroscopie 0.41 en uit potentiometrische titraties 0.55. De CEC gemeten met de zilver-thioureum methode is 57 µmole/g, terwijl die met de ammonium acetaat methode 30 µmole/g is. Tussen pH 4 - 10 wordt geen pzc of iep gevonden. Extrapolatie van de electroforetische beweeglijkheid geeft een iep (pzc) van 2. Het ladingsnulpunt van de randen (epzc) werd geschat uit het buigpunt van de lading/potentiaal curven. Dat buigpunt valt binnen het gebied van de minimale zoutinvloed. Van de kationen, Li^+, Na^+ en Cs^+ wordt cesium het sterkst geadsorbeerd. Daarom is het epzc van Cs-kaoliniet wat lager dan dat van Li-kaoliniet en van Na-kaoliniet.

Protonen worden zowel aan de kaoliniet randen als aan de platen specifiek geadsorbeerd. De adsorptie van protonen is exotherm. De adsorptieënthalpie neemt toe met de pH. De invloed van de zoutsterkte op de enthalpie van protonadsorptie is minder dan die van de pH. Deze conclusie kon weer bevestigd worden met de beweeglijkheid metingen. De beweeglijkheid van kaoliniet deeltjes verandert sterker met de pH dan met de zoutconcentratie. De enthalpie van de protonadsorptie bij een bepaalde pH komt overeen met die voor oxiden met dezelfde ladingsnulpunten.

Hoofdstuk 3 beschrijft de eigenschappen van kationogene zepen. De enthalpie van micelvorming werd gemeten met een isotherme calorimeter (Therma Activity Monitor). De temperatuur werd gevarieerd

tussen 6 en 60°C. Als tijdens de adsorptie zeepmoleculen aan het oppervlak aggrereren lijkt het proces op dat van de micelvorming van de zeepmoleculen in een oplossing. Omdat de hydrofobe staart een zeer grote rol speelt in het micelvormings proces, hebben wij getracht de bijdrage van elke individuele CH_2 in thermodynamische parameters uit te drukken. Om dit doel te bereiken werden zepen met verschillende staartlengten bestudeerd, namelijk decyl-, dodecyl- en tetradecylpyridiniumchloride. Wij hebben de invloed van temperatuur en van zout op de kmc van deze surfactants bekeken.

De kmc waarden zijn respektievelijk 60-80, 10-20 en 5-10 mmol per liter voor decyl-, dodecyl en tetradecylpyridiniumchloride. De molaire micelvormings enthalpieën $\Delta_{mic}H_m$ zijn sterk afhankelijk van de temperatuur. De tekens van deze enthalpieën keren om bij een bepaalde temperatuur (T_{trans}). Deze T_{trans} is sterk afhankelijk van de staartlengte maar in mindere mate van de concentratie van het electrolyt. De geëxtrapoleerde $\Delta_{mic}H_m(T)$ curven van die zepen snijden elkaar bij −12°C. Bij deze temperatuur is de gemeenschappelijke enthalpie geheel toe te schrijven aan de hydrofobe kop; de bijdrage van de staart tot de totale enthalpie is daar nul. Als de temperatuur hoger dan −12°C wordt, worden de watermoleculen in de buurt van de staart minder gestruktureerd. Dit effect is vooral verantwoordelijk voor de afname van de enthalpie.

Er is een poging gedaan om de Gibbs energie ($\Delta_{mic}G_m$), enthalpie ($\Delta_{mic}H_m$) en entropie ($\Delta_{mic}S_m$) van micelvorming te splitsen in hun electrische, hydrofobe en chemische bijdragen. Wij hebben het massawerkingsmodel gebruikt om $\Delta_{mic}G_m$ te benaderen. Als de zoutconcentratie 0.1 M is, hebben de thermodynamische parameters van de micelvorming van de zepen per CH_2 groep ongeveer dezelfde waarden als voor het overbrengen van een methylgroep uit de waterfase naar de oliefase. Onze berekeningen tonen aan dat hydrofobe binding de belangrijkste bijdrage levert tot $\Delta_{mic}G_m$. De elektrische bijdrage is klein en werkt tegen. De (constante) chemische bijdrage werkt eveneens tegen en komt waarschijnlijk van de afnemende hydratiekrachten van het oplosmiddel in de buurt van de kopgroep.

Er zijn twee methoden om de adsorptieënthalpie te bepalen; (a) bestudering van de temperatuursinvloed op de adsorptie; dit geeft de zogenaamde isostere warmte $\Delta_{ads}H_m$(isost), (b) het direkt meten van de adsorptie warmte met een calorimeter $\Delta_{ads}H_m$. In hoofdstukken 4 en 5 zijn de adsorpties van DPC en DTAB bestudeerd en werd $\Delta_{ads}H_m$(isost) van die twee zepen experimenteel bepaald. In hoofdstuk 6 is de warmte-ontwikkelling van het proces direkt gemeten.

In hoofdstuk 4 zijn de invloed van zout en pH op de adsorptie gemeten. Alle isothermen (de adsorptie als funktie van de evenwichtssurfactant-concentratie) hebben een steile beginhelling. Het meest opvallende aspect van de isothermen, gemeten bij verschillende zoutconcentraties, is dat deze een gemeenschappelijk snijpunt (cip) vertonen. Het cip is binnen de meetfout gelijk aan het isoëlectrisch punt van kaoliniet in de aanwezigheid van de zeep. Vóór het cip wordt de adsorptie onderdrukt door zout, maar na het cip stijgt de adsorptie met de zoutconcentratie. Deze resultaten bewijzen dat de electrostatica een belangrijke rol speelt in het adsorptie proces. Vóór het cip, d.w.z. vóór het iep, is de wisselwerking tussen het negatieve oppervlak en de positieve zeepmoleculen attractief. Echter, voorbij het cip treedt aan het grensvlak associatie op tussen de staarten van de geadsorbeerde zeepmoleculen. Het zout vermindert dan de afstoting tussen de kopgroepen en maakt de adsorptie dus gunstiger. De pyridinium kopgroep heeft een iets grotere affiniteit voor het grensvlak dan de trimethylammonium kopgroep.

DPC en DTAB adsorberen beiden vooral aan de platen. Als de pH toeneemt, neemt de (totale) adsorptie wel toe, maar deze toename is veel minder dan de toename van het aantal beschikbare plaatsen aan de randen. Het kan zijn dat bij hogere pH de geadsorbeerde protonen aan de platen worden vervangen door de zeepmoleculen. Wij heben een bilaagadsorptie-model ontwikkeld op basis van de Frumkin-Fowler-Guggenheim vergelijking. Onze resultaten passen prima in dit model.

In hoofdstuk 5 is de temperatuursinvloed van de adsorptie van organische kationen aan het hydrofiele kaoliniet grensvlak vergeleken met die aan het hydrofobe AgI. De adsorptie van tetrabutylammonium-

nitraat (TBAN) aan AgI gaat niet verder dan een monolaag, terwijl de adsorptie van DPC en DTAB aan Na-kaoliniet doorgaat tot een bilaag.

Het is nuttig om de adsorptie, Γ, bij een bepaalde evenwichts-concentratie van het adsorbaat als funktie van de temperatuur uit te zetten. Voor TBAN/AgI hebben zulke curven één maximum. De temperatuur heeft echter nauwelijks invloed op de vorming van de eerste laag van DPC of van DTAB aan Na-kaoliniet. Wel vertoont Γ één maximum als de functie van de temperatuur bij de vorming van de tweede laag. Omdat in de eerste laag de geadsorbeerde zeepmoleculen het oppervlak van kaoliniet meer hydrofoob maken, is de temperatuursinvloed in dit geval dezelfde als voor het hydrofobe AgI oppervlak. De temperatuursafhankelijkheid van de adsorptieënthalpie aan de hydrofobe oppervlakken, AgI en tweedelaag adsorptie aan Na-kaoliniet, vertoont dezelfde trend als de micelvormings enthalpie. Dit feit ondersteunt dat de hydrofobe binding één van de belangrijkste drijvende krachten is voor zowel de micelvorming als voor de vorming van de tweede laag. Aldus kan aan micelvorming en adsorptie van surfactants aan een hydrofoob oppervlak een gemeenschappelijke basis toegeschreven worden.

Hoofdstuk 6 gaat over de direkte bepaling van de adsorptieënthalpie met behulp van een isotherme microcalorimeter. Deze waarden zijn gemeten als functie van temperatuur en zoutconcentratie. De adsorptie-enthalpieën zijn temperatuurafhankelijk, met een T_{trans} van ~24°C. Als de adsorptiewarmten, $q_{ads}(cum)$, tegen Γ worden uigezet, ontstaat een curve met een knik. In alle gevallen is de adsorptie in de knik (binnen de meetfout) gelijk aan die in het cip en het iep. De gebieden zowel voor de knik als die daarna zijn redelijk rechte lijnen. De verandering van de helling bewijst dat het adsorptiemechanisme voor de eerste laag anders is dan dat voor de tweede. Uit de hellingen van de $(q_{ads}(cum)/\Gamma)$ grafiek is de molaire adsorptieënthalpie ($\Delta_{ads}H_m$) berekend. De constante helling en de constante waarden van $\Delta_{ads}H_m$ tonen aan dat het oppervlak behoorlijk homogeen is. Uit Ar/N_2 adsorptie calorimetrie waren we al tot de conclusie gekomen dat de adsorptieplekken op de platen homogeen zijn maar die op de randen niet. Dit is een van de argumenten voor onze conclusie dat de surfactant moleculen vooral aan de platen adsorberen.

Door $\Delta_{ads}H_m$ voor de eerste en de tweede laag met elkaar te vergelijken kan men concluderen dat de belangrijkste drijvende kracht voor de vorming van de eerste laag electrostatische wisselwerking tussen de koppen en het geladen oppervlak is. In de tweede laag zijn het echter dezelfde wisselwerkingen tussen de moleculen werkzaam als in micellen.

Vergelijking van $\Delta_{ads}H_m$(isost) met $\Delta_{ads}H_m$ leidt tot de volgende conclusies: (a) Voor de vorming van de eerste laag verschilt $\Delta_{ads}H_m$(isost) enigszins van $\Delta_{ads}H_m$. (b) Voor de vorming van de tweede laag komen $\Delta_{ads}H_m$(isost) en $\Delta_{ads}H_m$ overeen. Deze laatste waarden zijn bijna gelijk aan $\Delta_{mic}H_m$. De benaderingen achter de berekeningen van $\Delta_{ads}H_m$(isost) zijn waarschijnlijk de redenen voor de afwijking tussen $\Delta_{ads}H_m$(isost) en $\Delta_{ads}H_m$. Een belangrijke benadering is dat Γ_i bij verschillende temperaturen niet constant is. Omdat na het iep de lading van het klei-oppervlak gecompenseerd is, is de bovengenoemde benadering niet meer aan de orde en daarom wordt in dit tweede gebied perfecte overeenstemming tussen $\Delta_{ads}H_m$(isost) en $\Delta_{ads}H_m$ gevonden.

Samengevat;

- Adsorptie van kationogene zepen aan geladen klei-oppervlakken vindt plaats aan de platen. Of er ook adsorptie optreedt aan de randen is niet zeker. De Gibbs energie van de adsorptie is enkele tientallen kJ/mol, zodat er sprake is van fysische adsorptie.
- Adsorptie gaat door tot een bilaag gevormd is. Voor de vorming van de eerste laag is electrische aantrekking de belangkrijkste drijvende kracht, voor de vorming van de tweede laag is dat hydrofobe binding.
- De vorming van de tweede laag lijkt op micelvorming. Als functie van de temperatuur hebben de enthalpieën van die twee processen dezelfde trend, hun grootten zijn dicht bij elkaar en hun T_{trans} 's verschillen slechts enkele graden.
- De aard van de kopgroep blijkt (relatief) geen grote rol te spelen in beide processen; de aard van het tegenion mogelijk wel.

De adsorptie van amfifiele moleculen hangt af van parameters zoals de aard van de oppervlaktelading, de concentratie van het indifferente electrolyt, pH en temperatuur. Daarom moet men verschillende adsorptiecapaciteiten van bodems verwachten voor verschillende

klimaten en als gevolg daarvan verschillende snelheden van water verontreiniging. Een voorbeeld: voor bodems die een vrij grote fractie van deeltjes met permanente lading hebben, is de adsorptie capaciteit zeer waarschijnlijk hoger dan voor de bodems die vooral deeltjes met variabele lading bevatten. In dit verband hebben tropische bodems relatief meer last van vervuiling van het grondwater.

Omdat de adsorptie van surfactants verder voortschrijdt dan compensatie van de oppervlaktelading, kan de CEC de adsorptie-capaciteit van de bodem onderschatten.

Omdat door de adsorptie van surfactants voor zover deze in de eerste laag plaatsvindt de hydrofobiciteit van het oppervlak wordt veranderd, kan de bodemverontreiniging ook grote invloed hebben op de bodempermeabiliteit.

De algemene conclusie is dat dit onderzoek zowel tot de kennis van het adsorptie mechanisme als tot de meer toegepaste landbouwweten-schappen bijdragen heeft.

چکیده

ترمودینامیك جذب یونهای مثبت آلی روی سطح کایولینیت

کار برد جذب مواد آلی روی سطح کایولینیت (یك نوع رس) در امور مربوط به حفاظت محیط زیست و مخصوصاً برای پیش بینی و پیشگیری آلوده شدن آبهای زیر زمینی حایز اهمیت است. کایولینیت (ماده جاذب) یك نوع سیلیکات آلومینیوم میباشد (رجوع کنید به شکل ۱ صفحه ۱۸٤).

در واحد ساختمانی اتمهای مرکزی آلومینیم و سیلیسیم قرار دارند که ظرفیتهای آلومینیوم توسط هیدروکسیل (OH) و ظرفیتهای باقیمانده سیلیسیوم توسط اتمهای اکسیژن تکمیل میشود. بعلت غیرسیمتری بودن واحد ساختمانی حدود ٤٠ لایه از این واحدها توسط پل هیدرژنی به یکدیگر متصل میشوند و کریستالهای شش وجهی تشکیل میدهند. قاعده های این کریستالها دارای بار منفی ثابت و سطوح جانبی آنها دارای بار متغیر میباشد. مقدار و نوع بار متغیر بستی به اسیدیته محیط دارد.

مواد جذب شونده که در این تحقیق بکار رفته اند دو نوع ماده صابونی میباشند: کلرور دودسیل پیریدینیم و برمور دودسیل تری متیل آمونیوم. این مواد از نظر جذب سطحی فعال هستند زیرا ملکول آنها شامل یك قسمت دوست دارنده آب (هیدروفیل) و یك قسمت طرد کننده آب(هیدروفوب) میباشد. خواص پاك کنندگی و قدرت مخلوط کننده آب و روغن از این ذات دوگانه منتج میردد. در محلولهای غلیظ از تجمع ملکولها ذرات بزرگتری تشکیل میگردد که میسل نام دارد. حد اقل غلظت لازم برای تشکیل میسل، غلظت بحرانی نامیده میشود.

در این کار تحقیقاتی پارامتر های ترمودینامیکی واکنش مورد بررسی قرار گرفته استازاین پارامتر هاگرمای واکنش(انتالپی) با روش مستقیم و غیر مستقیم اندازه گیری شده است. انرژی آزاد واکنش (انرژی گیبس) بوسیله کاربرد مدل اثر جرم محاسبه گردیده است. برای اندازه گیری مستقیم انتالپی از کالریمتر ایزوترم Thermal Activity Monitor

ساخت سوید استفاده شده است. پژوهش با مطالعه دقیق خواص سطحی (جسم) جاذب و مواد جذب شونده آغاز شده است. کلیه آزمایشات در محلول آبی انجام گرفته است. درجه حرارت آزمایش ثابت و بین ٦ تا٦٠ درجه سانتیراد و اسیدیته pH محیط ثابت و بین ٤ تا ١٠ بوده است.آزمایشات متعدد نشان میدهد که کایولینیت بسیار خالص و عاری از پوشش اکسید ها و بویژه سایر انواع رس است.

مقدار انتالپی تشکیل میسل به نسبت قابل ملاحظه ای تابع درجه حرارت و تا اندازه ای تابع قدرت یونی محیط میباشد. دردرجه حرارتهای پایین واکنش تشکیل میسل اندوترم و در درجات بالاتر اگزوترم است. گرمای ویژه محلولهای صابونی فوق الذکر ثابت و تابعی از اندازه قسمت هیدروفوب (تعداد متیل) میباشد. قسمت هیدروفیل ملکول در این مورد رل موثری ندارد.

جذب مواد صابونی بطور کلی روی سطح خارجی قاعده های کریستال رس انجام میپیرد. هیچ نشانه ای دردست نیست که دلالت بر جذب در روی سطوح جانبی کریستال نماید. مواد صابونی در دو لایه روی سطح قاعده کایولینیت جذب میشوند. تشکیل لایه اول یك واکنش تبادل یونی است. در حقیقت یونهای صابونی مثبت با کاتیونهایی که در سطح رس وجود داشته اند (برای خنثی کردن بار سطحی) مبادله میشوند. تشکیل لایه اول به خنثی شدن بار کایولینیت منجر میشود. در این لایه از نظر فضایی ملکولهای جذب شده خیلی نزدیك به سطح کریستال قرار دارند. انتالپی تشکیل لایه اول بسیار نا چیز است. انتالپی تشکیل لایه دوم تابعی

از درجه حرارت میباشد. دردرجات حرارت پایین واکنش اندوترم و در درجات بالا تر اگزوترم میباشد. چون تغییرات انتالپی تشکیل لایه دوم با درجه حرارت شبیه تغییرات انتالپی تشکیل میسل است ، استنتاج میشود که ملکولهای مواد صابونی روی سطح رس تجمع پیدا میکنند و یك نوع نیمه میسل hemimicelle را تشکیل میدهند.

هرچه درصدذرات دارنده بار ثابت در خاك بالا باشد امکان جذب مواد صابونی بیشتر میشود. صرفنظراز تمایل جذبی واکنش جذب این مواد صابونی شبیه یکدیگر و پارامترهای ترمودینامیکی آنها بسیاربهم نزدیك میباشد

Resume

Tahereh (Nick name : Mary) Mehrian Isfahany was born in Isfahan in Iran. At the secondary school she won the first prize in the provincial competition of pupils in General Knowledge. She completed high school in Mathematics where she won the national gold medal in a General-Mathematics competition. She passed in the national contest for the entrance examination for higher education with the possibility of studying either Chemistry in Faculty of Science in Isfahan University or Physics in Tehran University. Her interest in chemistry made the choice easy. After four years she obtained her BSc degree with distinction. She worked for a few months in a yeast production company and later for 13 years in a Soil and Water Research Institute, of the Ministry of Agriculture in Iran. There she had the position of Soil Laboratory Researcher and the Deputy of the head of the laboratory. In 1985 she emigrated to *The Netherlands* where she graduated in the "MSc Course Soil Science and Water Management" in Wageningen Agricultural University with a major thesis in Soil Chemistry and a minor thesis in Colloid Chemistry. Since 1988 she has worked upon her PhD in the department of Physical and Colloid Chemistry in Wageningen. It has been resulted in this thesis which has been accepted by the Wageningen Agricultural University for a PhD degree.

Nawoord

Terug naar het begin. Ik heb in september 1985 met de vakgroep fysische en kolloïedchemie kennis gemaakt door de serieuze, getalenteerde en professionele scheikundehoogleraar professor Fleer. Ik was toen bezig met " Master of Science Course in Soil Science and Water Management". Van alle colleges vond ik scheikunde het leukste vak en kreeg ik het idee om bij de FYSKO een PhD te doen. Uiteindelijk kwam ik terecht bij Arie de Keizer voor een (extra) afstudeervakje en later voor die AIO baan. De tijd ging vreselijk snel. Het eerste 1,5 jaar leverde geen publiceerbaar resultaat! Propachlore (een pesticide) adsorbeert helemaal niet aan de kleimineralen. Ik heb zelfs een negatieve adsorptie (afstoting) gevonden! Mijn projectomschrijving is toen veranderd naar het onderwerp waarover mijn proefschrift gaat.

Er waren goede en slechte tijden gezien mijn werk en mijn leven in een andere land. Een nieuwe taal, een nieuwe cultuur, een nieuwe vak en de verwaringen die soms in een soort onzekerheid en ongeduld beëindigden. Maar gelukkig waren er altijd aardige collega's die mij met hart en ziel steunden. Ik heb veel kolloïdchemie geleerd en ik beheers nu de nederlandse cultuur goed o.a. de grappen, de goed bedoelde pesterijen enzovoort. Ik ben in vele aspecten niet de beste maar ik ben er zeker van dat ik in laatste 5 jaar meer dan alle anderen geleerd heb!

Hans Lyklema: de vrijheid en de vriendelijke werksfeer van het lab en de hoge werkkwaliteit zijn even belangrijk, het werksfeer en het onderzoeks-niveau weerspiegelen elkaar en dat is door jou voortgebracht. Bovendien ben jij een ideale promotor. Jouw kritische bestudering en grondige correcties en zelfs jouw kleine opmerkingen op mijn verslagen, geven altijd nieuwe ideeën. Jouw stimulaties en aanmoedigingen zal ik niet vergeten.

Arie: mijn experimenten zouden nooit zo goed lukken zonder jouw technische begeleiding. Jouw stimulerende karakter, vooral in het begin, was onmisbaar. Jij hebt zoveel voor ons onderzoek gedaan dat ik vaak aan *ons* proefschrift denk en niet aan *mijn* proefschrift!

Gerard: Jouw assistente te zijn voor de MSci cursussen is prachtig geweest. Bovendien hielp jij mij als ik engelse- of nederlanse taal-problemen had, buiten of binnen jouw verantwoordelijkheid. Niet veel mensen zijn zo goed in talen als jij.

Anton Korteweg: de geweldige samenwerking met jou is een heel leuke ervaring geweest. Jij was altijd bereid om zelfs in het weekend wat tijd te besteden om een nieuw experiment te beginnen, omdat tijd een grote beperking was. Onze en jouw familie zijn nu meer dan kennisen.

Bert van der Wal: jij hebt in het kader van jouw doctroraalonderzoek een significante bijdrage aan de hoofdstukken 4 en 5 geleverd. Iedere keer als ik jouw doctoraalverslag terug zie, herken ik weer jouw nawkeurige werk en jouw enthousiasme. Wij hebben veel *gemeenschappelijke* resultaten voor twee zepen met dezelfde staart. *Dus de invloed van de kopgroep op de thermodynamische parameters van de adsortie is gering.*

Maarten Bakkenens en Ab van der Linde en Klaas Besseling hebben mij ook geholpen. Maarten met het maken van onze zuivere zepen. Ab en Klaas met het programmeren in Pascal en bij de Newtoniteratie. Verder ben ik dankbaar aan alle secreteriaat medewerksters (de zogenaamde opvangsters voor probleemhebbenden). Bert Bouman: bedankt voor je medewerking op velerlei gebied. Alle medewerk(st)ers, (ex)AIO's en (ex)OIO's dank ik van harte voor hun solidariteit en medewerking, o.a. Riet van de Steeg en Jakomien Solfstra. Janet van Vreeswijk, mijn laatste kamergenote: bedankt vooral voor het verdragen van mijn rondslingerende papieren. Gert Buurman heeft in de vorm van figuren tekenen en fotografie zichtbare bijdragen aan dit boekje geleverd. Zijn kunsttalent is bijzonder nuttig voor deze absoluut wetenschappelijke vakgroep. Ik ben Rudy Hengelmolen dankbaar voor het corrigeren van de engelse tekst. Ik dank Drs. C. Hanssen van de afdeling Oosterse Talen en Cultuur van de Rijksuniversiteit Utrecht voor zijn hulp bij het uitwerken van de perzische samenvatting.

Irene (mijn paranimf) en Ruud Jordens mijn vrienden voor het leven: jullie hebben een zeer grote bijdrage geleverd tot mijn succes de laatste 7 jaar.

Katy: bedankt voor jouw geduld en jouw hulp bij de nederlandse teksten.

Ten slotte wil ik, mijn man Iraj bedanken voor zijn grote steun en inspiratie zonderwelke dit proefschrift niet tot stand had kunnen komen.

IK kijk met plezier terug op de laatste 5 jaar. Mary